

In compliance with the
Canadian Privacy Legislation
some supporting forms
may have been removed from
this dissertation.

While these forms may be included
in the document page count,
their removal does not represent
any loss of content from the dissertation.

**Synthesis, Characterization, Thermomechanical and Rheological
Properties of Long Chain Branched Metallocene Polyolefins**

By

Edward B. Kolodka, B. Sc.

A Thesis

Submitted to the School of Graduate Studies

in Partial Fulfillment of the Requirements

for the Degree

Doctor of Philosophy

McMaster University

Hamilton, Ontario, Canada

**Synthesis, Characterization, Thermomechanical and Rheological
Properties of Long Chain Branched Metallocene Polyolefins**

**SYNTHESIS, CHARACTERIZATION, THERMOMECHANICAL
AND RHEOLOGICAL PROPERTIES OF LONG CHAIN
BRANCHED METALLOCENE POLYOLEFINS**

BY

EDWARD B. KOLODKA

B. Sc.

Doctor of Philosophy (2002)

McMaster University

(Chemical Engineering)

Hamilton, Ontario

TITLE: Synthesis, Characterization, Thermomechanical and Rheological
Properties of Long Chain Branched Metallocene Polyolefins

AUTHOR: Edward B. Kolodka B.Sc. (University of North Dakota)

SUPERVISORS: Professor Shiping Zhu
Professor Archie E. Hamielec

NUMBER OF XVI, 172

PAGES:

ABSTRACT

The objectives of this research were to prepare model long chain branched polyolefin samples with controlled molecular weights and chain structural properties, and to elucidate the effects of long chain branching on the rheological and mechanical properties of polyethylene and polypropylene using a variety of synthesis and characterization techniques.

Significant long chain branch (LCB) formation was found by ^{13}C NMR measurements in polyethylene (PE) samples produced using the homogeneous catalyst bis(cyclopentadienyl) zirconium dichloride in a semi-batch slurry polymerization. Enhanced levels of LCB were attributed to the in-situ reaction of ethylene macromonomer and the encapsulation of active centres by precipitated polymer chains.

PE samples with controlled levels of LCB were synthesized using a two-stage polymerization process. Narrowly dispersed poly(ethylene-co-propylene) (EPR) macromonomer was first produced in a continuous stirred tank reactor (CSTR). The macromonomer was subsequently copolymerized with ethylene in a semi-batch reactor using the constrained geometry catalyst (CGC-Ti). The two-stage reaction process was also employed to synthesize polypropylene (PP) with EPR long chain branches using the catalyst system *rac*-dimethylsilylenebis(2-methylbenz[e]indenyl)zirconium dichloride / MMAO. It was found that the stoichiometry of the macromonomer could be used to efficiently control the long chain branch frequency (LCBF) of the copolymers without

greatly influencing the copolymer molecular weight. It was also possible to control the long chain branch length by varying the molecular weight of the macromonomer.

The rheological properties of various long chain branched polyolefins were measured. These polymers exhibited significantly higher zero shear viscosities (η_0) and displayed greater shear thinning than linear polymers with similar molecular weights. It was observed that the branch M_N had to be greater than 7000 g/mol in order to form sufficient entanglements to significantly influence the rheological responses. The η_0 was found to be a sensitive indicator of branch frequency and branch length. Increasing the branch M_N led to enhanced values of η_0 , improved shear-thinning, and elevated flow activation energies.

Long chain branching played a significant role in the dynamic mechanical behaviour of polyolefins. Increasing the frequency of branching increased the stiffness of polyethylene, as reflected by the storage modulus. Long chain branching also served to enhance the damping or energy dissipation of PE, shown by increased values of the loss modulus. The dynamic mechanical behaviour of polypropylenes with EPR long chain branches was also characterized. There appeared to be a critical EPR branch length at a M_N of approximately 6000 g/mol. When the branch length was below this critical M_N , a homogenous system resulted. If this critical M_N was exceeded, a two-phase system developed, with fine rubbery domains dispersed in a PP matrix. When a two-phase system developed, it enhanced the loss modulus of the copolymer in a manner similar to impact modified PP.

ACKNOWLEDGEMENTS

I would like to take this opportunity to express my gratitude to the many people who enriched my time at McMaster University.

First and foremost I would like to thank Professor Zhu for guidance, time, and finite patience throughout this work. Working with Professor Zhu for the past five years has indeed been a privilege. I am also grateful to my thesis co-supervisor, Professor Hamielec, who has contributed invaluable to this thesis.

I would also like to thank Dr. Wen-Jun Wang for his advice, encouragement, and wry sense of humour.

I owe a large debt of gratitude to my parents. They believed in me and helped me to become the person I am.

Finally, I would like to thank the members of JEDE for helping me to forget.

TABLE OF CONTENTS

	Page
ABSTRACT	iii
ACKNOWLEDGEMENTS	v
LIST OF FIGURES	ix
LIST OF TABLES	xiii
NOMENCLATURE	xv
CHAPTER 1 – INTRODUCTION	1
1.1 Background	1
2.2 Objectives and outlines of this thesis work	3
CHAPTER 2 – LITERATURE REVIEW	5
2.1 Historical Review of Polyolefins	5
2.2 Metallocene Catalysts	8
2.3 Long Chain Branching in Polyolefins	25
2.3 Rheological Characterization	28
2.4 Dynamic Mechanical Analysis	32
CHAPTER 3 – SYNTHESIS OF LONG CHAIN BRANCHED POLYOLEFINS WITH METALLOCENE CATALYSTS	35
3.1 Introduction	35
3.2 Long Chain Branching in Ethylene Slurry Polymerization	37
3.2.1 Experimental	37
3.2.2 Results and Discussion	42
3.2.3 Conclusions	52
3.3 Copolymerization of Poly(Ethylene-co-Propylene) Macromonomer with Ethylene	53
3.3.1 Experimental	54

3.3.2 Results and Discussion	58
3.3.3 Conclusions	64
3.4 Copolymerization of Poly(Ethylene-co-Propylene) Macromonomer with Propylene	65
3.4.1 Experimental	65
3.4.2 Results and Discussion	70
3.4.3 Conclusions	
 CHAPTER 4 – RHEOLOGICAL PROPERTIES OF LONG CHAIN BRANCHED POLYOLEFINS	 83
4.1 Introduction	83
4.2 Rheological Behaviour of Long Chain Branched Polyethylene	86
4.2.1 Experimental	86
4.2.2 Results and Discussion	90
4.2.3 Conclusions	105
4.3 Rheological Behaviour of Long Chain Branched Polypropylene	107
4.3.1 Experimental	107
4.3.2 Results and Discussion	109
4.3.3 Conclusions	121
 CHAPTER 5 – DYNAMIC MECHANICAL PROPERTIES OF LONG CHAIN BRANCHED POLYOLEFINS	 122
5.1 Introduction	122
5.2 Dynamic Mechanical Behaviour of Long Chain Branched Polyethylene	127
5.2.1 Experimental	127
5.2.2 Results and Discussion	128
5.2.3 Conclusions	136
5.3 Dynamic Mechanical Behaviour of Polypropylene with Poly(ethylene-co-propylene) Long Chain Branches	137
5.3.1 Experimental	137

5.3.2 Results and Discussion	139
5.3.3 Conclusions	144
CHAPTER 6 – SIGNIFICANT RESEARCH CONTRIBUTIONS AND RECOMMENDATIONS FOR FUTURE WORK	146
6.1 Significant Research Contributions of the Thesis Work	146
6.2 Recommendations for Future Research	151
6.3 List of Publications from this Work	152
REFERENCES	154

LIST OF FIGURES

CHAPTER 2		page
Figure 2.1	Generic structure of a metallocene catalyst.	9
Figure 2.2	Proposed structures of methylaluminoxane.	11
Figure 2.3	Formation of cationic metallocene alkyl active site.	12
Figure 2.4	Mechanism of propagation.	13
Figure 2.5	Mechanisms of β -hydride elimination and chain transfer to monomer.	14
Figure 2.6	Termination mechanisms of metallocene catalysts.	16
Figure 2.7	Mechanism of in-situ long chain branch formation.	27
Figure 2.8	Influence of molecular weight on zero shear viscosity.	31
Figure 2.9	Schematic representation of DMA.	33
CHAPTER 3		
Figure 3.1	Schematic of the 1 litre high-pressure semi-batch reactor.	38
Figure 3.2	^{13}C NMR spectrum with chemical shifts in TCB and d-ODCB at 120 °C of Sample 4.	41
Figure 3.3	Mechanism of the formation of long chain branching.	42
Figure 3.4	The effect of temperature on LCB density and frequency.	47
Figure 3.5	The effect of pressure on LCB density and frequency.	48
Figure 3.6	^{13}C NMR spectrum with chemical shifts in TCB and d-ODCB at 120 °C of Sample 9.	50
Figure 3.7	The effect of $[\text{MMAO}]/[\text{Cp}_2\text{ZrCl}_2]$ on long chain branch density and frequency.	51
Figure 3.8	Mechanism of EPR incorporation into a growing PE chain forming a LCB.	54
Figure 3.9	Schematic of semi-batch reactor setup.	56
Figure 3.10	Influence of ethylene pressure on the degree of grafting.	61
Figure 3.11	Influence of pressure on the catalyst activity.	61

Figure 3.12	Influence of temperature on the degree of grafting of EPR macromonomer copolymerized with ethylene.	62
Figure 3.13	The influence of temperature on the catalyst activity for the copolymerization of ethylene and EPR macromonomer.	64
Figure 3.14	GPC trace of Sample 13 overlaid with the trace of macromonomer.	72
Figure 3.15	FTIR spectrum of Sample 3 macromonomer before and after copolymerization.	73
Figure 3.16	¹³ C NMR spectrum of Sample 12.	75
Figure 3.17	Influence of low MW macromonomer concentration on conversion, M _w and LCBF.	77
Figure 3.18	Influence of high MW macromonomer concentration on conversion, M _w and LCBF.	77
Figure 3.19	Influence of macromonomer MW on conversion, M _w , and LCBF.	79
Figure 3.20	Influence of reaction temperature on conversion, M _w , and LCBF.	81
 CHAPTER 4		
Figure 4.1	Dynamic viscosity at 190 °C fit using the Cross Equation.	89
Figure 4.2	Dynamic viscosity of PE samples with M _w approximately 155 kg/mol.	91
Figure 4.3	Dynamic viscosity of PE samples with M _w approximately 60 kg/mol.	92
Figure 4.4	Schematic representation of long chain branching at high and low shear rates.	93
Figure 4.5	The influence of LCBF on the power-law exponent n.	94
Figure 4.6	Normalized dynamic viscosity of semi-batch PE samples.	96
Figure 4.7	Influence of LCBF on G' and G'' for Samples 2 and 8.	98
Figure 4.8	Influence of LCBF on G' and G'' for Samples 9 and 10.	99

Figure 4.9	Apparent master curve of Sample 7 ($E_a = 31.4$ kJ/mol).	100
Figure 4.10	Rheologically simple behavior of Sample 10.	101
Figure 4.11	Rheologically complex behavior of Sample 7.	102
Figure 4.12	Determination of modulus-dependent shift factor for Sample 5.	103
Figure 4.13	Frequency dependent activation energy.	104
Figure 4.14	Influence of branch MW on the dynamic viscosity.	110
Figure 4.15	Influence of branch length on the Power-law exponent n and on the η_0 .	111
Figure 4.16	Influence of branch length on G' and G'' .	112
Figure 4.17	Influence of branch length on activation energy.	113
Figure 4.18	Influence of LCBF on dynamic viscosity having branches of $M_N 2500 =$ g/mol.	114
Figure 4.19	Influence of LCBF on G' and G'' with branches of $M_N = 2500$ g/mol.	115
Figure 4.20	Influence of LCBF on E_a with branches of $M_N = 2500$ g/mol.	115
Figure 4.21	Influence of LCBF on dynamic viscosity with branches of $M_N = 17000$ g/mol.	117
Figure 4.22	Influence of LCBF on G' and G'' with branches of $M_N = 17000$ g/mol.	117
Figure 4.23	Influence of LCBF on E_a with branches of $M_N = 17000$ g/mol.	118
Figure 4.24	Rheological Complexity of Sample 6	119
Figure 4.25	Time dependent activation energies of Samples 1 and 6.	120

CHAPTER 5

Figure 5.1	Dynamic mechanical behavior of high density polyethylene.	129
Figure 5.2	Storage Modulus of Samples 3, 4 and 5.	130
Figure 5.3	Loss modulus of Samples 3, 4 and 5.	131

Figure 5.4	Storage modulus of Samples 2 and 8.	131
Figure 5.5	Loss modulus of Samples 2 and 8.	132
Figure 5.6	Chain architecture of branched polyethylene.	134
Figure 5.7	Storage modulus of Samples 1 and 10.	135
Figure 5.8	Loss modulus of Samples 1 and 10.	135
Figure 5.9	Temperature dependence of mechanical storage modulus (E') and loss modulus (E'') at 1Hz for the PP-graft-EPR copolymers with varying EPR M_N .	139
Figure 5.10	Morphological development of PP-g-EPR with increasing branch length.	141
Figure 5.11	Temperature dependence of mechanical storage modulus (E') and loss modulus (E'') at 1Hz for PP-graft-EPR copolymer and commercial HIPP.	142
Figure 5.12	Temperature dependence of mechanical storage modulus (E') and loss modulus (E'') at 1Hz for PP-graft-EPR copolymers with varying EPR concentrations.	143

LIST OF TABLES

Chapter 3

Table 3.1	Experimental Conditions For Ethylene Homopolymerization Using Metallocene Systems.	39
Table 3.2	Summary of GPC, ¹³ C NMR, and MFI Data.	44
Table 3.3	Experimental Conditions For EPR / Ethylene Copolymerization.	57
Table 3.4	Chain properties of EPR.	59
Table 3.5	Copolymerization of EPR / Ethylene.	60
Table 3.6	Chain properties and reaction conditions of poly(ethylene-co-propylene) macromonomer samples prepared by high-temperature continuous stirred-tank reactor.	67
Table 3.7	Experimental conditions for the copolymerization of propylene with poly(ethylene-co-propylene) macromonomers using a semibatch reactor.	68
Table 3.8	Results of the copolymerization of propylene with poly(ethylene-co-propylene) macromonomers using semibatch reactor.	70

CHAPTER 4

Table 4.1	Molecular properties of long chain branched polyethylene samples.	87
Table 4.2	Results of the copolymerization of propylene with poly(ethylene-co-propylene) macromonomers using semi-batch reactor.	107

CHAPTER 5

Table 5.1	Molecular properties of long chain branched polyethylene samples.	127
Table 5.2	GPC and ^{13}C NMR results of the polymer samples.	138

NOMENCLATURE

CCD	chemical composition distribution
CGC	constrained geometry catalyst
CSTR	continuous stirred tank reactor
DSC	dynamic scanning calorimetry
E	Young's modulus
EPDM	ethylene-propylene-diene
EPR	ethylene-propylene rubber
FTIR	Fourier transform infrared
G'	storage modulus
G''	loss modulus
GPC	gel permeation chromatography
HDPE	high density polyethylene
LCB	long chain branch
LCBD	long chain branch density
LCBF	long chain branch frequency
LDPE	low density polyethylene
LLDPE	linear low density polyethylene
MAO	methylaluminoxane
MMAO	modified methylaluminoxane
MW	molecular weight
MWD	molecular weight distribution
¹³ C NMR	carbon-13 nuclear magnetic resonance
PDI	polydispersity index
PE	polyethylene
PP	polypropylene
SAOS	small-amplitude oscillatory shear
SCB	short chain branching
TCB	1,2,4-trichlorobenzene

Z-N	Ziegler-Natta
E_a	flow activation energy
M_N	number average molecular weight
M_W	weight average molecular weight
T_g	glass transition temperature
ω	frequency
η	dynamic viscosity
$\tan(\delta)$	loss tangent
τ	shear stress
η_0	zero shear viscosity

Chapter 1

Introduction

1.1 Background

Polyolefins are the single largest synthetic commodity polymers with over 40 billion pounds produced annually in North America alone (Modern Plastics, 2002). The polyolefin family is composed of low and high density polyethylene, polypropylene, and copolymers of other alkene (olefin) monomers. The unique combination of mechanical properties, ease of processing, and low cost have enabled polyolefins to be employed in such diverse applications as films, injection molding of household goods, fibres, coatings and adhesives.

Polyolefins are produced commercially using free radical initiators, Phillip's type catalysts and Ziegler-Natta catalysts. Ziegler-Natta catalysts, the most important catalyst type, have evolved significantly since their inception in the 1950s, with large improvements in activity, stereoselectivity and versatility. These catalysts are used extensively in gas phase and slurry phase reactions for the production of a wide array of polyolefins. Polymers produced with Ziegler-Natta catalysts inevitably have broad molecular weight distributions, and in the case of copolymerizations, broad chemical composition distributions. This phenomenon is generally attributed to multiple active sites, each with distinct polymerization properties.

Recently a new generation of soluble Ziegler-Natta catalysts has been developed. The metallocene/aluminoxane catalysts are poised to revolutionize the polyolefin industry. These novel homogeneous catalysts offer an unprecedented control over polyolefin architecture. Metallocenes are thought to be single site type catalysts, and consequently, metallocene polymers have narrow molecular weight distributions and narrow chemical composition distributions, leading to improved mechanical properties including clarity, tear strength and stiffness. Furthermore, metallocenes can be tailored to an almost limitless number of site types for a single monomer or monomer pair by varying: a) ligand type, b) bridge joining ligands, c) substituents on ligands and bridge to alter the steric and electronic surroundings of the active centre, and d) transition metal type.

Metallocene polymers, due to their narrow molecular weight distributions, exhibit a distinct lack of shear thinning. This characteristic has led to difficulties in processing using existing equipment. However, several metallocene catalysts have been developed which enable the production of long chain branches. These branches have been found to have significant influences on the rheological properties of polymers. Low levels of long chain branching have been associated with increased low shear viscosities, enhanced shear thinning, elevated melt strengths, and increased elasticities. Unfortunately, the precise effects of LCB are not well understood due to the difficulty of producing well-defined samples with a broad range of molecular attributes.

1.2 Objectives and outlines of this thesis work

The objectives of this research were to prepare model long chain branched polyolefin samples having controlled molecular weight and chain structural properties, and to elucidate the effects of long chain branching on the rheological and mechanical properties of polyethylene and polypropylene using a variety of synthesis and characterization techniques.

Long chain branched polyethylene, with a variety of branch densities, was synthesized in a slurry phase, semi-batch reaction using the metallocene catalyst Cp_2ZrCl_2 and modified methylaluminoxane. The polymer architecture was characterized using ^{13}C NMR and gel permeation chromatography (GPC)

A novel two-stage polymerization was developed to produce polyethylene with poly(ethylene-co-propylene) long chain branching. Poly(ethylene-co-propylene) macromonomer was first synthesized in a continuous stirred tank reactor using a constrained geometry metallocene catalyst (CGC). In a subsequent reaction, the macromonomer was copolymerized with ethylene using CGC in a semi-batch reactor. The resultant polymer was characterized using ^{13}C NMR, GPC, and FTIR.

This two-stage polymerization was then applied to produce isotactic polypropylene with poly(ethylene-co-propylene) long chain branching. The branch

densities and branch lengths were varied to produce model long chain branched polymers.

The rheological properties of the various polymers were measured using a parallel plate rheometer. The effects of branch density, branch length, and branch type were characterized.

The mechanical properties of the long chain branched polymers were measured using dynamic mechanical analysis. The influences of branch length and branch type on the stiffness, damping characteristics and crystallinity of branched PE and PP were observed.

A detailed understanding of long chain branching is essential. Many polymers produced using metallocene catalysts have low levels of long chain branching. These polymers have significantly altered rheological properties and require different processing conditions. In order to optimize the processing of metallocene catalysts, the influences of long chain branching must be understood.

CHAPTER 2 - LITERATURE REVIEW

2.1 Historical Review of Polyolefins

Polyolefins are a class of polymer which include the various grades of polyethylene (PE), polypropylene (PP) and (co-)polymers of other alkene monomers. They are among the most important modern commodity polymers with over 42 billion pounds produced annually in North America (Modern Plastics, 02). Polyolefins are commercially produced using free radical initiators, Ziegler-Natta catalysts, and Phillips type catalysts.

Low density PE was first synthesized in 1933 by Imperial Chemical Industries using a high temperature, high pressure, free radical process (tubular reactor at 140-325 °C and 250 MPa). Due to the free radical mechanism, the resultant polymer structure cannot be controlled, leading to a broad molecular weight distribution (MWD) and a highly branched backbone composed of both short chain branches (SCB) and long chain branches (LCB). These branches disrupt the crystallinity of PE (40-60 %), reduce the density (0.91-0.93 g/cm³), and decrease the physical and mechanical characteristics of the polymer. Low density PE, due to a combination of desirable properties, is still used extensively today. It has a good combination of strength, flexibility, impact resistance, and melt flow behaviour. LDPE is used primarily in film applications (60 percent) and in the injection molding of toys and household goods (20 %). The production of LDPE is expanding at a significantly lower rate than that of linear low density polyethylene due to

high plant costs, lack of flexibility, and relatively poor physical and mechanical properties.

The development of Ziegler-Natta catalysts revolutionized the polyolefin industry. These catalysts were first developed in 1953 by Ziegler for ethylene production and later developed by Natta in 1954 to synthesize isotactic polypropylene. These catalysts are widely applied in the polyolefin industry today. They are used in the synthesis of high density polyethylene (HDPE), linear low density polyethylene (LLDPE), isotactic polypropylene (iPP), ethylene-propylene-diene rubbers (EPDM), and *cis*-1,4-polybutadiene among others.

Ziegler-Natta catalyst systems are composed of a transition metal salt of Groups IV to VIII (catalyst), and a metal alkyl of Groups I to III (cocatalyst). Although there are thousands of different combinations with a range of behaviours and applications, most industrial processes are based on titanium salts and aluminum alkyls (Boor, 1979). Z-N catalysts have undergone several major changes since their first introduction with three distinct generations recognized. There has been a 20-fold increase in catalyst activity and at the same time significant improvements in stereochemical control (Whitely et al., 1992).

Ziegler-Natta catalysts allowed the production of high density polyethylene (HDPE). HDPE, produced via Z-N catalysts, is linear in nature, with very low levels of short chain branching. Because of this lack of branching, HDPE is far more crystalline

than LDPE and consequently has a higher density and a higher thermal stability. It also has increased tensile strength, stiffness, chemical resistance, and upper temperature range. However, HDPE has reduced low temperature impact strength, elongation, permeability, and resistance to stress cracking. HDPE is primarily used in blow molding of bottles and toys (40 %), and the injection molding of household goods (30 %) but is also used a wide array of other applications including film production (O dian, 1991).

The third major classification of PE, known as linear low density polyethylene (LLDPE), saw widespread commercial production with the emergence of gas phase technologies employing Z-N catalysts (James, 1989). LLDPE is a copolymer of ethylene and a small amount of α -olefin, such as 1-butene, 1-hexene, or 1-octene. It is composed of a linear backbone with α -olefins forming a controlled amount of short chain branching. LLDPE exhibits many of the properties of LDPE yet can be produced under far milder conditions (70 – 100 °C and 2 MPa), greatly reducing the capital investment and energy operating costs. LLDPE is gradually replacing LDPE in the blown film industry (O dian, 1991).

Perhaps an even more important advancement made possible by Z-N catalysts was the advent of isotactic and syndiotactic polypropylene (PP). Atactic PP is an amorphous, tacky polymer with no physical strength and little commercial value. However, several types of Z-N catalysts are highly stereospecific. The insertion of an asymmetric monomer into the growing polymer chain in a given orientation is favoured. PP is an industrially significant polymer with many useful properties. It has a high

strength-to-weight ratio, a working temperature of up to 120 °C, is easily processed, and has a low cost. PP has many applications as plastic and as fibrous materials.

Polymers produced with Z-N catalysts invariably share a common trait. The polymers have a broad molecular weight distribution (MWD), and in the case of copolymers, a broad chemical composition distribution (CCD). It is generally accepted that heterogeneous Z-N catalysts possess several active site types, each with distinct chemical properties. Polymer chains produced at separate sites have different average molecular weights, comonomer compositions, and variable degrees of stereoregularity. Therefore, polymers synthesized using Z-N catalysts are complex mixtures of dissimilar chain types with broad MWDs and CCDs. Several soluble Z-N catalysts, including bis(cyclopentadienyl)zirconium dichloride, were known to produce narrowly dispersed PE when combined with organoaluminum cocatalysts (Andressen, 1976). However, these catalysts had extremely low activities and were used primarily to elucidate the elementary steps in the polymerization process.

2.2 Metallocene Catalysts

Metallocene catalysts are a new generation of Ziegler-Natta catalysts which offer unprecedented control over polymer architecture and are poised to revolutionize the polyolefins industry. The first metallocene catalyst was the low activity, soluble Z-N catalyst bis(cyclopentadienyl)zirconium dichloride activated by diethylaluminumchloride

(AlEt₂Cl). The activity of this complex was observed to be greatly enhanced by the introduction of minute traces of water into trimethyl aluminum (Sinn and Kaminsky, 1980). It was determined that the water reacted with the cocatalyst, yielding methylaluminoxane (MAO), a very active cocatalyst. The activity of the bis(cyclopentadienyl)zirconium dichloride / MAO combination was greater than that offered by traditional Z-N catalysts.

Metallocene catalysts, often referred to as fourth generation Z-N catalysts, are soluble in the reaction medium. They are generally composed of a transition metal atom bonded to one or two cyclopentadienyl or substituted cyclopentadienyl rings (Huang and Rempel, 1995). Metallocenes can be tailored to an almost limitless number of site types for a single monomer or monomer pair by varying: a) ligand type, b) bridge joining ligands, c) substituents on ligands and bridge to alter the steric and electronic surroundings of the active centre, and d) transition metal type (Hamielec and Soares, 1996). Figure 2.1 shows the generic structure of a metallocene catalyst.

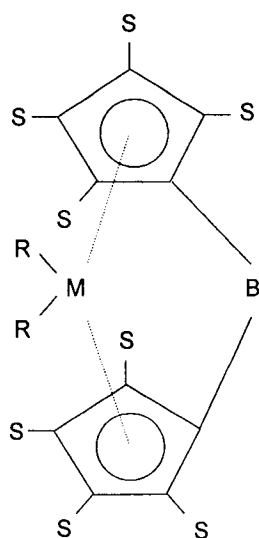


Figure 2.1 Generic structure of a metallocene catalyst

Several metallocene catalyst types can provide an excellent degree of stereospecific control for asymmetric monomers, such as propylene. Racemic-bridged metallocenes, first developed in the mid eighties, were the first soluble Z-N catalysts used to produce isotactic PP (Wild et al., 1985) and later syndiotactic PP (Kaminsky et al., 1985). The bridge structure between the indenyl rings prevents rotation of the rings around the coordination axes, imparting stereoregularity to the metallocene catalyst. The spatial arrangement of the racemic enantiomers favours the coordination of propylene monomers in a specific orientation, producing mainly isotactic chains.

The greatest advantage of metallocene catalysts over traditional Z-N catalysts is their single site nature. The active sites each have the same chemical properties and produce similar polymer chains (Kaminsky, 1988). As a consequence, polymers produced using metallocenes have narrow molecular weight distributions, and chemical composition distributions.

One of the most serious disadvantages of metallocene catalysts is the high concentration of MAO required to achieve sufficient activities, with aluminum / catalyst ratios of 1000 to 20000 commonly reported. Other cocatalysts such as ethylaluminumoxane and isobutylaluminumoxane have been shown to be far less effective than MAO (Kaminsky and Steiger, 1988). Aluminoxanes are difficult to synthesise and handle and are extremely expensive. In addition, at elevated concentrations they can adversely affect the polymer properties and must be removed, further increasing production costs.

Wang, 1990), as shown in Figure 2.3. MAO is also believed to aid in the reactivation of dormant active sites (Kaminsky et al., 1985).

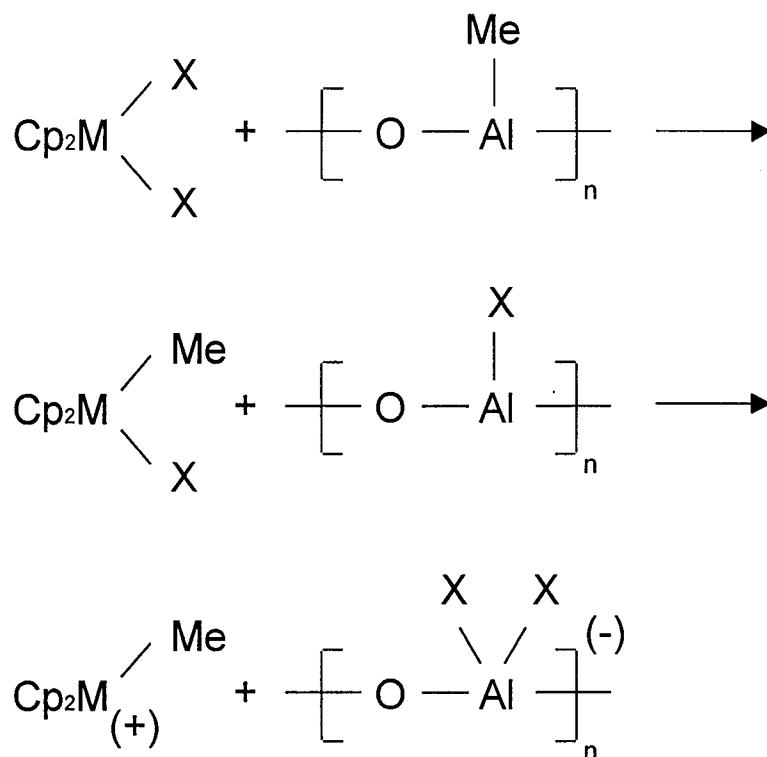


Figure 2.3 Formation of cationic metallocene alkyl active site

The activity of the metallocene complex was found to be strongly dependent on the MAO/catalyst ratio (Chien and Wang, 1988). Increasing the MAO concentration led to an almost 20 fold increase in activity. In order to determine the influence of MAO concentration on the active site concentration, Han et al., proposed using CO as an inhibitor (Han et al., 1996). It was determined that the concentration of active sites increases with increasing Al/Zr. The activity of the catalyst showed a dramatic increase when the ratio was raised to 2000.

The active centre of metallocene catalysts are believed to be alkylated cations of the type $\text{Cp}_2\text{M}^+-\text{R} \cdot \text{MAOX}^-$ (Barsan et al., 1998, Chien and Wang, 1990). This theory was further verified when enhancements in the activity of $(\text{C}_5\text{H}_5)_2\text{TiCl}_2-(\text{C}_2\text{H}_5)_2\text{AlCl}$ were observed in polar organic solvents such as ethyl chloride, with activities approaching that of classic metallocenes (Matkovskii et al., 1998).

The generally accepted mechanism of polymerization using metallocenes is the monometallic mechanism proposed for Z-N catalysis, shown in Figure 2.4 (Cossee, 1964). A vacant coordination site is generated by interaction with MAO, followed by olefin complexation (Mashima et al., 1997). Polymer chain growth occurs by 1-olefin coordination to a vacant site followed by olefin insertion via a transition-state. After monomer insertion the coordination site is vacated for the next monomer. The polymerization rate R_p is proportional to the propagation rate constant k_p , monomer concentration $[\text{M}]$, and active site concentration $[\text{C}^*]$.

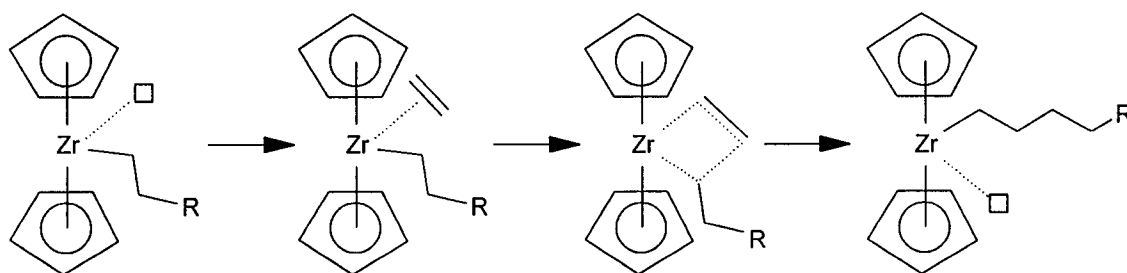


Figure 2.4 Mechanism of propagation

Chain transfer to monomer and β -hydride elimination are generally believed to be the dominant chain transfer reactions in olefin polymerization with metallocene catalysts

(Brintzinger et al., 1995). The mechanisms of β -hydride elimination and chain transfer to monomer are shown in Figure 2.5. In chain transfer to monomer the β -H is transferred from the growing polymer chain to an approaching monomer. After the monomer coordinates with the active site, the π -bond of the monomer opens and the β -H is transferred. The saturated end of the new growing polymer chain contains a linear alkyl chain of length R_2 . In ethylene polymerization the dead polymer chain contains a terminal vinyl group while α -olefin polymerizations contain a vinylidene group (Tsutsui et al., 1989).

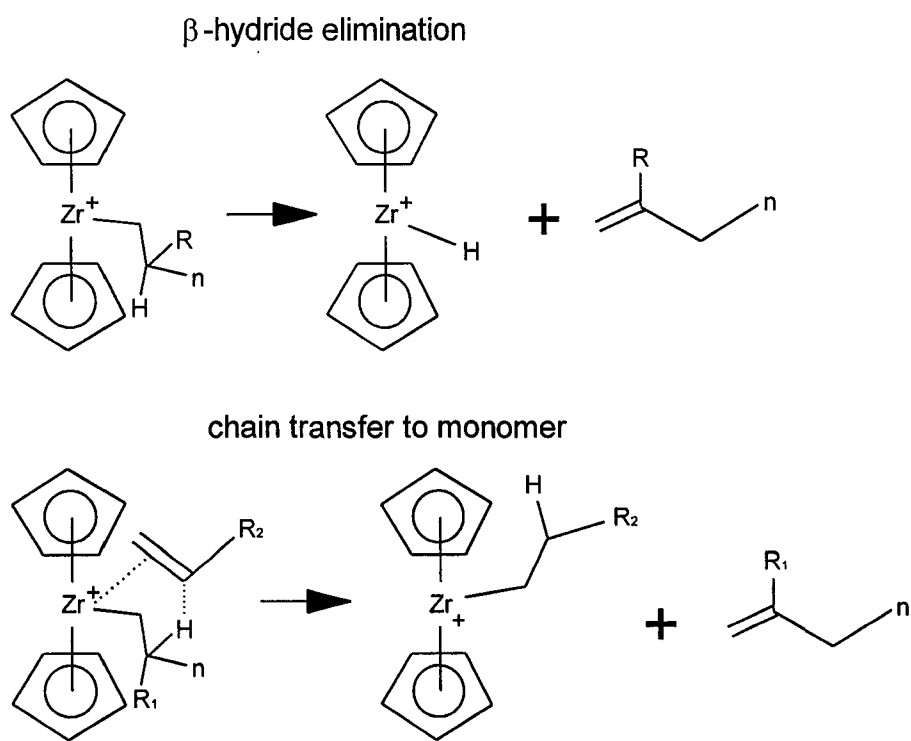


Figure 2.5 Mechanisms of β -hydride elimination and chain transfer to monomer

In β -hydride elimination, shown in Figure 2.5, the β -H is transferred to the metal active site (Sinn and Kaminsky, 1980). A terminal vinyl end group is formed in ethylene homopolymerizations, while a vinylidene forms in α -olefin polymerizations.

There are several other termination mechanisms common to metallocene catalysts, some of which are shown in Figure 2.6. Polymerizations involving propylene are subject to β -CH₃ elimination, as shown in Figure 2.6. This results in the formation of propylene with a vinyl termination and a Zr⁺-CH₃ site (Resconi, 1992).

In σ -bond metathesis, shown in Figure 2.6, chain transfer to monomer occurs via C-H activation. The alkene π -bond is not opened but the Zr-C- bond and H-C= groups exchange constituents. A saturated dead polymer chain and a Zr-C= group are formed via the metathesis reaction (Siedle, 1998).

Hydrogen is a common chain transfer agent used to control the molecular weight of olefin polymerizations. In chain transfer to hydrogen, shown in Figure 2.6, a hydrogen molecule inserts into a growing polymer chain. This results in a saturated dead polymer chain and a Zr⁺-H cation (Kissin and Brandolini, 1999).

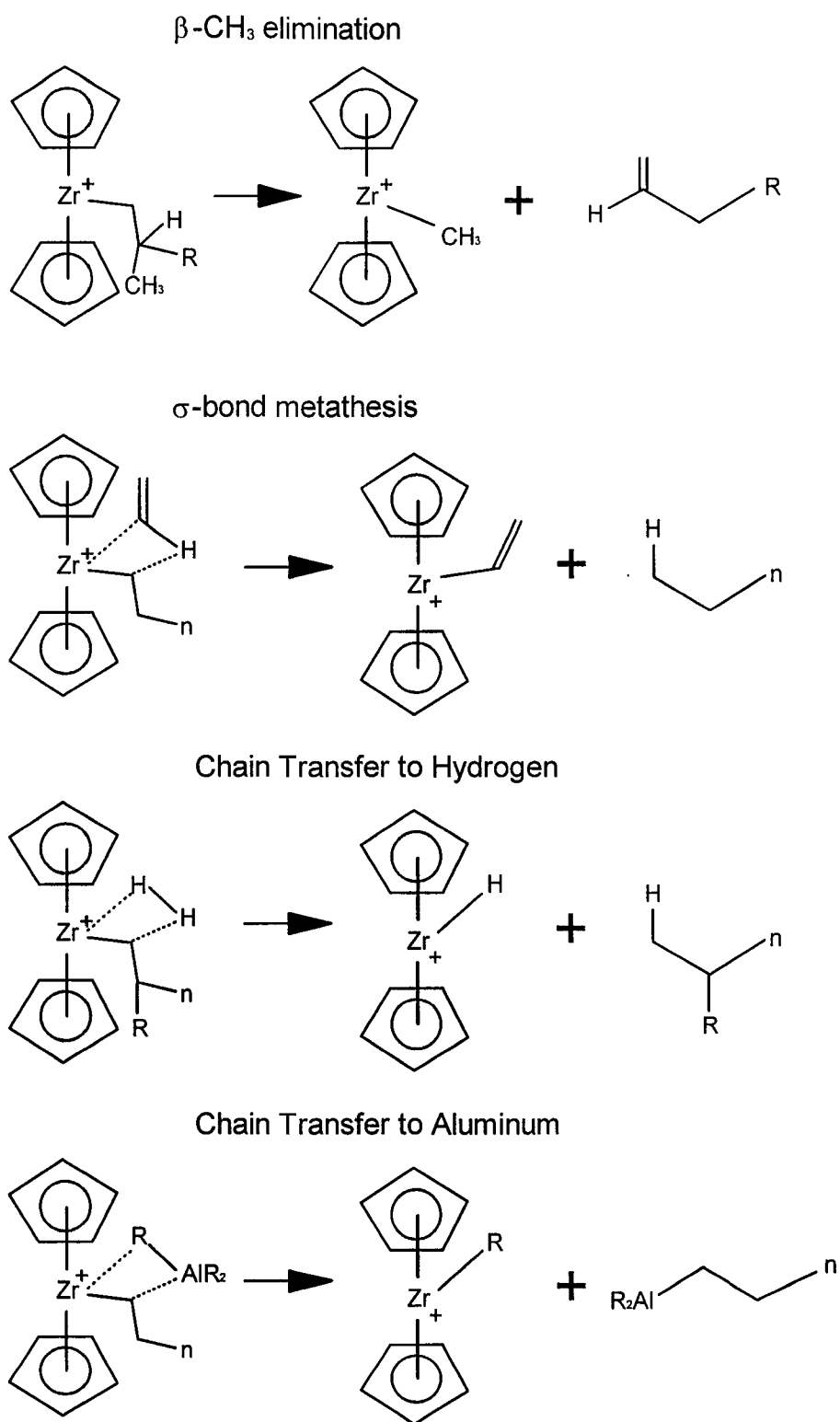


Figure 2.6 Termination mechanisms of metallocene catalysts

A final termination mechanism common to metallocene catalysis is chain transfer to aluminum, shown in Figure 2.6. An alkyl group bonded to an aluminum alkyl or MAO is transferred to the metallocenium ion and a R_2Al -group is attached to the polymer chain. This bond is extremely reactive and can be removed with treatment of HCl/MeOH (Shiono and Soga, 1992).

Many metallocene catalysts show a comonomer effect. The addition of α -olefins to a reaction has been shown to significantly increase the reaction rate and enhance the activity of the catalyst while reducing the resultant polymer molecular weight (Herfert et al., 1993, Yano et al., 1999). This phenomenon has been attributed to an increase in active sites, and / or an increase of the rate constant of the ethylene insertion. Cruz et al., using semi-empirical modeling, report that the comonomer enhancement affect is due to an increase in the ethylene insertion rate following a comonomer insertion (Cruz et al., 1998). The activation energy of ethylene insertion following hexene insertion was determined to be 6.0 kcal/mol while the insertion activation energy of an ethylene homopolymerization was calculated as 9.4 kcal/mol. Kravchenko and Waymouth observed a similar phenomenon with the addition of small amounts of ethylene to a propylene polymerization (Kravchenko and Waymouth, 1998). The increase in reaction rate was too significant to be explained by faster ethylene insertion. Instead they suggest that the added ethylene activates dormant active sites. Other researchers offer different explanations. Munoz-Escalona et al., using semi-empirical modeling, concluded that the presence of a second ethylene monomer in the back-side position of a front-side ethylene insertion significantly reduced the insertion energy (Munoz-Escalona et al., 2000).

Siloxy-substituted *ansa*-metallocenes have an oxygen bonded directly to the 1- or 2- position of an η^5 -indenyl moiety. These novel metallocenes were shown to have high activities with significantly reduced concentrations of MAO (Harkki et al., 1999). Furthermore, siloxy-substitution of the 1 position yielded greater comonomer incorporation. Kokko et al. demonstrated that siloxy-substituted *ansa*-metallocenes produced PE with significant levels of short and long chain branching (Kokko et al., 2000). This was attributed to the excellent incorporation of bulky α -olefins, including PE macromonomer.

More recent innovations in metallocene catalyst technology include silylene-bridges. These catalysts offer significantly higher molecular weights and activities while still providing excellent stereoregularity. Schneider et al. have conducted extensive research to determine the influences of indenyl ligand substitution patterns on the catalyst activity and on the resultant polymer characteristics of ethylene and propylene (Schneider et al., 1997a, Schneider and Mulhaupt, 1997). It was determined that 2-methyl substitution yielded higher molecular weight polymers but reduced the catalyst activity. More significantly, they report that benzannelation significantly increased the ability of the catalyst to incorporate large α -olefin molecules. Suhm et al. reported the temperature dependence of copolymerizations using the silylene-bridged metallocene *rac*-Me₂Si(2-MeBenz[e]Ind)₂ZrCl₂ (MBI-Cl₂) (Suhm et al., 1997). This catalyst exhibited a high incorporation of 1-octene, particularly at low temperatures. Beck et al. explored MBI-Cl₂ and MBI-Me₂ using several cationic activators (Beck et al., 1998). They report the

successful use of MBI-Me₂ activated with *N,N*-dimethylanilinium tetra(pentafluorophenyl)borate or trityl tetra(pentafluorophenyl) borate without the use MAO and without the loss of significant activity. Polymer properties were unaffected by the cationic activator. Van Reenen et al. demonstrated the ability of MBI-Cl₂ to copolymerize bulky α -olefins (Van Reenen et al., 2000). Propylene was copolymerized with 1-octadecene, 1-tetradecene and 1-decene. Wester et al., working with Me₂Si(Ind)₂ZrCl₂ and Me₂Si(2-Me-Ind)₂ZrCl₂, report that at polymerization temperatures greater than 70 °C, PP isotacticity sharply decreases (Wester et al., 1998). Yano et al. investigated the affect of metal type on the polymerization of propylene using silylene-bridged metallocenes activated with MAO (Yano et al., 1999). They report that titanium based catalysts yielded the lowest activity and produced PP with the lowest tacticity. Hafnium based catalysts had higher activities but were significantly outperformed by zirconium based silylene-bridged metallocenes.

Polyethylene produced with metallocene catalysts have a significant amount of short chain branching composed primarily of methyl branches. Several researchers have proposed that this branching occurs in a three-step reaction (Kokko et al., 2002, Wang et al., 1998): 1) partial transfer of the β -hydrogen to the active site, 2) relative rotation of the coordinated olefin, 3) reinsertion of the olefin into the Zr-H bond.

Metallocene catalysts can be produced which offer excellent control of the tacticity of the polymer. Syndiotactic PP was synthesized using isopropyl(cyclopentadienyl-1-fluorenyl) hafnium dichloride / MAO and the zirconium

analogue (Ewen et al., 1988). Uozumi and Soga report the synthesis of statistically random, isotactic and syndiotactic poly(propylene-co-hexene) (Uozumi and Soga, 1992) using various metallocene catalysts. It was observed that the incorporation of higher α -olefins was favoured by the syndiotactic catalyst, $i\text{-Pr}(\text{Cp})(\text{Flu})\text{ZrCl}_2$ over the isotactic catalyst, $\text{Et}[\text{IndH}_4]_2\text{ZrCl}_2$.

Elastomeric PP with low levels of isotactic pentads (<22 percent) with high molecular weight was synthesized using unbridged “oscillating” metallocenes (Mansel et al., 1999). The resulting polymers showed several unique thermal and mechanical properties. Rieger et al. report the synthesis of ultra high molecular weight polypropylene elastomers with asymmetric hafnocene / borate complexes (Rieger et al., 2002). The resultant polymers had molecular weights in the range of 700 000 to 5 million g/mol with isotacticities ranging from 17 to 25 percent.

A great deal of research has been conducted in order to prepare supported metallocene catalysts. These catalysts would be ideally suited to both slurry and gas phase polymerizations. Supported catalysts offer far superior control of polymer morphology and reduce reactor fouling. Metallocenes have been supported on both organic and inorganic supports (Ribeiro et al., 1997), including silica, alumina, magnesium compounds, and crosslinked polymers. The method of supporting metallocene catalysts has a significant impact on the polymerization properties and careful study is required to determine the optimal support conditions (Soares and Hamielec, 1995). Kaminaka and Soga supported $\text{Et}(\text{IndH}_4)_2\text{ZrCl}_2$ on Al_2O_3 , MgCl_2 and

SiO₂ (Kiminaka and Soga, 1991). Polypropylene synthesized using Et(IndH₄)₂ZrCl₂/Al₂O₃ showed the best properties, with enhanced stereoregularity and low polydispersity. Santos et al., supported zirconocene on SiO₂ (Santos et al., 1999). They report a decrease in the required concentration of Al / Zr and also replaced some MAO with TEA. Meng et al., in an attempt to reduce the amount of inorganic residues in polymers, supported Cp₂ZrCl₂ to crosslinked poly(styrene-*co*-4-vinylpyridine) (Meng et al., 1999). They reported little decrease in activity with a slower deactivation.

In an effort to produce reactor blends of Ziegler-Natta and metallocene-derived propylene homopolymers, Lisovskii et al. successfully utilized metallocene / Ziegler-Natta mixed catalyst systems (Lisovskii et al., 1998). These polymers showed intimate blending and displayed several advantageous properties. However, interactions between MMAO and the Ziegler-Natta catalyst significantly reduced the tacticity of the PP. Eskelinen and Seppala attempted to increase the molecular weight distribution of metallocene polymers by operating at two different temperatures (Eskelinen and Seppala, 1996). This solution, however, has little practical application.

Chien reported a novel solution to the necessity of high MAO concentrations (Chien and Xu, 1993). Metallocenium species, formed from stable metallocene precursors by reaction with triphenyl carbenium tetrakis(pentafluorophenyl) borate, require only TEA which functions as an impurity scavenger. Metalloceniums display high activity and can be used to polymerize ethylene and α -olefins.

Leino prepared several novel metallocene catalysts for ethylene and α -olefin polymerizations including *rac*-[ethylenebis(2-(*tert*-butyldimethylsiloxy)-4,5,6,7-tetrahydro-1-indenyl)]zirconium dichloride and *rac*-[ethylenebis(2-(*tert*-butyldimethylsiloxy)indenyl)]hafnium dichloride (Leino et al., 1997). These stereospecific catalysts, combined with MAO and trityl tetrakis(pentafluorophenyl) borate, were highly active with very low concentrations of MAO ([Al]/[Zr] between 100 to 200) and showed good comonomer responses.

A new method of producing low density PE using only ethylene feed was proposed by Quijada (Quijada et al., 2001). He reported branching levels of up to 2.9 branches per 100 ethylene units using an iron / metallocene catalyst tandem. An iron catalyst, $\{[(2\text{-ArN}=\text{C}(\text{Me}))_2\text{C}_5\text{H}_3\text{N}]\text{FeCl}_2\}$ (Ar = 2-C₆H₄(Et)), was employed to produce low molecular weight oligomers in-situ while a metallocene catalyst, Me₂SiInd₂ZrCl₂ or EtInd₂ZrCl₂, was used to copolymerize ethylene and the formed oligomer.

Ethylene and ethylene / α -olefin oligomers were produced using zirconocene / MAO catalysts (Micholotti et al., 1996). The liquid oligomers had low molecular weights (C₆-C₃₀) and vinylidene end groups.

End group analysis of polypropylene synthesized with *ansa*-zirconocenes showed four distinct terminal unsaturations (Carvill et al., 1998). Catalyst type and reaction condition had a strong influence on the unsaturation type and concentration. Vinylidene,

2-butenyl, allyl, and 4-butenyl terminal groups were identified using ^{13}C NMR and ^1H NMR.

Kim has recently proposed a method of generating metallocene catalysts capable of producing iPP without the presence of MAO (Kim and Zhou, 1999). An ansa-zirconocene diamide complex, $\text{rac-Me}_2\text{Si}(1\text{-C}_5\text{H}_2\text{-2-Me-4-}^t\text{Bu})_2\text{Zr}(\text{NME}_2)_2$ is combined with AlR_3 (R = Me, Et, *i*-Bu) and $[\text{CPh}_3]^+[\text{B}(\text{C}_6\text{F}_5)_4]^-$ in situ in toluene. The resulting catalyst is highly active and produces PP with an isotacticity greater than 90 percent.

A novel method of producing iPP with grafted polystyrene has been suggested (Henschke et al., 1997). Styrene macromonomer was first synthesized using a living polymerization technique with *sec*-butyllithium / allyl bromide. The macromonomer was subsequently copolymerized with propylene using the metallocene catalyst $[\text{Me}_2\text{Si}(2\text{-Me-Benzind})_2]\text{ZrCl}_2$ / MAO. Graft densities of up to 3.6 branches per main chain were achieved.

A wide array of innovative copolymers has been synthesised using metallocene catalysts. A constrained geometry catalyst has been used to produce poly(ethylene-co-*p*-methylstyrene) copolymers (Chung and Lu, 1997). The open configuration of the catalyst allowed high incorporation of *p*-methylstyrene which was subsequently functionalized. Several oxygen-functionalized, long-chain olefins were also copolymerized with ethylene using *rac*-ethylene-bis(1-indenyl) zirconium dichloride / MAO (Hakala, et al., 2000). 10-undecenyl methyl ether was incorporated into the

polymer with the methyl ether group remaining untouched. This suggests the formation of aluminum alkoxides via reaction with MAO is not a prerequisite for comonomer insertion.

The “half-sandwich” metallocenes, which have only one cyclopentadienyl ring, have seen application in ethylene / styrene copolymerizations. Sernetz et al. investigated the influence of various substituents on the Cp ring on the catalyst activity and styrene incorporation (Sernetz et al., 1997a). Sukhova et al. report a high activity catalyst, $\text{Me}_2\text{SiCp}^*\text{N}^t\text{BuTi}(\text{CH}_3)_2 / (\text{CPh}_3)(\text{B}(\text{C}_6\text{F}_5)_4)$, which was used to incorporate up to 20 mol percent styrene (Sukhova et al., 1999). The resultant high molecular weight copolymers had low crystallinities with melting points around 110 °C. Similarly, Sernetz et al. reported the terpolymerization of ethylene, 1-octene, and styrene using $\text{Me}_2\text{Si}(\text{Me}_4\text{Cp})(N-t\text{-butyl})\text{TiCl}_2$ (Sernetz and Mulhaupt, 1997b). There was a relatively high incorporation of styrene, but a large decrease in catalyst activity compared to ethylene 1-octene copolymerizations. Other researchers, working with $\text{CpTi}(\text{OPh})_3$ synthesized random poly(ethylene-co-styrene) with up to 54.5 mol percent styrene (Xu and Lin, 1997).

Metallocenes, coupled with a bulky counter ion, have been used as living cationic catalysts for the ring opening polymerization of 1,5,6,11-tetraoxaspiro[5,5]undecane to give polycarbonate (Ariffin et al., 1998). This polymerization, conducted under mild conditions, yielded a low dispersity (PDI = 1.2), low molecular weight polymer. Barsan et al. similarly demonstrated the carbocationic polymerization of isobutylene and isoprene using the metallocene derivative $\text{Cp}^*\text{TiMe}_2(\mu\text{-Me})\text{B}(\text{C}_6\text{F}_5)_3$ (Barsan et al.,

1998). The resultant polymer, synthesised at the relatively mild condition of $-40\text{ }^{\circ}\text{C}$ in toluene, was similar to commercial samples produced using traditional Lewis acids.

2.3 Long Chain Branching in Polyolefins

The influence of long chain branching (LCB) on the thermorheological properties of polymers can be remarkable (Small, 1975, Santamaria, 1985). A long chain branch is defined as a branch whose length is comparable to, or longer, than the critical entanglement length (M_C). This length is polymer specific and for PE it is approximately 3800 g/mol . When a branch is shorter than M_C its impact on the rheological properties is minimal, however, longer branches significantly alter the rheological properties and therefore the processing characteristics of polymers.

LDPE, produced in a high temperature, high pressure, free radical process, has a broad molecular weight distribution and a combination of short and long chain branches. HDPE produced using conventional Z-N catalysts, has a broad molecular weight distribution but is primarily linear. The broad molecular weight dispersities of these polymers reduce mechanical properties such as clarity, tear strength and stiffness, but lead to a significant shear thinning phenomenon. These polymers have high viscosities at low shear rates but at the elevated shear rates of processing conditions the viscosities are markedly lower.

Polymers produced using metallocene catalysts have comparatively narrow molecular weight distributions. This narrow distribution leads to superior mechanical properties, but also contributes to a significant lack of shear thinning. The processing pressures and subsequent capital and energy expenditures required to process metallocene polymers are higher than for conventional Z-N polymers. However, long chain branched, narrowly dispersed polymers have been shown to exhibit significantly higher shear thinning than their linear analogues. Unfortunately, the precise effects of LCB are not well understood due to the difficulty of producing well-defined samples with a broad range of molecular attributes.

Metallocenes, unlike traditional Ziegler-Natta catalysts, have been shown to produce polyethylenes with long chain branching. Malmberg et al. reported the presence of low levels of long chain branching in PE synthesized using $\text{Et}[\text{Ind}]_2\text{ZrCl}_2 / \text{MAO}$ and $\text{Et}[\text{IndH}_4]_2\text{ZrCl}_2 / \text{MAO}$ in a slurry polymerization (Malmberg et al., 1998). This phenomenon is attributed to an in situ incorporation of vinyl-terminated polyethylene macromonomers. Figure 2.7 shows the mechanism of in-situ long chain branch formation.

In order to maximize the amount of long chain branching an innovative metallocene catalyst, called the Dow Chemical Constrained Geometry Catalyst (CGC) was developed (Brant et al., 1995a, Brant et al., 1995b, Lai et al., 1993). This catalyst has a relatively open configuration which allows the incorporation of higher α -olefins and macromonomers with greater ease than traditional metallocenes (Wang et al., 1999,

Wang et al., 2000a). The presence of long chain branching in poly(ethylene-co-propylene) was also reported, with long chain branch densities of up to 0.96 branches per 10 000 carbons (Wang and Zhu, 2000b).

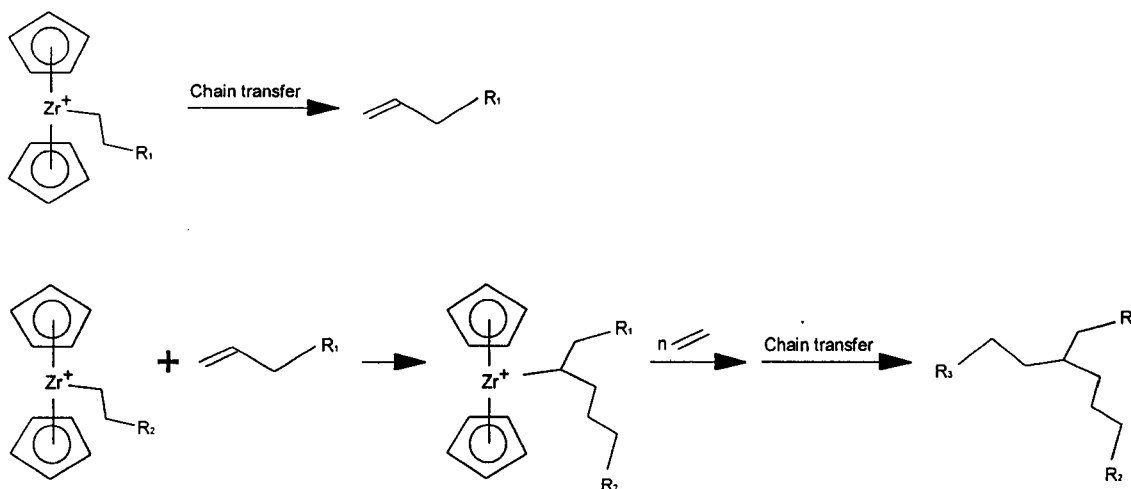


Figure 2.7 Mechanism of in-situ long chain branch formation.

Several researchers have produced branched polyolefins using a two-step polymerization. Soga et al. first produced oligoethylene with vinyl end groups using Cp_2ZrCl_2 (Soga et al., 1996). Ethylene was then copolymerized with the oligoethylene with $[(\text{C}_5\text{Me}_4)\text{SiMe}_2\text{N}(\text{t-Bu})]\text{TiCl}_2 / \text{MAO}$. Shiono et al. later synthesized atactic PP macromonomer with terminal unsaturation using bis(pentamethylcyclopentadienyl)zirconium dichloride (Shiono et al., 1997). The macromonomer was then copolymerized with ethylene using CGC-Ti to form polyethylene with long chain atactic PP branches. In a later experiment, Shiono et al copolymerized the PP macromonomer with propylene using the silylene-bridged metallocene *rac*- $\text{Me}_2\text{Si}(\text{2-MeBenz}[\text{e}]\text{Ind})_2\text{ZrCl}_2$ (Shiono et al., 1999). Using a similar

method, Weng et al. later produced both long chain branched PE and PP (Weng et al., 2001).

2.4 Rheological Characterization

Rheology is the study of the flow of materials. The polymer architecture has a strong influence on the rheological properties of polymers. The polymer type, molecular weight, molecular weight distribution, branch length, and branch density all interact to determine the final polymer properties. The precise effects of each influence are not well understood due to the difficulty of producing model polymers with controlled architecture.

A powerful method of determining several important rheological properties of a polymer, using parallel plate rheometry, is to subject the polymer to a periodic (cosine function) shear rate function called small-amplitude oscillatory shear (SAOS). The frequency of the cosine function is termed ω . When a sample is strained in this manner at low strain amplitudes the shear stress that results is a sine wave of the same frequency as the input strain wave. The shear stress is generally out of phase with the input strain. The quantity δ gives the phase difference between the strain wave and the stress response.

There are several important material properties that can be observed using small-amplitude oscillatory shear rheology. The storage modulus, G' , as shown in Equation

2.1, is defined as the amplitude of the portion of the stress wave that is in phase with the strain wave divided by the amplitude of the strain wave.

$$G'(\omega) = \frac{\tau_0}{\gamma_0} \cos \delta \quad (2.1)$$

where τ_0 is the shear stress and γ_0 is the strain amplitude. The loss modulus, G'' , as shown in Equation 2.2, is defined as the amplitude of the portion of the stress wave that is out of phase with the strain wave, divided by the amplitude of the strain wave.

$$G''(\omega) = \frac{\tau_0}{\gamma_0} \sin \delta \quad (2.2)$$

Other important material properties are the complex modulus magnitude ($|G^*|$), the loss tangent ($\tan \delta$), dynamic viscosity (η'), out of phase component of viscosity (η''), and the complex viscosity magnitude ($|\eta^*|$). These relationships are given in Equations 2.3 to 2.7, respectively.

$$|G^*| = \sqrt{G'^2 + G''^2} \quad (2.3)$$

$$\tan \delta = \frac{G''}{G'} \quad (2.4)$$

$$\eta' = \frac{G''}{\omega} \quad (2.5)$$

$$\eta'' = \frac{G'}{\omega} \quad (2.6)$$

$$|\eta^*| = \sqrt{\eta'^2 + \eta''^2} \quad (2.7)$$

The importance of SAOS data is further emphasized by the Cox-Merz rule, given in Equation 2.8. This rule states that for many materials the steady shear viscosity versus

shear rate curve (η vs. $\dot{\gamma}$) has the same shape and values as the complex viscosity versus frequency ($|\eta^*|$ vs. ω) if they are compared at $\dot{\gamma} \text{ (s}^{-1}\text{)} = \omega \text{ (rad/s)}$ (Morrison, 2001).

$$\eta(\dot{\gamma}) = |\eta^*(\omega)|_{\dot{\gamma}=\omega} \quad (2.8)$$

It has been determined that the zero shear viscosity (η_0) is a function of the weight average molecular weight (M_w) of the polymer. When the polymer molecular weight is below a critical entanglement length, M_C , the viscosity is directly proportional to the molecular weight. When the molecular weight is greater than M_C the entanglements become effective and the η_0 is related to the molecular weight by Equation 2.9.

$$\eta_0 = K \cdot M_w^{3.4} \quad (2.9)$$

where K is a polymer specific constant. This behaviour is represented schematically in Figure 2.8.

Long chain branching has been shown to have a dramatic influence on the rheological properties and hence the processing conditions of polyolefins (Dealy and Wissbrun, 1990). Long chain branching affects the melt viscosity, elasticity, shear thinning, extensional viscosity, melt fracture, and the die swell of polyolefins (Macosko, 1994). The effect of long chain branching on the thermorheological properties is due to two competing influences. Long chain branching decreases the effective radius of

gyration of polymers with the same molecular weight, but also increases the amount of entanglements. Depending on the dominant component, increases or decreases in the low shear melt viscosity can be realised (Graessley, 1977).

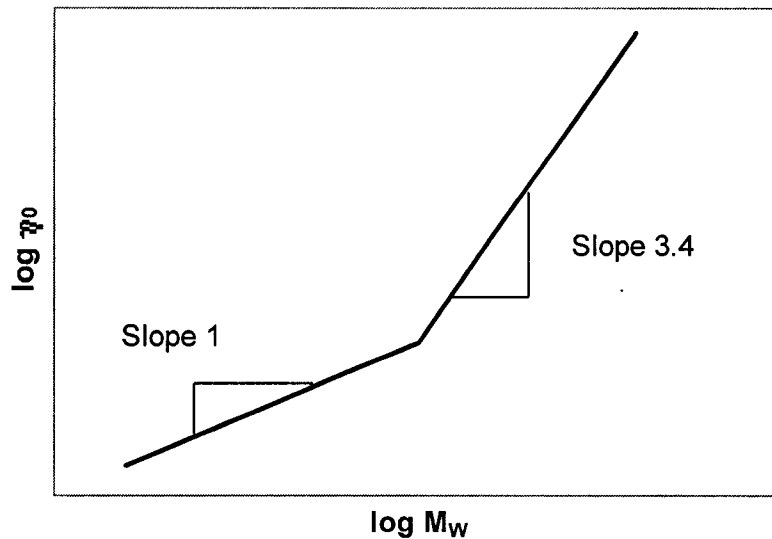


Figure 2.8 Influence of molecular weight on zero shear viscosity

There are many branch variables which can have a significant influence on the rheological properties and correlations are only valid if the branching architecture is fixed (Bersted, 1985). The branch density, branch length, and branch distribution have all been shown to have important roles in determining the melt behaviour of polyolefins (Bersted et al., 1981). Unfortunately, the precise effects of LCB are not well understood due to the difficulty of producing well-defined samples with a broad range of molecular attributes.

It has been shown that the density and length of long chain branching has a significant influence on the flow activation energy of PE (Carella et al., 1986, Mavridis

and Shroff, 1992). The activation energy, given in Equation 2.10, is often represented as an Arrhenius relationship.

$$\eta = A \exp\left(\frac{E_a}{RT}\right) \quad (2.10)$$

where η is the shear viscosity, A is the frequency factor, E_a is the flow activation energy, R is the gas constant, and T is the temperature. Increases in branch length or branch density increase the temperature sensitivity of the polymer melt by increasing the mobility of the branched chains to a larger extent than the mobility of the linear chains. The flow activation energy has been shown to be a sensitive indicator of the presence of branching (Wood-Adams and Costeux, 2001).

2.5 Dynamic Mechanical Analysis

Dynamic mechanical analysis (DMA) has been used extensively to characterize solid polymers and viscoelastic liquids. DMA involves applying an oscillating mechanical strain and resolving the stress into real and imaginary components. This procedure can be used to detect changes in the state of molecular motion with changing temperature. It is a powerful technique for studying the effect of molecular structure and phase morphology on the physical properties of a given polymer.

Dynamic mechanical analysis is often used in concert with differential scanning calorimetry (DSC). DSC offers quantitative measurements of heat changes during first order thermodynamic changes (melting and crystallization) but generally fails to detect

second order transitions (glass transition) in polyolefins. DMA however, detects molecular relaxations such as glass transitions with approximately 1000 times higher sensitivity than DSC (Wetton, 1984).

In DMA the sample polymer is rigidly clamped in place between two balanced support arms which are free to oscillate. The system is displaced and set into oscillation by a driver at a preselected amplitude. As the system oscillates the sample is subjected to deformation. The frequency of the oscillation is directly related to the modulus of the sample, while the energy needed to maintain constant amplitude oscillation is a measure of damping within the sample. Figure 2.9 shows a schematic of a sample prepared for DMA (Gill, et al., 1984).

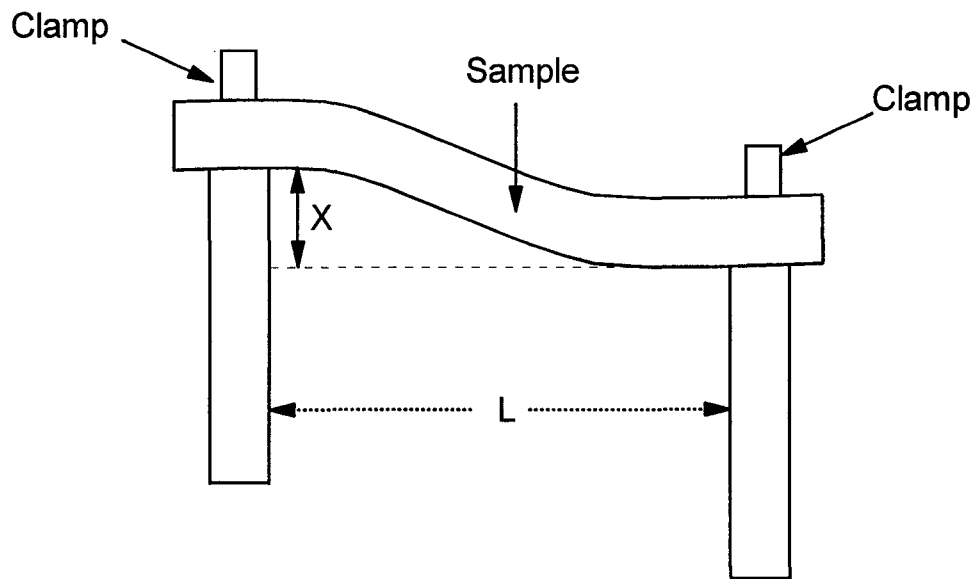


Figure 2.9 Schematic representation of DMA.

When a sinusoidal stress is applied to a perfectly elastic solid the deformation, and hence the strain, occurs exactly in-phase with the stress. However, when some internal molecular motion occurs at the same frequency range as the impressed stress, the material responds in a viscoelastic manner and the strain lags behind the stress. Dynamic mechanical results are given in terms of complex moduli, as shown in Equation 2.11.

$$E^* = E' + iE'' \quad (2.11)$$

where E^* is the complex Young's modulus, E' is the real part of the modulus, E'' is the imaginary part of the modulus, and $i = \sqrt{-1}$. The angle that reflects the time lag between the applied stress and strain is δ , and is defined by a ratio called the loss tangent, as shown in Equation 2.12.

$$\tan \delta = \frac{E''}{E'} \quad (2.12)$$

Tan δ is a damping term and is a measure of the ratio of energy dissipated as heat to the maximum energy stored in the material during one cycle of oscillation (Nielsen and Landel, 1994). Relaxation regimes in DMA appear as peaks in E'' and $\tan \delta$ and as a step transitions in E' . Typically, the relaxation points are studied using E'' or $\tan \delta$.

Chapter 3

Synthesis of Long Chain Branched Polyolefins with Metallocene Catalysts

3.1 Introduction

There has been considerable interest in the relationships between molecular architecture and the viscoelastic behavior of polyolefins in recent years (Vega et al., 1998, Harrell and Nakajima, 1984, Tsenoglou and Gotsis, 2001). It has been demonstrated that the influence of long chain branching (LCB) on the thermorheological properties of polymers can be remarkable (Small, 1975, Santamaria, 1985). The precise effects of LCB are not well understood due to the difficulty of producing well-defined samples with a broad range of molecular attributes. There are many molecular properties which influence the physical characteristics of polymers including: molecular weight (MW), molecular weight distribution (MWD), short chain branching (SCB), long chain branching (LCB), branch length, and branch distribution. These properties act in concert and separating individual influences has proven difficult. In an attempt to isolate the effect of branching from MW and MWD there has been considerable interest paid to both linear and star branched hydrogenated polybutadienes (HPB) synthesized via anionic polymerization (Carella et al., 1986, Milner et al., 1998, Milner and McLeish, 1998). This technique provides excellent control of the MW and MWD and has contributed fundamentally to the understanding of LCB. This technique, however, has only recently

been applied to the study of comb branched polymers (Lohse et al., 2001). Recent innovations in single-site type catalysts allow the production of model polymers with narrow molecular weight distributions (MWDs) and extremely narrow chemical composition distributions (CCDs) (Kaminsky et al., 1985, Chien and Wang, 1990). Dow Chemical's constrained geometry catalyst (CGC-Ti) has been used to synthesize LCB polyethylenes of various MWs and long chain branch densities (LCBD) (Lai et al., 1993, Yan et al., 1999). This catalyst, with its open configuration, produces long chain branching through the insertion of vinyl terminated PE formed in-situ through β -hydride elimination or chain transfer to monomer. A precise control of the branch length is not possible using this technique. Recent innovations have demonstrated the ability of several metallocene catalysts to incorporate previously produced macromonomers into growing polymer backbones, forming a comb structure (Soga et al., 1996, Shiono et al., 1997, Shiono et al., 1999, Weng, et al., 2001). Using this technique it is possible to produce polymers with controlled branch density, branch length, and with uniform backbones.

The objective of this chapter was to evaluate various methods for the preparation of long chain branched polyolefins. Section 3.2 outlines the synthesis of LCB PE using the metallocene catalyst system $\text{Cp}_2\text{ZrCl}_2 / \text{MMAO}$ in a semi-batch reactor system. This was the first reported systematic study of long chain branched PE using classical metallocene catalysts. Section 3.3 summarizes the synthesis of novel copolymers with polyethylene backbones and controlled levels of poly(ethylene-co-propylene) (EPR) long chain branching. Finally, Section 3.4 reports the synthesis of model polypropylene

copolymers with EPR branching. This work enabled, for the first time, the synthesis of comb-branched polyolefins with controlled branch lengths and branch densities, and with consistent copolymer molecular weights.

3.2 Long Chain Branching in Ethylene Slurry Polymerization

3.2.1 Experimental

Materials

All manipulations involving air and moisture sensitive compounds were carried out under dry nitrogen in a glove box. The catalyst Cp_2ZrCl_2 was purchased from Aldrich and modified methylaluminoxane (MMAO, 12 mol % of isobutylaluminoxane) was provided by Akzo as a 10 wt% solution in toluene. The catalyst and co-catalyst were used without further purification. Reagent grade toluene, provided by Caledon Laboratories, was refluxed over metallic sodium / benzophenone for 48 hours and was distilled under a nitrogen atmosphere prior to use. Ethylene (polymerization grade > 99.5%) was provided by Matheson Gas and further purified by passing through columns with CuO (Aldrich), Ascarite (Fisher Scientific) and molecular sieves (Grace-Davidson) to remove oxygen, carbon dioxide and moisture, respectively.

Polymerization procedure

Polymerization reactions were performed in our 1 liter semi-batch reactor. Figure 3.1 shows a flow sheet of the semi-batch system.

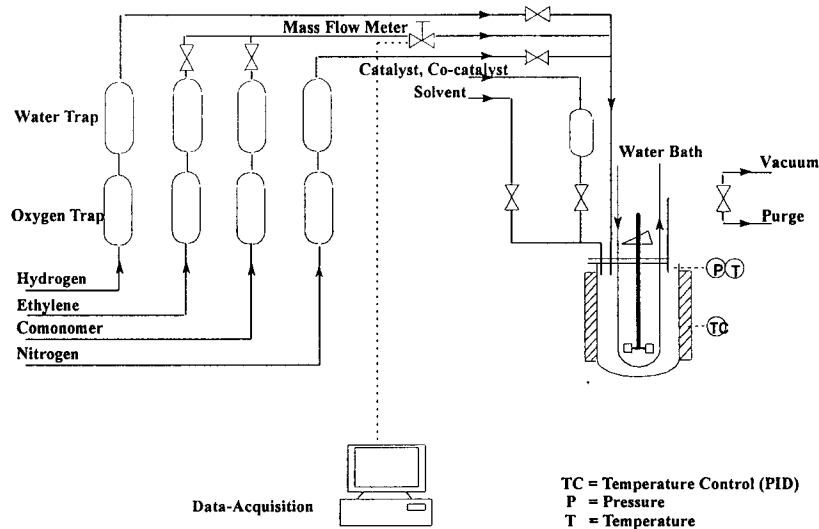


Figure 3.1 Schematic of the 1 liter high-pressure semi-batch reactor

All experiments were performed at 1200 rpm, with toluene as the diluent and with a catalyst concentration of $6.5 \mu\text{M}$. A measured amount of diluent was transferred into the nitrogen purged reactor with subsequent purging with nitrogen. The cocatalyst solution was injected by syringe into the reactor. After 5 minutes the catalyst solution was injected. The polymerization was initiated by the addition of ethylene to the reactor. This procedure was used for all reactions except for those otherwise noted. The reaction was terminated by depressurizing and purging the reactor with nitrogen. The formed polyethylene was washed with a 1% HCl in methanol solution to remove MMAO residue, filtered, and dried in a vacuum oven. The detailed polymerization conditions are summarized in Table 3.1.

Table 3.1 Experimental Conditions For Ethylene Homopolymerization Using Metallocene Systems

Run	Reaction Type	Temp. (°C)	Press. (psig)	[Cp ₂ ZrCl ₂] (μM)	[MMAO]/[Cp ₂ ZrCl ₂]	τ (min)
1	SB	60	10	6.5	1600	-
2	SB	70	10	6.5	1600	-
3	SB	80	10	6.5	1600	-
4	SB	70	2	6.5	1600	-
5	SB	70	5	6.5	1600	-
6	SB	70	20	6.5	1600	-
7	SB	70	10	6.5	800	-
8	SB	70	10	6.5	2400	-
9	Altered SB	70	10	6.5	1600	-
10	Altered SB	80	10	6.5	1600	-
11	Altered SB	70	5	6.5	1600	-
12	CSTR ^{a)}	140	1500	2	1000	5
13	CSTR ^{b)}	140	500	15	3	4

The polymerization conditions were: catalyst = Cp₂ZrCl₂, co-catalyst = MMAO, solvent = toluene, solvent volume = 700 ml. SB = Semi-Batch Reactor; τ = residence time for continuous reactor; CSTR = Continuous Stirred Tank Reactor.

a) Catalyst = Cp₂ZrCl₂, co-catalyst = MMAO, solvent = toluene, ethylene flow rate = 7.7 g/min.

b) Catalyst = The Dow Chemical's CGC-Ti, co-catalyst = tris(pentafluorophenyl) boron, 2nd co-catalyst = MMAO at 150 μ M, solvent = Isopar-E, ethylene flow rate = 6.0 g/min., and [hydrogen] = 8.01 × 10⁻⁴ M.

Polymer Characterization

Molecular weight (M_w) and MWD of the polymers were measured using a Waters-Millipore 150 C High Temperature GPC with a differential refractive index (DRI) detector. The polymer samples were dissolved in 1,2,4-trichlorobenzene (TCB) at a concentration of 0.1 wt% and measured at 140 °C with a flow rate of 1 mL/min. The GPC was equipped with three linear mixed Shodex AT806MS columns. The retention times were calibrated at 140 °C against known monodisperse TSK polystyrene (PS) standards from TOYO SODA Mfg. Co. The Mark-Houwink constants for the universal

calibration curve were $K = 2.32 \times 10^{-4}$ and $\alpha = 0.653$ for PS and $K = 2.32 \cdot 10^{-4}$ and $\alpha = 0.726$ for PE.

^{13}C NMR spectra were acquired on a Bruker AC 300 pulsed NMR spectrometer operated at 75.4 MHz with broad band decoupling. The samples were dissolved in deuterated o-dichlorobenzene (d-ODCB) and TCB, and were measured at 120 °C using 10 mm sample tubes. d-ODCB was used to provide an internal lock signal, and TCB was the internal reference. Spectra required more than 7000 scans to attain an acceptable signal-to-noise ratio. A repetition time of 10 s was utilized (Wang et al., 1998).

Figure 3.2 shows a spectrum of a polyethylene sample produced in this work (run 4). The chemical shifts assigned to different carbonyl groups followed the references (Randall, 1997, De Pooter et al., 1991). The long chain branching density (LCBD, the number of branch points per 10,000 carbons), short chain branching density (SCBD, the number of branching points per 10,000 carbons), unsaturated chain end density (UCED, the number of unsaturated chain ends per 10,000 carbons), and long chain branching frequency (LCBF, the number of long chain branch points per polymer molecule) were calculated using the following equations.

$$LCBD = \frac{IA_{\alpha}}{3IA_{Tot}} \times 10,000 \quad (3.1)$$

$$SCBD = \frac{IA_{\alpha M}}{2IA_{Tot}} \times 10,000 \quad (3.2)$$

$$UCED = \frac{IA_a}{IA_{Tot}} \times 10,000 \quad (3.3)$$

$$LCBF = \frac{2LCBD}{SCED + UCED - LCBD} \quad (3.4)$$

where the saturated chain end density $SCED = (IA_{1s} + IA_{2s}) / 2IA_{Tot} \times 10,000$; IA_{α} , $IA_{\alpha M}$, IA_{1s} , IA_{2s} , IA_a , and IA_{Tot} are the integral areas of α -CH₂, α M-CH₂, 1s, 2s, a-CH₂, and total intensity of carbons, respectively. In integrating the resonance peaks close to the peak δ^+ , the baseline effect by the “tree trunk” of peak δ^+ was subtracted from the signals.

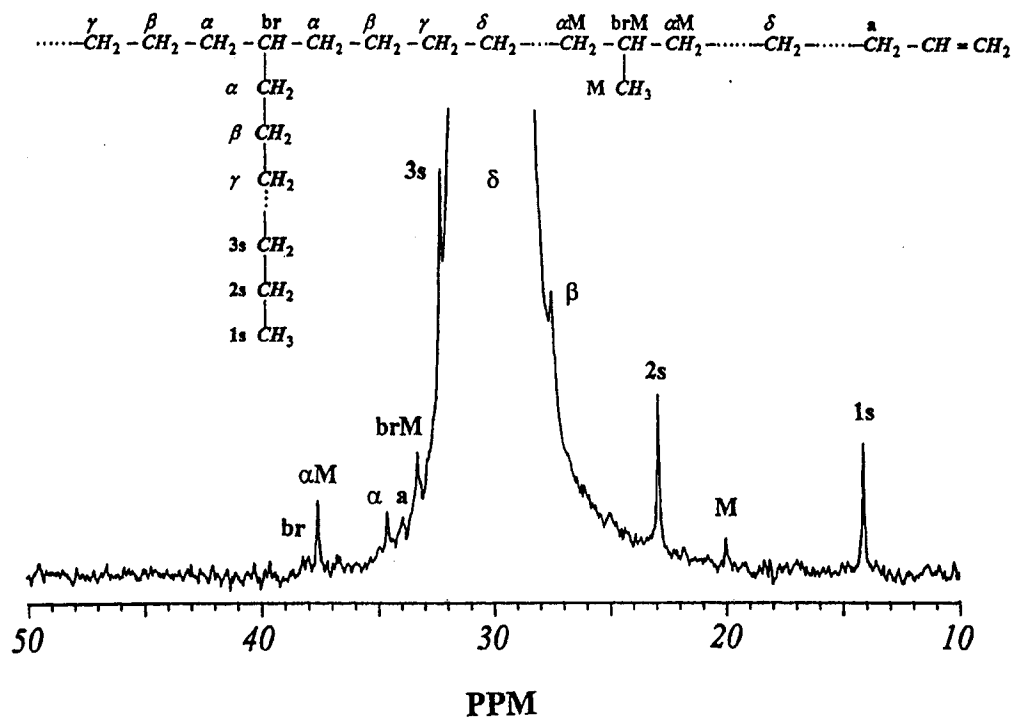


Figure 3.2 ¹³C NMR spectrum with chemical shifts in TCB and d-ODCB at 120 °C of Sample 4.

The polymerization conditions were: $[Cp_2ZrCl_2] = 6.5 \mu M$, $[MMAO] / [Cp_2ZrCl_2] = 1600$, $T = 70 \text{ }^\circ C$, $P = 2 \text{ psig}$

Melt flow indexes were determined with a Kayeness Melt Flow Indexer at 190 °C according to the ASTM D-1238 method. The test loads for I_2 and I_{10} were 2.16 and 10 kilograms, respectively. Polyethylene samples were prepared by mixing 0.6 wt. %

Irganox 1010 (an antioxidant) in acetone, adding PE, followed by subsequent drying in a vacuum oven. The polymer samples were typically white.

3.2.2 Results and Discussion

The formation of long chain branching is believed to be a two-step reaction. The first step is the formation of a polymer chain with a terminal vinyl end group through β -hydride elimination or chain transfer to monomer. This macromonomer is then incorporated into a growing polymer chain yielding a branch. If the molecular weight of the macromonomer is above the critical entanglement length the branch will behave as a long chain branch. This mechanism is shown schematically in Figure 3.3.

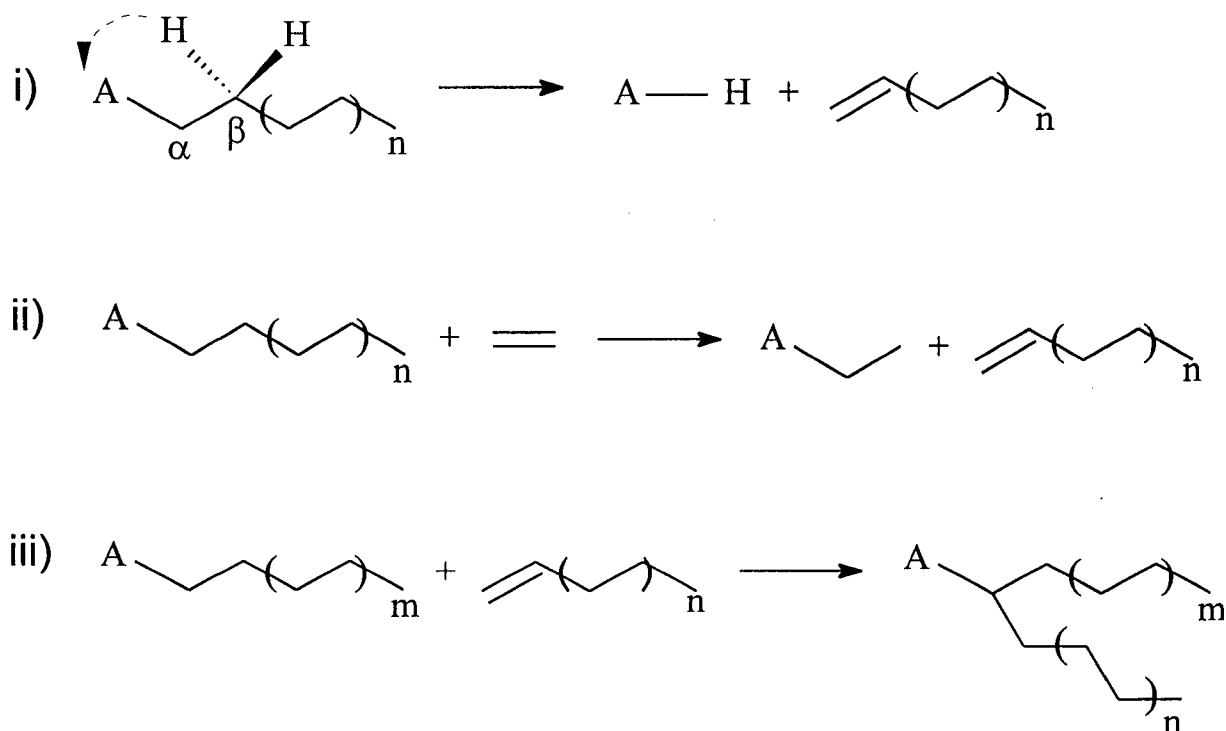


Figure 3.3 Mechanism of the formation of long chain branching

Long Chain Branching in Slurry Polymerization

Table 3.2 summarizes the high temperature GPC, ^{13}C NMR, and MFI characterization results. Also included in this table is a PE sample produced in a high temperature, high pressure continuous stirred-tank reactor (CSTR) with toluene as the diluent using the same catalyst system (Charpentier et al. 1997). The CSTR reaction temperature was higher than the melting point of PE, ensuring a homogeneous system with no polymer precipitation. Homogeneous polymerization at high temperature is believed to increase the diffusion of the polymer chains, hence making ethylene macromonomers more mobile and reactive. However, no LCB was observed in the polymer sample produced by the CSTR using Cp_2ZrCl_2 with only short chain branching present owing to chain isomerization (Wang et al. 1998, Johnson et al., 1995, Deng et al, 1997). In comparison, ^{13}C NMR spectra of PE samples produced in the slurry polymerization (Figure 3.2) clearly show the presence of LCB structures. This indicates that the slurry polymerization enhances LCB formation using Cp_2ZrCl_2 .

During the slurry polymerization, the catalyst and co-catalyst interact to form cationic active sites which polymerize ethylene monomer to form polymer chains. The polymer chains, due to poor solubility at low reaction temperature (Orwoll, 1989) are believed to precipitate out of solution upon formation and encapsulate the active centres. The precipitated polymers, swollen with solvent, form a polymer rich phase. Ethylene diffuses into this polymer-rich phase and propagates. While the ethylene propagation

reaction proceeds, β -hydride elimination and/or transfer to monomer occur to form ethylene macromonomers (see Figure 3.1). These macromonomers are “frozen” in the polymer-rich phase and trapped in close proximity to the active centres, allowing further reactions at the same active site to form LCBs. Moreover, the formation of long chain branches depends on the competing reactions between monomer propagation and macromonomer insertion. The high ratio of macromonomer to monomer within the polymer rich phase facilitates the LCB formation.

Table 3.2 Summary of GPC, ^{13}C NMR, and MFI Data

Run	M_w ($\times 10^{-5}$)	M_w/M_N	LCBD ($\times 10^4$)	SCBD ($\times 10^4$)	UCED ($\times 10^4$)	LCBF	I_2	I_{10}/I_2
1	2.80	2.44	0.25	0.63	0.76	0.16	---	---
2	1.54	2.54	0.33	1.59	0.74	0.12	0.04	21.5
3	1.08	2.34	0.10	1.03	0.79	0.03	0.70	8.8
4	0.95	2.44	0.73	1.66	1.23	0.22	0.22	17.6
5	1.22	2.63	0.65	1.16	1.06	0.21	0.17	15.5
2	1.54	2.54	0.33	1.59	0.74	0.12	0.04	21.5
6	1.97	2.66	0.30	0.93	0.71	0.15	0.03	21.3
7	1.60	2.40	0.35	0.81	0.89	0.17	0.07	14.8
2	1.54	2.54	0.33	1.59	0.74	0.12	0.04	21.5
8	1.52	2.81	0.21	2.21	0.43	0.07	0.18	13.0
9	0.63	2.15	1.00	1.77	0.89	0.20	2.33	12.9
10	0.57	2.05	0.86	1.94	0.89	0.17	4.20	12.4
11	0.73	2.69	1.01	1.50	0.92	0.21	1.59	11.5
12	0.33	2.55	0	3.10	4.67	0	29.0	5.64
13	1.04	2.04	0.35	0	0.65	0.11	0.21	17.8

LCB polyethylenes were also synthesized by chromium (Shaffer and Ray, 1997), vanadium (Reinking et al., 1998), and palladium-based catalysts (Guan et al., 1999) as well as some metallocenes such as $\text{Et}[\text{Ind}]_2\text{ZrCl}_2$ and $\text{Et}[\text{IndH}_4]_2\text{ZrCl}_2$ in slurry and gas-phase polymerizations (Malmberg et al., 1998, Harrison et al., 1998). Three mechanisms were proposed to explain the long chain branching in ethylene/catalyst systems: 1) copolymerization of ethylene with ethylene macromonomer generated in-situ via β -hydride elimination and/or chain transfer to ethylene (Wang et al., 1998); 2) chain walking followed by ethylene insertion (Guan et al., 1999); 3) intermolecular C-H bond activation through σ -bond metathesis reaction (Reinking et al., 1998). Which of these mechanisms is actually involved in branching depends on the catalyst type and the experimental conditions. Since there was no long chain branching observed in our solution ethylene polymerization experiments using the same catalyst system (Charpentier et al., 1997), we believe that the branching mechanism involved in this work is via the ethylene macromonomer copolymerization.

The LCB polyethylenes showed increased shear thinning properties. The melt flow index ratios I_{10}/I_2 were in the range of 8.8 - 21.5 as shown in Table 2. It should be pointed out that the shear thinning behaviour of a polymer is determined by many chain parameters including molecular weight, molecular weight distribution, long chain branching density, and chain length of branches. Although an increase in the I_{10}/I_2 with LCBD can be clearly seen in Table 2 (data with the same reactor type), a comprehensive relationship between the chain structure and polymer shear thinning is yet to be developed.

^{13}C NMR determination also indicates the existence of methyl side groups in the PE samples. It is believed that this is due to a same-site 2-1 insertion of ethylene macromonomer immediately after β -hydride elimination. This phenomenon was also observed in the continuous solution polymerization of ethylene at temperatures over 180 °C using the CGC system (Wang et al., 1998).

Compare the sample of semi-batch run 4 (LCBD 0.73, MW 0.95×10^5 and MWD 2.44) to the CSTR CGC-PE (LCBD 0.35, MW 1.04×10^5 , and MWD 2.04). The melt flow indexes (I_2 and I_{10}/I_2) for both samples are very similar (run 4 sample: $I_2 = 0.22$ and $I_{10}/I_2 = 17.6$; CGC-PE: $I_2 = 0.21$ and $I_{10}/I_2 = 17.8$). However, these polymers have a large difference in LCBD. This may indicate that the branches generated in the CGC solution polymerization have longer chain lengths and induce higher shear sensitivities than those in the Cp_2ZrCl_2 slurry process.

Effect of Polymerization Temperature

The temperatures studied were 60, 70, and 80 °C (runs 1, 2, and 3). Figure 3.4 shows the effect of temperature on the LCB density and frequency. Increasing the temperature from 60 to 80 °C significantly reduced the polymer molecular weight and LCBF. However, temperature had a minor effect on the level of residual unsaturated chain ends. The effect of temperature on LCB can be explained by the solubility of the polymer chains (Orwoll, 1989). At higher temperatures, more polymer chains are dissolved in solvent and there is consequently a smaller polymer rich phase. Thus elevating the temperature from 70 to 80 °C lowered LCBDs from 0.33 to 0.10. On the

other hand, temperature also affects the monomer solubility in solvent (Gerrard, 1976), and thus influences the concentration ratio of ethylene monomer to macromonomer in the polymer rich phase. Increasing the temperature not only decreases the polymer rich phase, but also decreases the ethylene concentration in solvent and in turn the ethylene concentration in the polymer rich phase. These competing factors raised the LCBD from 0.25 to 0.33 for the temperatures from 60 to 70 °C. The long chain branching frequency (LCBF) is the combination of the polymer molecular weight and LCBD. At lower temperatures the molecular weights were much higher and consequently the LCBF increased. Therefore the LCBF increased from 0.03 to 0.16 when the temperature decreased from 80 to 60 °C.

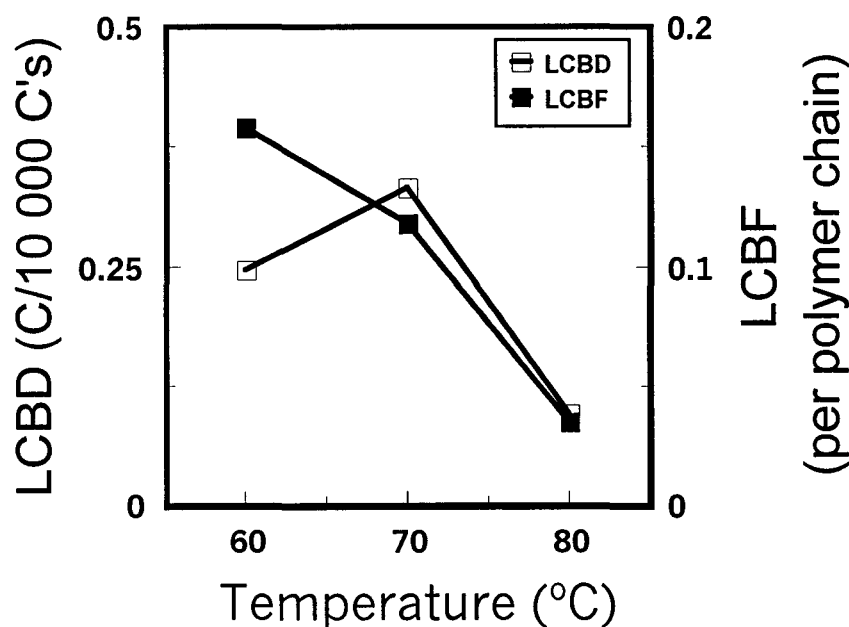


Figure 3.4 The effect of temperature on LCB density and frequency.
 The polymerization conditions were: $[Cp_2ZrCl_2]=6.5 \mu M$, $[MMAO]/[Cp_2ZrCl_2]=1600$, $P=10 \text{ psi}_g$.

Effect of Polymerization Pressure

Four polymerization pressures, 2 (run 4), 5 (run 5), 10 (run 2) and 20 psig (run 6), were investigated in this work. The effect of pressure on the LCBD and LCBF is shown in Figure 3.5.

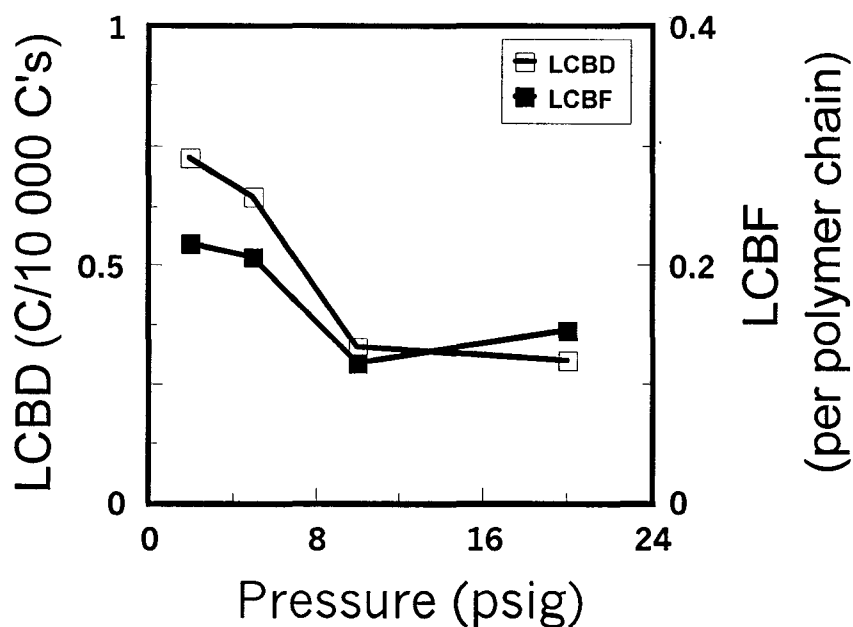


Figure 3.5 The effect of pressure on LCB density and frequency

The polymerization conditions were: $[\text{Cp}_2\text{ZrCl}_2] = 6.5 \mu\text{M}$, $[\text{MMAO}] / [\text{Cp}_2\text{ZrCl}_2] = 1600$, $T = 70 \text{ }^\circ\text{C}$.

The pressure of the polymerization system determines the ethylene concentrations in the solvent and polymer rich phases. The formation of ethylene macromonomers depends on the competition between monomer insertion and chain transfer reactions (β -hydride elimination and chain transfer to monomer). Lowering monomer concentration in the polymer rich phase leads to higher unsaturation of polymer chains and thus higher UCED and SCBD. The effect of pressure on the monomer concentrations also influences

molecular weight, LCBD and LCBF. Increasing the pressure from 2 to 20 psig increased MW from 0.95×10^5 to 1.97×10^5 , while decreasing LCBD from 0.73 to 0.30.

Effect of Polymerization Procedure

The order in which the reactor was charged with reactants had a strong influence on the molecular weight and branching formation of the PE. In the altered procedure the system was saturated with ethylene immediately after the injection of MMAO. The reaction was then initiated by the injection of catalyst five minutes later. Runs 9, 10, and 11 used this altered procedure and correspond to the experimental conditions in runs 2, 3, and 5 respectively, as shown in Table 3.1. In all cases, the altered procedure produced polymers with higher LCBD, SCBD, UCED, and with lower molecular weights compared with their analogous runs. A ^{13}C NMR spectrum of Run 9, given in Figure 3.6, clearly shows the increase of branching intensities.

Because the polymerization system was initially saturated by ethylene, there existed a high monomer concentration at the start of the reaction in the altered procedure. When the catalyst was injected into the system it immediately reacted with MMAO to form active sites. Note that the same experimental conditions, excepting the initial monomer concentration in the system, were used in both procedures. It appears that the different experimental results are due to the immediate encapsulation of catalyst and active centres by instantaneous polymer formation in the altered procedure. A larger proportion of active sites were entrapped in the polymer rich phase with significant

limitations on monomer diffusion into the active zone. This in turn served to reduce the MW and enhance LCB formation. This instant encapsulation also affected the morphology of the resultant polymers. PE produced with the standard procedure was composed of fine, uniform particles, while PE formed in the altered procedure was composed of larger, irregular particles.

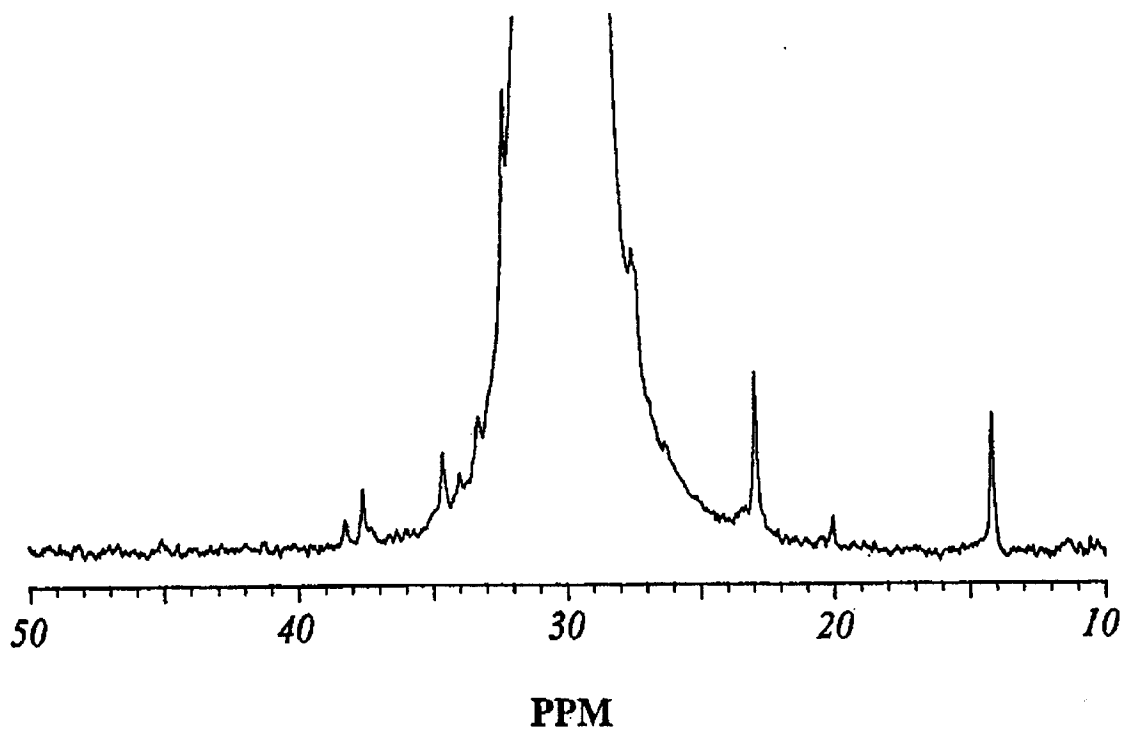


Figure 3.6 ¹³C NMR spectrum with chemical shifts in TCB and d-ODCB at 120 °C of Sample 9.

The polymerization conditions were: [Cp₂ZrCl₂] = 6.5 μM, [MMAO]/ [Cp₂ZrCl₂] = 1600, T = 70 °C, P = 10 psig

Effect of MMAO Concentration

The effects of the co-catalyst MMAO concentration on the polymer chain structures are shown in Figure 3.7 and Table 3.2.

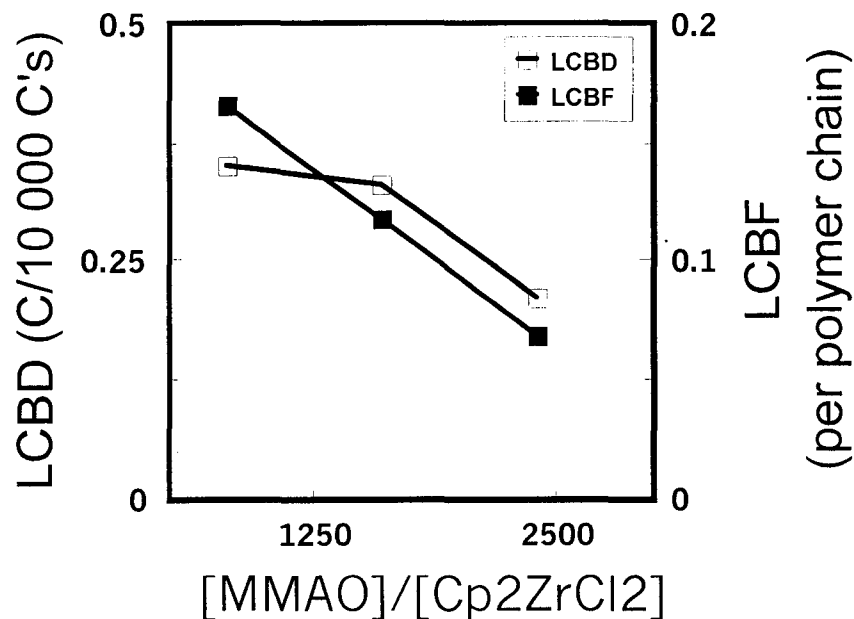


Figure 3.7 The effect of [MMAO]/[Cp₂ZrCl₂] on long chain branch density and frequency

The polymerization conditions were: [Cp₂ZrCl₂] = 6.5 μM, T = 70 °C, P = 10 psig

The ratios of MMAO to Cp₂ZrCl₂ concentrations of 800 (run 7), 1600 (run 2), and 2400 (run 8) were used in the present work. This concentration ratio had only a minor effect on the molecular weight of the PE samples, but broadened the MWD at higher MMAO concentrations. This affect is attributed to increased chain transfer to MMAO. Chain transfer to MMAO also reduces the formation of terminal double bonds. Therefore at high MMAO concentrations the UCED was lower, which lowered both LCBD and

LCBF and increased I_2 . Elevated MMAO concentrations also increased the rate of 2-1 insertion of ethylene macromonomer and thus the SCBD.

3.2.3 Conclusions

Significant long chain branch formation was found by ^{13}C NMR measurements in PE produced using the homogeneous catalyst bis(cyclopentadienyl) zirconium dichloride in a semi-batch slurry polymerization, with LCBD (carbons per 10,000 carbons) up to 1.0. A slurry polymerization process was believed responsible for the formation of LCB. Enhanced levels of LCB were attributed to the in-situ reaction of ethylene macromonomer and the encapsulation of active centres by precipitated polymer chains. The experimental conditions of reaction temperature, pressure, initial polymer concentration, and MMAO concentration, all affected LCB formation. High initial polymer concentration had a great influence on the long chain branching density, increasing the LCBD in the PE samples. Increasing the temperature from 60 °C to 80 °C reduced the LCBD from 0.33 to 0.10, while increasing the pressure from 2 psig to 20 psig reduced the LCBD from 0.73 to 0.30. Different MMAO to Cp_2ZrCl_2 ratios also influenced the formation of LCB, with LCBDs ranging from 0.21 to 0.35 at ratios of 2400 to 800. The LCBed polyethylenes showed enhanced shear thinning properties. The melt flow index ratios I_{10}/I_2 were in the range of 8.8 ~ 21.5, with an I_2 ranging from less than 0.1 ~ 0.701 g/10 min.

This work was published by Kolodka et al. (Kolodka et al., 2000).

3.3 Copolymerization of Poly(Ethylene-co-Propylene) Macromonomer with Ethylene

Section 3.2 outlined a method of producing long chain branched polyethylene using a metallocene catalyst in a slurry phase semi-batch reactor. It proved to be impossible to simultaneously control the molecular weight of the polymer, the branch length, and the long chain branch density (LCBD) using this method. The greatest difficulty is controlling the branch length while maintaining a constant molecular weight (MW) polymer as macromonomer produced in-situ has the same MW as the polymer. It was proposed that macromonomer could be produced in a separate reaction and copolymerized with ethylene forming a long chain branched polymer. The major considerations in choosing macromonomer are the presence of a reactive vinyl end group and the macromonomer solubility in polymerization system. The macromonomer must be able to dissolve in the solvent and diffuse to the active sites where the vinyl end group can insert into a growing polymer chain. Using a CSTR reactor it is possible to synthesize narrowly dispersed, well characterized PE macromonomers. However, PE is only slightly soluble in toluene and could not diffuse to a growing polymer chain. Poly(ethylene-co-propylene) (EPR), also produced in a CSTR, is significantly less crystalline than PE and has a much higher solubility in toluene. It was therefore chosen as the macromonomer in this study. Figure 3.8 shows the mechanism of the incorporation of EPR into a growing PE chain to form a long chain branch.

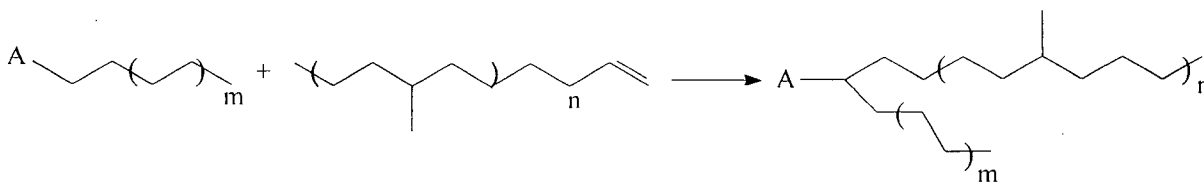


Figure 3.8 Mechanism of EPR incorporation into a growing PE chain forming a LCB

3.3.1 Experimental

Materials

All manipulations involving air and moisture sensitive compounds were carried out under dry nitrogen in a glove box. The catalyst, $[C_5Me_4(SiMe_2N^tBu)]TiMe_2$ (Me: methyl; tBu : isobutyl; C_5 : cyclopentadiene) (CGC-Ti) was donated by Dow Chemical as a 10 wt % solution in Isopar-E. The co-catalyst, tris(pentafluorophenyl)boron (TPFPB) was purchased from Strem Chemicals and modified methylaluminoxane (MMAO-3A) was provided by Akzo-Nobel Corporation as a 7.2 wt % aluminum solution in heptane. The catalyst, co-catalyst, and MMAO were used without further purification. Isopar-E, provided by Van Waters & Rogers Ltd., was refluxed over metallic sodium / benzophenone for 48 hours, and was distilled under a nitrogen atmosphere prior to use. Ethylene (polymerization grade > 99.5%) was provided by Matheson Gas and further purified by passing through columns with CuO (Aldrich), Ascarite (Fisher Scientific) and molecular sieves (Grace-Davidson) to remove oxygen, carbon dioxide, and moisture, respectively.

Synthesis of EPR Macromonomer

Poly(ethylene-co-propylene) (EPR) was prepared in a high temperature, high pressure continuous stirred tank reactor with CGC-Ti according to the procedure outlined in the literature (Wang et al., 2000). Polymerizations were carried out at 500 psig and 140 °C with a mean residence time (τ) of 4 minutes. The CGC-Ti/MMAO/Isopar-E, TFPFB/Isopar-E, and propylene/Isopar-E solutions were prepared and stored separately. The solvent, catalyst, co-catalyst, and comonomer tanks were kept at 15 psig under dry nitrogen. By adjusting the feed rates of the inlet streams, the mean residence time of 4 minutes, CGC-Ti concentration of 15 μM , TFPFB of 45 μM , and MMAO of 150 μM , were obtained and remained constant.

The CSTR system was heated to the desired temperature, and controlled at the set pressure. Isopar-E was then fed into the reactor. When the flow rate of Isopar-E reached 50% of the set value, ethylene and propylene were charged and the catalyst and co-catalyst pumps were turned on. During the polymerization process, polymer samples were collected and mixed with anhydrous ethanol. The solvent was evaporated and the resultant viscous polymer was dried at 50 °C under vacuum.

Polymerization Procedure

Polymerization reactions were performed in a 1 liter glass semi-batch reactor equipped with a magnetic stir bar. Temperature control was obtained through use of an

oil bath with temperature fluctuations within ± 1 °C. The reaction setup is shown schematically in Figure 3.9.

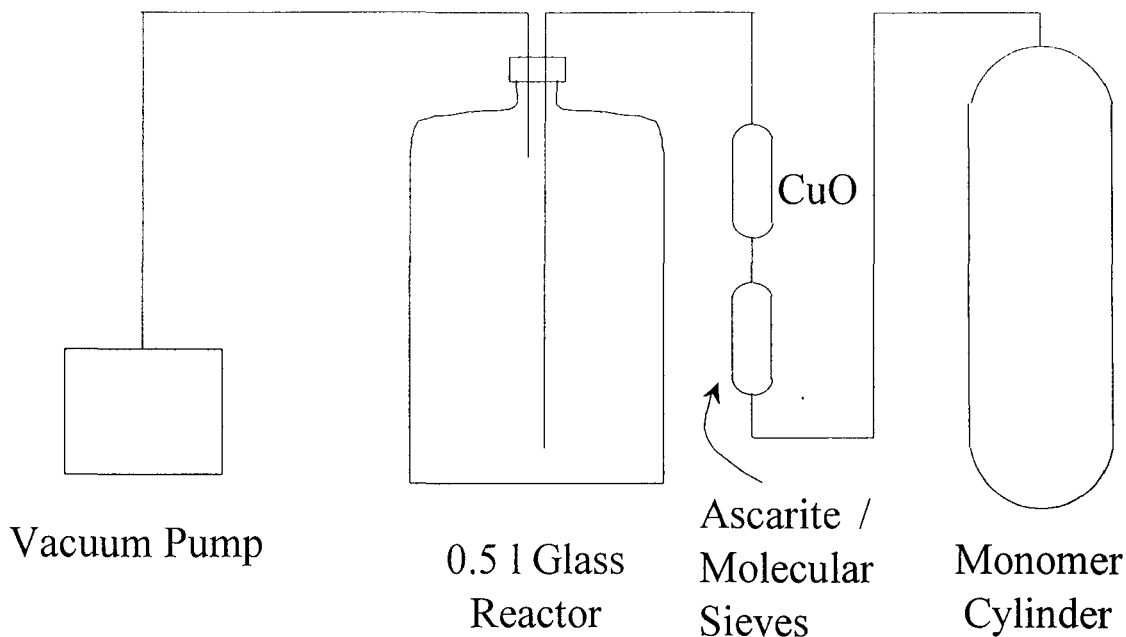


Figure 3.9 Schematic of semi-batch reactor setup

All experiments were performed with Isopar-E as the diluent and with a CGC-Ti concentration of 75 μM , a TFPFB concentration of 225 μM , and a MMAO concentration of 750 μM . The EPR macromonomer was completely dissolved in a measured amount of diluent and transferred into the nitrogen purged reactor. MMAO was subsequently injected into the reactor and after 5 minutes CGC-Ti was added, followed by TFPFB. The nitrogen was removed under vacuum, and the polymerization initiated by the addition of ethylene to the reactor at the set temperature. The reaction was quenched after 1 hour by the addition of 5 ml of dilute hydrochloric acid in methanol. The copolymer was filtered and the solvent was allowed to evaporate in order to collect any

unreacted EPR. To further remove any residual unreacted EPR, the copolymer was heated in toluene at 70 °C and filtered and dried in a vacuum oven. The detailed polymerization conditions are summarized in Table 3.3.

Table 3.3 Experimental Conditions For EPR / Ethylene Copolymerization

Run	Temp. (°C)	Press. (psig)	EPM (mmol/L)
1	70	12.5	4.9
2	80	20	4.9
3	60	20	4.9
4	80	5	4.9
5	70	12.5	4.9
6	60	5	4.9
7	70	12.5	0

The polymerization conditions were: volume of Isopar-E = 200 ml; CGC-Ti = 75 μM; TPFPB = 225 μM; MMAO = 750 μM; polymerization time = 1 hour; Initial EPR = 4.0 g.

Polymer Characterization

Molecular weight (MW) and MWD of the polymers were measured using a Waters Millipore 150 C High Temperature GPC with a differential refractive index (DRI) detector. The polymer samples were dissolved in 1,2,4 - trichlorobenzene (TCB) at a concentration of 0.1 wt % and measured at 140 °C with a flow rate of 1 mL/min. The GPC was equipped with three linear mixed Shodex AT806MS columns. The retention times were calibrated at 140 °C against known monodisperse TSK polystyrene (PS) standards from TOYO SODA Mfg. Co. The Mark- Houwink constants for the universal calibration curve were $K = 2.32 \times 10^{-4}$ and $\alpha = 0.653$ for PS and $K = 3.95 \times 10^{-4}$ and $\alpha = 0.726$ for PE.

^{13}C NMR spectra were acquired on a Bruker AC 300 pulsed NMR spectrometer operated at 75.4 MHz with broad band decoupling. The samples were dissolved in deuterated o-dichlorobenzene (d-ODCB) and TCB, and were measured at 120 °C using 10-mm sample tubes. d-ODCB was used to provide an internal lock signal, and TCB was the internal reference. Spectra required more than 7000 scans to attain an acceptable signal-to-noise ratio. A repetition time of 10 sec was utilized (Wang and Zhu, 2000).

The vinyl and vinylidene concentrations of the macromonomer were measured using an IR spectrometer according to ASTM D 3124-93 and ASTM D 5576-94 procedures (ASTM D 3124-93, 1994, ASTM D 5576-94, 1994). The samples were prepared in KBr cells with a thickness of 0.1 mm. Standard solutions were prepared using 1-octene and heptane.

3.3.2 Results and Discussion

EPR Macromonomer Properties

The EPR macromonomer was synthesised with CGC-Ti according to the method described in the experimental section. The resultant polymer was a viscous liquid which was highly soluble in Isopar-E and toluene. Table 3.4 summarizes the GPC and ^{13}C NMR data.

Table 3.4 Chain properties of EPR

M_N	4098
M_W	10 300
M_W/M_N	2.5
F_P^1	0.395
Terminal Vinyl	0.379
Terminal Unsaturation ²	
Terminal Vinylidene	0.311
Terminal Unsaturation ²	

- 1) Mole ratio of propylene within the EPR chains
 2) Determined using FTIR spectroscopy

Copolymerization of EPM with Ethylene

A two level factorial design was employed to study the influence of temperature and pressure on the copolymerization of EPR and ethylene. The observed variables were the degree of grafting, the weight percent of EPR, the grafting efficiency, and the catalyst activity. These variables are defined as:

$$\text{Degree of Grafting} = \frac{\text{mass of incorporated macromonomer}}{\text{mass of polyethylene produced}} \times 100 \quad (3.5)$$

$$\text{Weight Percent EPR} = \frac{\text{mass of incorporated macromonomer}}{\text{mass of total polymer}} \times 100 \quad (3.6)$$

$$\text{Grafting Efficiency} = \frac{\text{mass of incorporated macromonomer}}{\text{mass of macromonomer fed}} \times 100 \quad (3.7)$$

$$\text{Catalyst Activity} = \frac{\text{kg polyethylene produced}}{\text{mmol of CGC - Ti}} \quad (3.8)$$

Table 3.5 summarizes the copolymerization data.

Table 3.5 Copolymerization of EPR / Ethylene

Run	Degree of Grafting (%)	Wt. % EPM	Grafting Efficiency (%)	Activity (kg/mmol CGC-Ti)
1	50.0	33.3	47.5	253
2	32.8	24.6	50.0	407
3	23.7	19.1	45.0	507
4	70.3	41.3	47.5	180
5	56.7	36.2	42.5	200
6	56.5	36.1	32.5	266
7	na	Na	na	733

The polymerization conditions were: volume of Isopar-E = 200 ml; CGC-Ti = 75 μ M; TPFPB = 225 μ M; MMAO = 750 μ M; polymerization time = 1 hour; Initial EPR = 4.0 g.

Effect of Pressure

Pressure had a strong influence on the incorporation of EPR into the growing PE backbone. Figure 3.10 shows the influence of pressure on the degree of grafting at 60 °C and at 80 °C. When the pressure of ethylene was 20 psig the degree of grafting was less than 30 %. However, when the pressure was reduced to 5 psig the degree of grafting showed a significant improvement with values up to 70 %. This increase in branching is due to two complementing mechanisms. The pressure of the polymerization system determines the ethylene concentration in the solvent. The rate of formation of polyethylene is proportional to the ethylene pressure. At elevated pressures the concentration of ethylene was higher, increasing the rate of formation of PE and enhancing the activity of the catalyst. An increase in PE produced decreases the degree of grafting as defined in Equation 3.5. The influence of pressure on the catalyst activity is shown in Figure 3.11

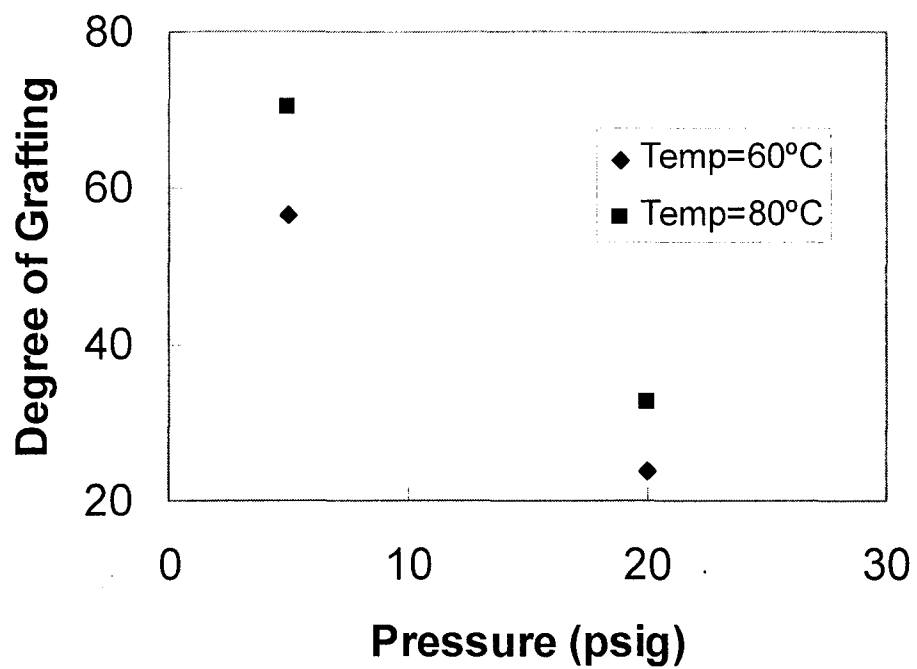


Figure 3.10 Influence of ethylene pressure on the degree of grafting

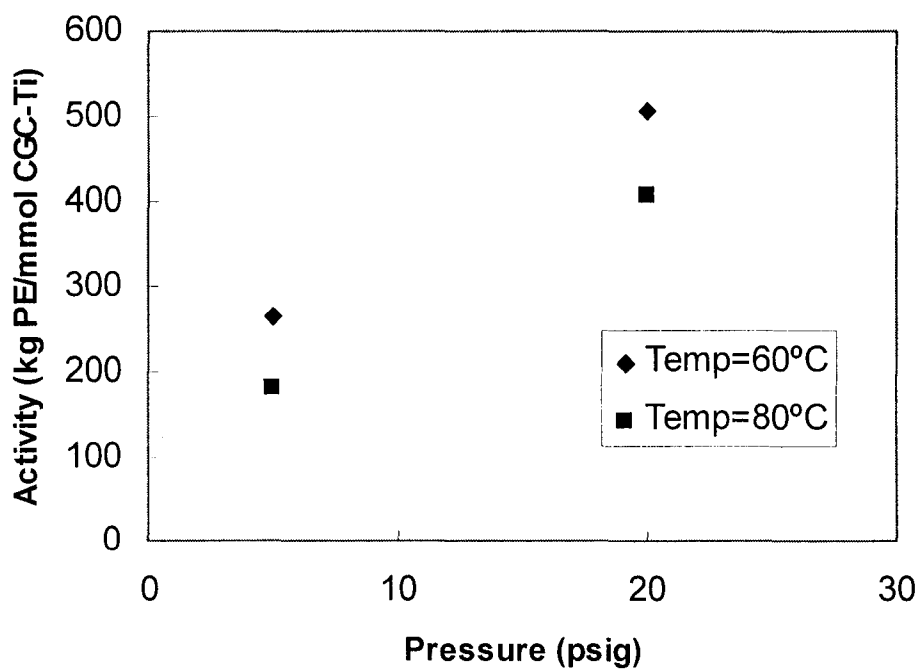


Figure 3.11 Influence of pressure on the catalyst activity

The second mechanism reducing the degree of grafting is the competition between monomer insertion and macromonomer insertion. Elevated concentrations of ethylene will tend to favour monomer insertion. Hence at higher pressures, there is significantly less EPR incorporation than at lower pressures. Consequently, the level of branching can be controlled by manipulating the pressure of the reaction.

Effect of Temperature

Temperature had a significant influence on the copolymerization of ethylene and EPR macromonomer. Figure 3.12 shows the affect of temperature on the degree of grafting of EPR at 60 and 80 °C.

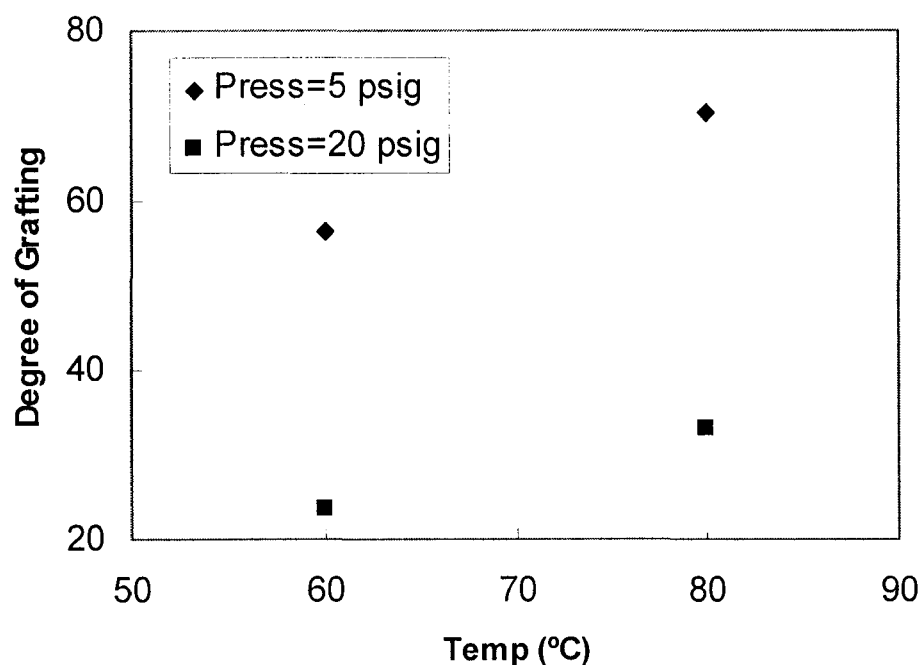


Figure 3.12 Influence of temperature on the degree of grafting of EPR macromonomer copolymerized with ethylene.

It can readily be seen in Figure 3.12 that there was an increase in the degree of grafting at elevated temperatures at both 5 and 20 psig. This effect is attributed to two complementing mechanisms. The first factor influencing the degree of grafting is the diffusion of macromonomer to the active sites. The EPR macromonomer chains display greater diffusional abilities at higher temperatures due to increased chain mobility. Consequently greater amounts of macromonomer can diffuse to, and be incorporated by, active sites at elevated temperatures. This tends to increase the degree of grafting. The second mechanism influencing the degree of grafting is due to the effect of temperature on the catalyst activity. The rate of reaction is related to the temperature by an Arrhenius relationship. Small increases in temperature greatly increase the rate of reaction. However, this reaction rate increase is accompanied by a significant increase in the rate of deactivation of catalyst. The overall effect of raising the temperature from 60 to 80 °C is a significant decrease in catalyst activity. This behaviour is shown graphically at two pressures in Figure 3.13. A decrease in the amount of PE produced increases the degree of grafting as shown by Equation 3.5. These two factors tend to significantly increase the degree of grafting at elevated temperatures.

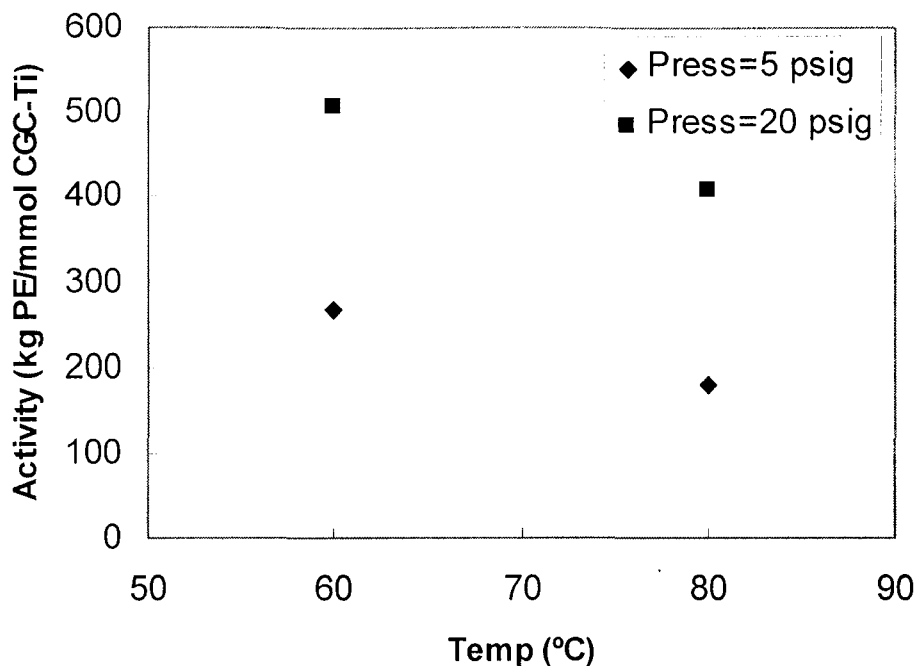


Figure 3.13 The influence of temperature on the catalyst activity for the copolymerization of ethylene and EPR macromonomer

3.3.3 Conclusions

Ethylene was copolymerized with a poly(ethylene-co-propylene) macromonomer (EPR) in a semi-batch reactor using Dow Chemicals homogeneous constrained geometry catalyst (CGC-Ti). A two level factorial design was used to study the influence of pressure and temperature on the degree of grafting (DoG) and the grafting efficiency. Pressure had a strong influence on the incorporation of EPR, with the degree of grafting (DoG) ranging from 32.8% to 70.3% at high and low pressures respectively. Pressure also strongly affected the activity of the catalyst, with activities ranging from 180 to 507 kg/(mmol CGC-Ti). Temperature also had a significant influence on the DoG. By manipulating the temperature, the DoG was varied from 56.5% to 70.3%. Temperature

also significantly affected the activity of the catalyst by increasing the rate of deactivation of the catalyst.

3.4 Copolymerization of Poly(Ethylene-co-Propylene) Macromonomer with Propylene

Section 3.2 described a method of producing long chain branched polyethylene using the metallocene catalyst Cp_2ZrCl_2 in a semi-batch, slurry phase reactor. Difficulties arose in controlling the branch length and the molecular weight of the total polymer. These difficulties were overcome through the copolymerization of ethylene with poly(ethylene-co-propylene) (EPR) in a two stage reaction, as described in Section 3.3. Using this method it was possible to control both the copolymer molecular weight and the long chain branch frequency. This technique was then further employed using propylene as the monomer and EPR as the macromonomer. Additionally, it was desired to produce polypropylene with various branch lengths and branch frequencies. These polymers were synthesised in order to determine the influence of branching on the physical characteristics of the polymers. This section details the synthesis of the model long chain branched polypropylenes.

3.4.1 Experimental

Materials

All manipulations involving air and moisture sensitive compounds were carried out under dry nitrogen in a glove box. The catalyst *rac*-dimethylsilylenebis(2-methylbenz[e]indenyl) zirconium dichloride (MBI), was provided by Mitsubishi Chemicals. The constrained geometry catalyst, $[\text{C}_5\text{Me}_4(\text{SiMe}_2\text{N}^t\text{Bu})]\text{TiMe}_2$ (CGC), and cocatalyst tris(pentafluorophenyl)boron (TPFPB) were provided by Dow Chemical as 10 and 3 wt % solutions in Isopar E. Modified methylaluminoxane (MMAO, 12 mol% of isobutylaluminoxane) was provided by Akzo as a 10 wt % solution in toluene. The catalysts and co-catalysts were used without further purification. Isopar E, used in the continuous stirred tank reactor (CSTR) for the macromonomer preparation, was purchased from Van Waters & Rogers Ltd., dried over a mixture of 5A and 13X molecular sieves from Fisher Scientific and silica gel from Caledon Laboratories Ltd. The solvent was also de-oxygenated by sparging with ultra high purity nitrogen (99.999%, Matheson Gas). Reagent grade toluene for the semi-batch reactor (SBR), provided by Caledon Laboratories, was refluxed over metallic sodium/benzophenone for 48 hours, and was distilled under a nitrogen atmosphere prior to use. Ethylene and propylene (polymerization grade > 99.5%) were purchased from Matheson Gas and further purified by passing through columns with CuO (Aldrich), Ascarite (Fisher Scientific) and molecular sieves (Grace-Davidson) to remove oxygen, carbon dioxide, and moisture, respectively.

Preparation of Macromonomer

The poly(ethylene-co-propylene) (EPR) macromonomer samples were prepared in a 0.6 liter high-temperature, high-pressure continuous stirred-tank reactor (CSTR). The details regarding the reactor system and operation were reported in our previous work (Park et al., 2000, Wang et al., 1999). Polymerizations were performed at 3.45×10^3 kPa and 130, 140, and 150 °C with a mean residence time of 4 minutes. The concentrations of CGC, TPFPB, and MMAO were 15 μ M, 45 μ M, and 150 μ M for all runs. Table 3.6 shows the measured properties of the various macromonomers.

Table 3.6 Chain properties and reaction conditions of poly(ethylene-co-propylene) macromonomer samples prepared by high-temperature continuous stirred-tank reactor

Macrom.	T °C	[E] ₀ mol/L	[P] ₀ mol/L	M _N g/mol	M _w /M _N	F _p	Vinyl Conc. %	Vinylidene Conc. %
1	150	0.33	1.09	2,560	2.6	0.57	36	42
2	140	0.31	1.13	3,900	2.5	0.58	37	39
3	130	0.59	0.83	6,010	2.5	0.42	40	43
4	150	0.08	0.13	7,820	2.4	0.28	42	44
5	140	1.02	0.42	11,200	2.5	0.21	44	43
6	130	0.11	0.11	17,100	2.0	0.28	43	45

Catalyst = CGC, Co-catalyst = TPFPB, 2nd cocatalyst = MMAO, solvent = Isopar-E, CGC concentration = 15 μ M, [TPFPB] = 3 μ M, [MMAO] = 150 μ M, mean residence time = 4 min, pressure 3.45×10^3 kPa

F_p: propylene molar fraction in copolymer

Copolymerization Procedure

The copolymerization reactions of propylene with EPR macromonomer were performed in our 0.5 liter semi-batch reactor (SBR). The schematic of the reactor system is shown in Figure 3.9. In all experiments, the soluble macromonomer was dissolved in

toluene and charged into the reactor. MMAO was injected into the system and five minutes later the catalyst was introduced. The MMAO and catalyst concentrations in the reactor were 0.025 mol/L and 2.5×10^{-5} mol/L, respectively. The reactor was evacuated and polymerization initiated by pressurizing with 12.5 psig propylene. The reaction was allowed to proceed for 30 minutes and was terminated by depressurizing and injecting 5 ml of methanol. The resultant polymer was filtered and washed three times with 60 °C toluene to remove any unreacted macromonomer. It was then washed with a 1 % HCl methanol solution to remove MMAO residue, filtered, and dried in a vacuum oven. The toluene extract was collected and the solvent evaporated. The unreacted macromonomer was dried for 72 hours in a vacuum oven and was weighed and analyzed. The detailed polymerization conditions are summarized in Table 3.7.

Table 3.7 Experimental conditions for the copolymerization of propylene with poly(ethylene-co-propylene) macromonomers using a semibatch reactor

Run	Macrom. number ¹	Load (g/L)	Temperature (°C)
1	1	20	30
2	2	20	30
3	3	20	30
4	4	26	30
5	5	25	30
6	6	17.5	30
7	1	0	30
8	1	5	30
9	1	10	30
10	1	15	30
11	6	5	30
12	6	10	30
13	1	20	20
14	1	20	40
15	1	20	50

Catalyst = *rac*-dimethylsilylenebis(2-methylbenz[e]indenyl) zirconium dichloride, Co-catalyst = modified methylaluminumoxane, Pressure = 12.5 psig, Volume toluene = 200 ml, [Zr] = 2.5×10^{-5} mol/L,, [Al] = 0.025 mol/L.
| refer to Table 3.6

Polymer Characterization

Molecular weight (MW) and MWD of the polymers were measured using a Waters- Millipore 150 C High Temperature GPC with a differential refractive index (DRI) detector. The polymer samples were dissolved in 1,2,4 - trichlorobenzene (TCB) at a concentration of 0.1 wt % and measured at 140 °C with a flow rate of 1 mL/min. The GPC was equipped with three linear mixed Shodex AT806MS columns. The retention times were calibrated at 140 °C against known monodisperse TSK polystyrene (PS) standards from TOYO SODA Mfg. Co. The Mark- Houwink constants for the universal calibration curve were $K= 2.32 \times 10^{-4}$ and $\alpha= 0.653$ for PS, $K= 3.95 \times 10^{-4}$ and $\alpha= 0.726$ for PE, and $K= 1.54 \times 10^{-4}$ and $\alpha= 0.760$ for PP.

¹³C NMR spectra were acquired on a Bruker AC 300 pulsed NMR spectrometer operated at 75.4 MHz with broad band decoupling. The samples were dissolved in deuterated o- dichlorobenzene (d-ODCB) and TCB, and were measured at 120 °C using 10-mm sample tubes. d-ODCB was used to provide an internal lock signal, and TCB was the internal reference. Spectra required more than 7000 scans to attain an acceptable signal-to-noise ratio. A repetition time of 10 sec was utilized (Wang, 1998).

The vinyl and vinylidene concentrations of the macromonomer were measured using an IR spectrometer according to ASTM D 3124-93 and ASTM D 5576-94 procedures (ASTM D 3124-93, 1994, ASTM D 5576-94, 1994). The samples were prepared in KBr cells with a thickness of 0.1 mm. Standard solutions were prepared using 1-octene and heptane.

3.4.2 Results and Discussion

Characterization

Table 3.8 summarizes the high temperature GPC, ^{13}C NMR, and FTIR characterization results.

Table 3.8 Results of the copolymerization of propylene with poly(ethylene-co-propylene) macromonomers using semibatch reactor

Run	M_N kg/mol	PDI	Yield (g)	EPR Conv. ¹ (%)	EPR Conv. ² (%)	Resid. macrom M_N	Wt. % EPR	LCBF ³	LCBF ⁴
1	59.0	2.7	13.1	25.0	25.4	3370	7.6	1.8	2.1
2	59.1	2.7	10.3	27.5	28.2	5100	10.7	1.6	2.0
3	54.8	2.6	14	30.0	30.8	7400	8.6	0.8	n.m.
4	41.0	3.2	10.8	32.7	n.m.	9780	15.7	0.8	n.m.
5	41.0	2.9	9.3	30.0	n.m.	14340	16.1	0.6	n.m.
6	99.0	2.8	6.9	17.1	n.m.	21720	8.7	0.4	n.m.
7	97.7	2.5	9.5	--	--	--	--	--	--
8	53.0	2.7	16.5	40.0	n.m.	n.m.	2.4	0.5	n.m.
9	55.2	2.4	15.7	35.0	34.8	n.m.	4.5	1.0	n.m.
10	48.3	2.7	15.6	28.3	n.m.	n.m.	5.4	1.0	n.m.
11	75.0	2.4	13.8	20.0	n.m.	n.m.	1.4	0.1	n.m.
12	80.0	2.3	15.3	25.0	n.m.	n.m.	3.3	0.2	0.25
13	248.9	2.5	1.2	2.5	2.8	3170	8.3	8.8	n.m.
14	31.7	2.4	22.5	30.0	31.3	3230	5.3	0.7	n.m.
15	29.4	2.4	20.2	32.5	33.4	3180	4.5	0.8	n.m.

- 1) Measured by weighing unreacted macromonomer
- 2) Determined using FTIR
- 3) Determined by massing unreacted macromonomer
- 4) Measured using ^{13}C NMR

The incorporation of EPR macromonomers onto growing PP chains was verified using several techniques. First, the unreacted macromonomer was extracted from the copolymer using toluene at 60 °C. The toluene was removed and the remaining macromonomer dried and weighed. This gave a direct estimate of the amount of macromonomer grafted in the copolymer.

Further analysis revealed that the separation of unreacted macromonomer from copolymer using hot solvent extraction was extremely effective. There were no discernable peaks where unreacted macromonomer would elute, indicating that there was no significant amount of residual macromonomer in the copolymer. Figure 3.14 shows a representative GPC trace of Sample 1 overlaid with the trace of unreacted macromonomer.

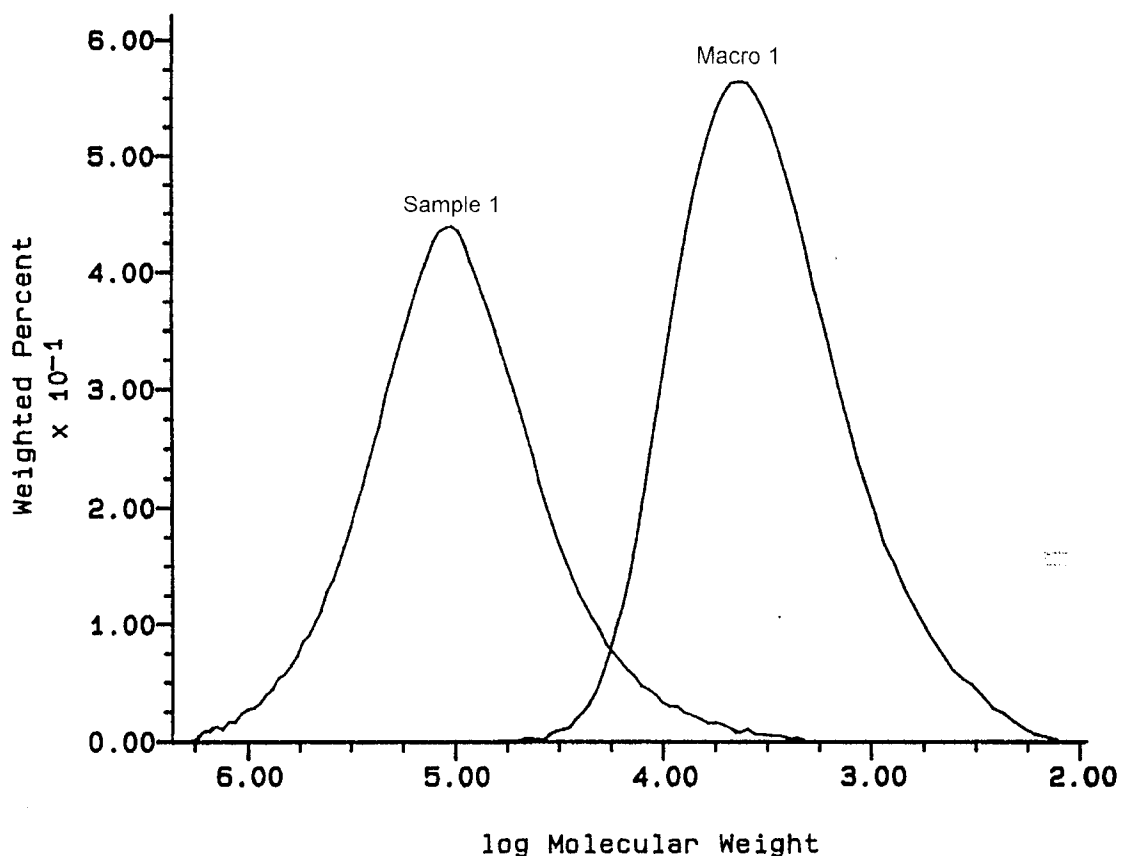


Figure 3.14 GPC trace of Sample 13 overlaid with the trace of macromonomer

An end group analysis using FTIR spectroscopy was performed to further verify the grafting reaction and to determine the extent of this reaction. The macromonomers were first analyzed to determine the concentration and type of end groups. The peaks were assigned using the method outlined in ASTM D 3124-93 and ASTM D 5576-94 (ASTM D 3124-93, 1994, ASTM D 5576-94, 1994). The two peaks observed at 887 and 910 cm^{-1} were attributed to vinylidene and vinyl end groups respectively. It was found that the EPR macromonomer was composed of approximately 80 % unsaturated end groups with similar concentrations of vinyl and vinylidene, as shown in Table 3.6.

Subsequently, several unreacted macromonomer samples were examined to determine the conversion of these end groups. This analysis revealed that the incorporation of macromonomer was efficient, with vinyl conversions of 70 to 90 %. Further inspection also showed that only vinyl end groups were incorporated into growing polymer chains. Macromonomer with terminal vinylidene did not participate in the copolymerization. These results match the conversions determined by massing the unreacted macromonomer, as seen in Table 3.8. Figure 3.15 shows the FTIR plots of the macromonomer used in Sample 3, before and after polymerization.

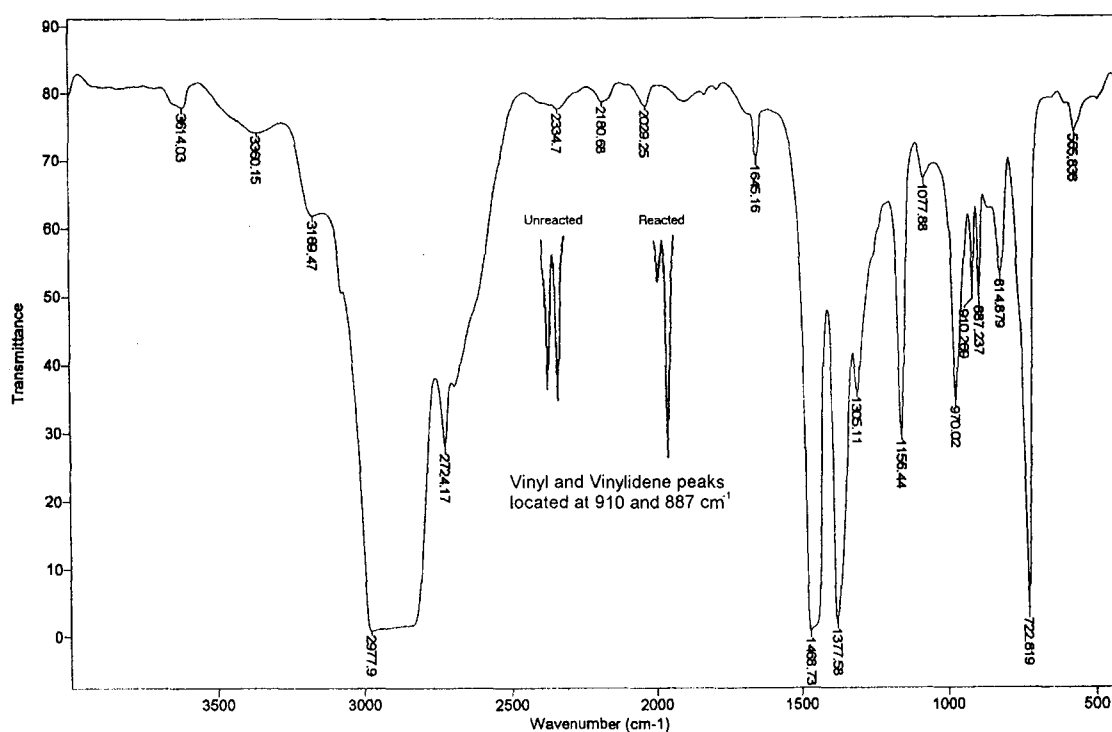


Figure 3.15 FTIR spectrum of Sample 3 macromonomer before and after copolymerization.

Further analysis using the MWs of the EPR and the copolymer, determined by GPC, allowed the calculation of the long chain branch frequencies using:

$$LCBF = \frac{\frac{mass(macrom, grafted)}{M_N(macrom, grafted)}}{\frac{mass(copolym)}{M_N(copolym)}} \quad (3.1)$$

A comparison of molecular weights was also conducted on the original and residual macromonomers. In all cases the residual macromonomer had a significantly higher molecular weight than the original. The original macromonomer used in Run 1 had a M_N of 2560 g/mol. After reacting, the residual macromonomer had a M_N of 3370 g/mol. Similarly, Macrom 2 (in Run 2) increased from 3900 to 5100 g/mol and Macrom 3 (in Run 3) increased from 6010 to 7400 g/mol after reacting. These data indicate that the copolymerization is dependent on the macromonomer MW with shorter chains preferentially reacted. This MW dependent behavior was also observed in a systematic study of increasing macromonomer MW shown in a later section.

The MW of the grafted macromonomer could not be measured directly. However, it could be estimated from the measured MWs of the original and residual samples,

$$\frac{mass(macrom, grafted)}{M_N(macrom, grafted)} = \frac{mass(macrom, original)}{M_N(macrom, original)} - \frac{mass(macrom, residue)}{M_N(macrom, residue)} \quad (3.2)$$

The M_N of the residual macromonomer was not available for all the runs. For these samples, the original M_N was used in Eq.(3.1) for the LCBF estimation.

The LCBF values estimated from Eqs.(3.1) and (3.2) were then verified using ^{13}C NMR with peaks assigned using the method outlined by Shiono et al. (Shiono et al., 1999). Figure 3.16 shows the ^{13}C NMR spectra of Sample 12. The peak associated with the conjunction carbon of iPP backbone with EPR side chain was assigned a chemical shift of 31.7. The intensity of this peak was used to determine the level of long chain branching. Three samples were measured with ^{13}C NMR and the values, shown in Table 3.8 were found to be in agreement with those calculated using weighed unreacted macromonomer.

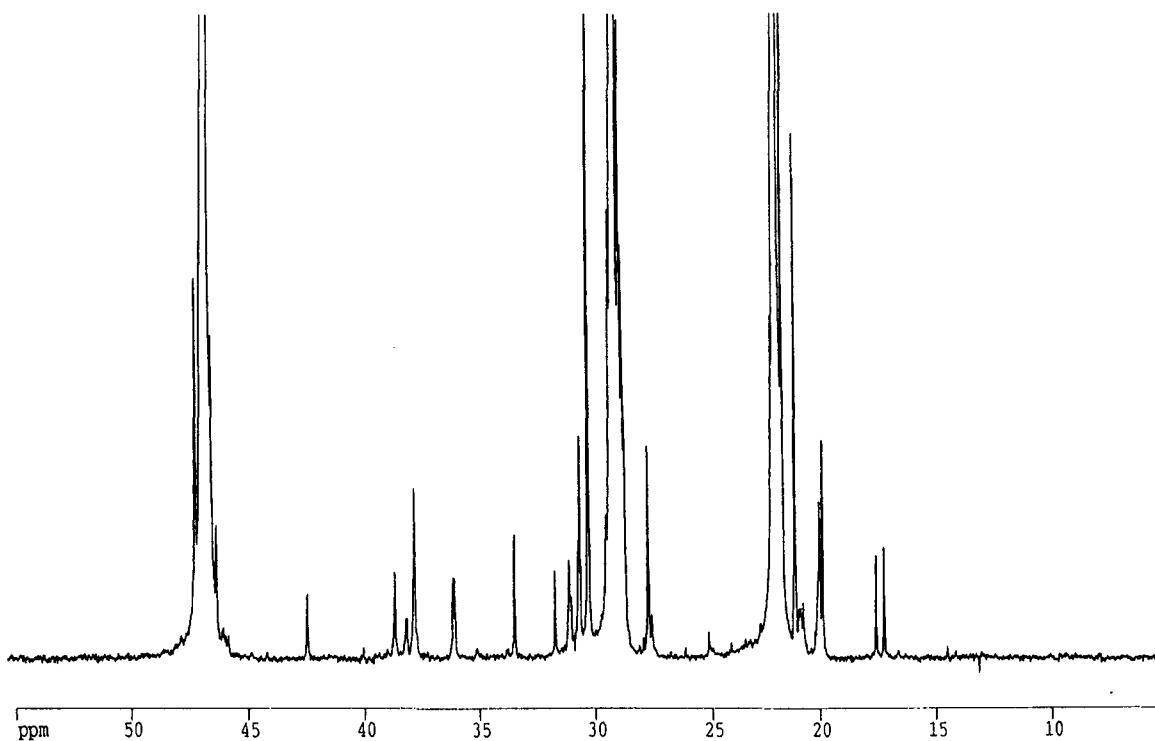


Figure 3.16 ^{13}C NMR spectrum of Sample 12

Effect of Macromonomer Concentration on the copolymerization

The influences of the initial concentration of macromonomer on the molecular weight, and LCBF of the copolymer, as well as the conversion of macromonomer was studied. Two different macromonomers were used, one well below the critical entanglement length (runs 8, 9, 10 and 1) and the other well above (runs 11, 12 and 6). The initial concentration was varied from 0 to 20 g/L. Figures 3.17 and 3.18 show the influence of macromonomer concentration on the conversion, molecular weight of copolymer, and incorporation of macromonomer for both series. It was found that when Macromonomer 1 was copolymerized the initial concentration had little influence on the molecular weight of the resultant copolymer. Varying the charge of EPR from 5 to 20 g/L had a strong influence on the LCBF. The LCBF changed from 0.5 to 2.8 branches per chain. Controlling the stoichiometry of the macromonomer provided an effective method for controlling the branch density while maintaining a constant molecular weight copolymer. It can also be seen that increasing the initial charge of macromonomer decreased the conversion. The conversion varied from 40 to 25 % when the macromonomer charge was increased from 5 to 20 g/mol. When Macrom 6 was copolymerized however, the initial concentration influenced both LCBF and M_N . Increasing the initial charge of Macrom 6 from 5.0 to 17.5 g/L increased the LCBF from 0.1 to 0.4 branches per chain. It also increased the M_N from 75000 to 99000 g/mol. Further, the conversions of Macrom 6 were approximately at 20~30 %, lower than those of Macrom 1.

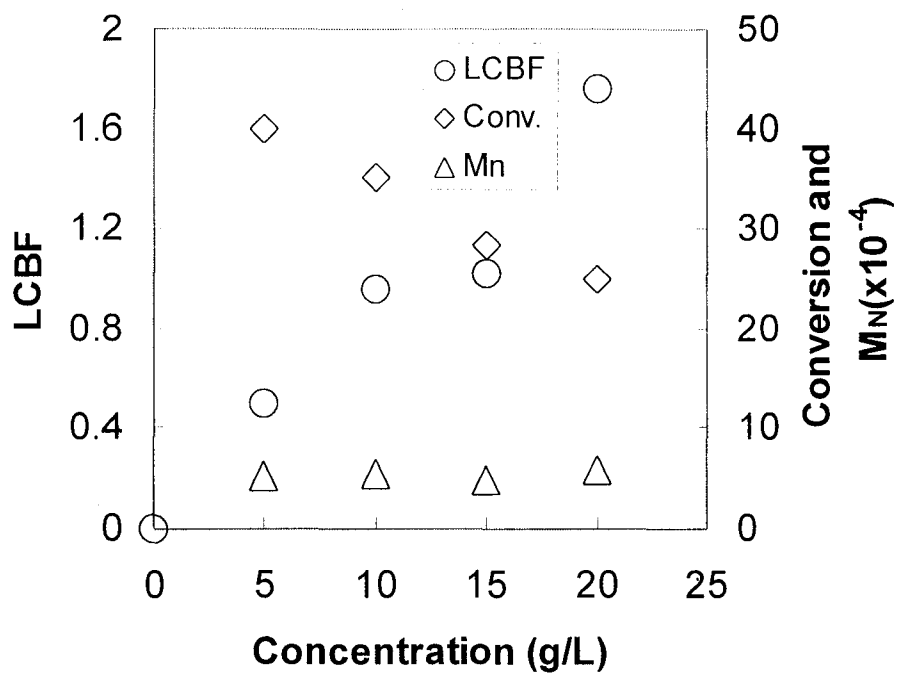


Figure 3.17 Influence of low MW macromonomer concentration on LCBF, copolymer M_N and conversion.

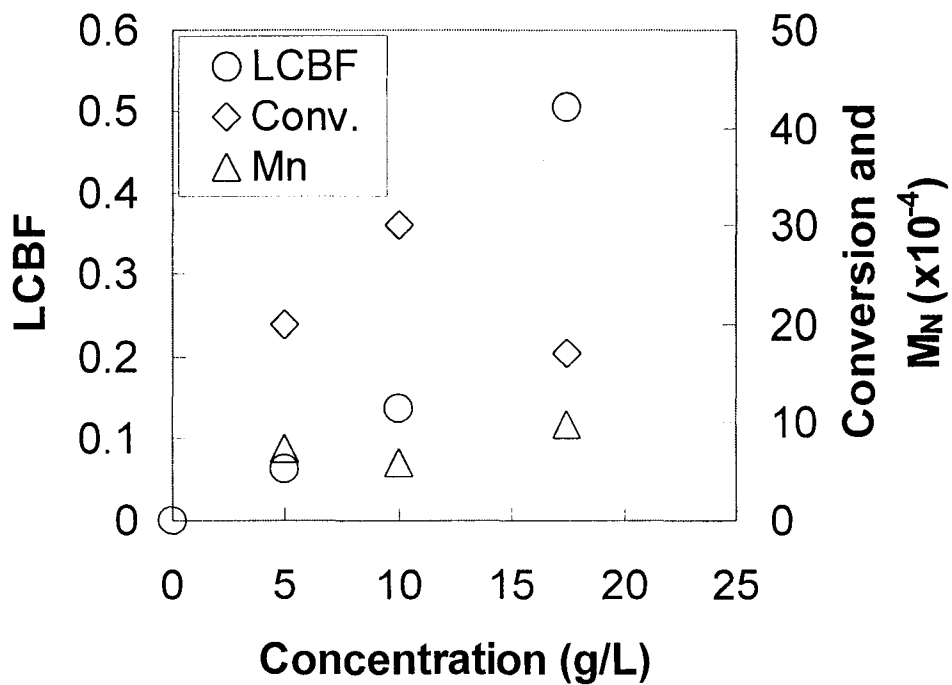


Figure 3.18 Influence of high MW macromonomer concentration on LCBF, copolymer M_N and conversion.

Effect of Macromonomer Molecular Weight on the Copolymerization

The influences of the macromonomer molecular weight on the copolymer molecular weight and LCBF, as well as the macromonomer conversion were studied. The macromonomer M_N was varied from 2500 to 17000 g/mol. Figure 3.19 shows the LCBF, copolymer MW, and macromonomer conversion versus the macromonomer M_N . An effort was made to prepare a series of model long chain branched samples having similar LCBFs while varying the branch M_N for rheological characterization purposes. This was attempted by varying the initial charge of macromonomer in the reaction. The macromonomer charge was increased from 20 g/L in Runs 1-3 to about 25 g/L in Runs 4 and 5 (see Table 2). However, the charge in Run 6 was reduced to 17.5 g/L due to solubility limitations of the high molecular weight macromonomer. Except for the Run 1 and Run 2 samples, the others had the LCBFs approximately equal to 1. The charge of Macrom 1 was lowered from 20 to 10 g/L (Run 9) to prepare the low molecular weight side chain sample having the LCBF about 1.0.

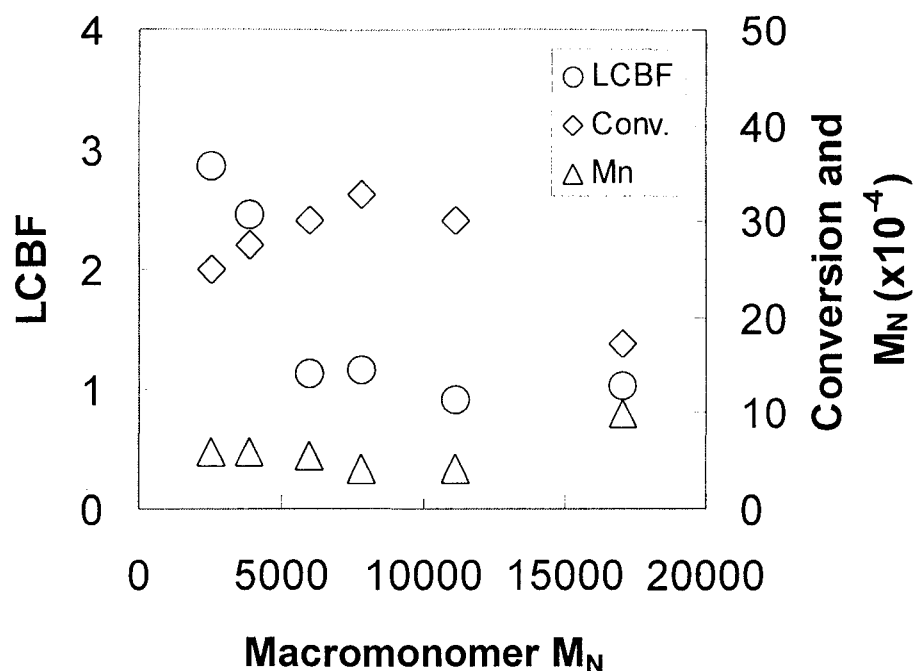


Figure 3.19 Influence of macromonomer M_N on LCBF, copolymer M_N and conversion.

At the same macromonomer charge, increasing the macromonomer M_N decreased the LCBF, particularly at the low M_N range. It is more difficult for the higher M_N macromonomer chains to be incorporated into the growing polypropylene backbones due to chain translational diffusion limitations and/or trapping of terminal vinyl groups in large chain coils. The conversion versus macromonomer M_N curve showed a maximum. The conversion initially increased with increasing macromonomer M_N . When the M_N exceeded 7800 g/mol, the conversion started to decrease. The conversion depended on the molar concentration of charged macromonomer. It was also affected by the chain length dependent incorporation. Lowering the molar concentration of macromonomer would lead to a higher conversion. The weight charges in Runs 1, 2, and 3 were the same at 20 g/L. However, the molar content of Run 1 was the highest, followed by Run 2 and

Run 3, due to their different M_N s, resulting in the higher conversion in Run 3 than Run 2 and Run 1. The conversion decrease in the high macromonomer M_N range was mainly caused by the chain length dependent incorporation. The copolymer molecular weights remained relatively constant, except for Run 6, which had significantly higher M_N .

Effect of Polymerization Temperature

The polymerization temperature was varied in order to study its influence on the reactivity of the macromonomer. Figure 3.20 shows the effect of temperature on the LCBF, copolymer MW, and macromonomer conversion. It was observed that the macromonomer conversion increased with increasing temperature. However, the reactivity of the propylene also greatly increased. There was significantly more sample produced. Despite the increase in the mass of incorporated macromonomer, the ratio of macromonomer to propylene in the copolymer actually decreased, leading to lower LCBFs. As was also expected, the temperature had a strong influence on the molecular weight of the resultant copolymers, with significantly higher MWs at low temperatures.

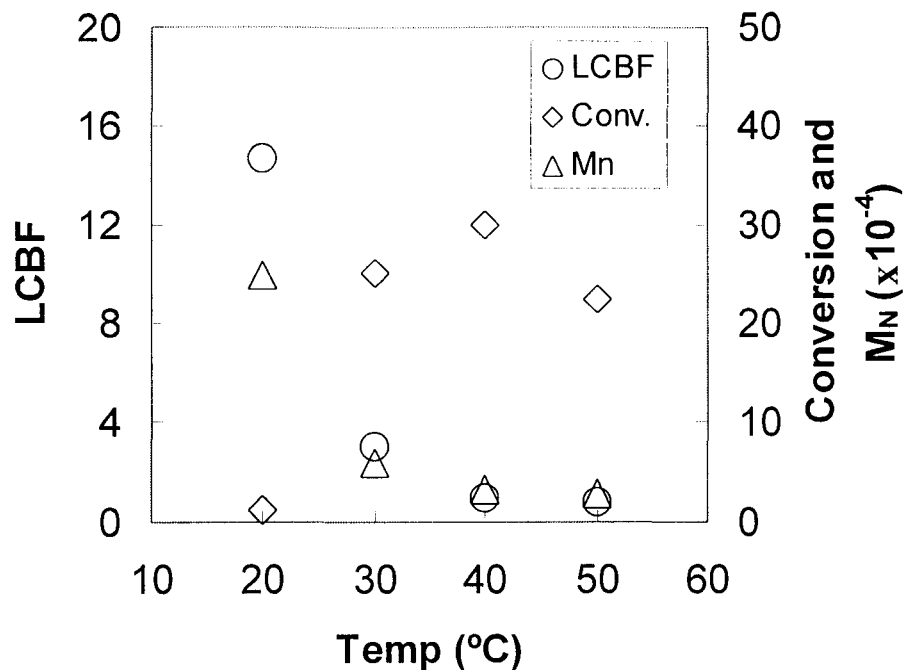


Figure 3.20 Influence of reaction temperature on LCBF, copolymer M_N and conversion.

3.4.2 Conclusions

Propylene was copolymerized with poly(ethylene-co-propylene) (EPR) macromonomers in a semi-batch polymerization using rac-dimethylsilylenebis(2-methylbenz[e]indenyl)zirconium dichloride / modified methylaluminoxane. The resultant polymer was composed of an isotactic polypropylene backbone with EPR branching forming a single branched or comb type structure. It was found that the stoichiometry of the macromonomer could be used to efficiently control the long chain branch frequency (LCBF) of the copolymers without greatly influencing the molecular weights. It was also possible to control the length of the long chain branches by controlling the M_N of the macromonomer with branch lengths ranging from 2500 to 17000 g/mol.

The work of Section 3.4 has been organized together with Section 4.3 and submitted to the journal *Macromolecules* for publication (Kolodka et al., 2002).

Chapter 4

Rheological Properties of Long Chain Branched Polyolefins

4.1 Introduction

There has been considerable interest in the relationships between molecular architecture and the viscoelastic behavior of polyolefins in recent years (Vega et al., 1998, Harrell and Nakajima, 1984, Tsenoglou and Gotsis, 2001). It has been demonstrated that the influence of long chain branching (LCB) on the thermorheological properties of polymers can be remarkable (Small, 1975, Santamaria, 1985). The precise effects of LCB are not well understood due to the difficulty of producing well-defined samples with a broad range of molecular attributes. There are many molecular properties which influence the physical characteristics of polymers including: the molecular weight (MW), molecular weight distribution (MWD), short chain branching (SCB), long chain branching (LCB), branch length, and branch distribution. These properties act in concert and separating individual influences has proven difficult. In an attempt to isolate the effect of branching from MW and MWD there has been considerable interest paid to both linear and star branched hydrogenated polybutadienes (HPB) synthesized via anionic polymerization (Carella et al., 1986, Milner et al., 1998, Milner and McLeish, 1998). This technique provides excellent control of the MW and MWD and has contributed fundamentally to the understanding of LCB. This method, however, has only recently been applied to the study of comb branched polymers (Lohse et al., 2001). Current innovations in single-site type catalysts allow the production of model polymers with

narrow molecular weight distributions (MWDs) and extremely narrow chemical composition distributions (CCDs) (Kaminsky et al., 1985, Chien and Wang, 1990). It has recently been shown that certain metallocene catalysts produce high density polyethylene with low levels of long chain branching (Kolodka et al. 2000). Other innovations in single site technology include Dow Chemical's constrained geometry catalyst which has been used to synthesize LCB polyethylenes of various MWs and long chain branch densities (LCBD) (Lai et al., 1993, Yan et al., 1999). This catalyst, with its open configuration, produces long chain branching through the insertion of vinyl terminated PE formed in-situ through β -hydride elimination or chain transfer to monomer. A precise control of the branch length is not possible using this technique. Recent advances have produced several metallocene catalysts with the ability to polymerize ethylene and propylene and to incorporate previously produced macromonomers into growing polymer backbones, forming comb structures (Soga et al., 1996, Shiono et al., 1997, Shiono et al., 1999, Weng, et al., 2001). Using this technique it is possible to produce polymers with controlled branch density, branch length, and with uniform backbones.

Extremely low levels of long chain branching have been shown to have significant influences on the viscoelastic behavior of polyolefins. Graessley et al., working with star branched hydrogenated polybutadienes, observed significantly increased zero shear viscosities (η_0) compared to linear polymers with similar molecular weights (Carella et al., 1984). It was demonstrated that the η_0 of star branched HPB varied exponentially with the arm molecular weight. Further studies on asymmetric 3 arm star HPB determined that the length necessary for a branch to behave as a long chain

branch was $2M_e$ (Jordan et al., 1989, Gell et al., 1997). It has been shown that the M_e for PE is 1250. Yan et al. observed significant increases in η_0 , shear thinning, and flow activation energies in LCB PE produced in a CSTR using CGC (Yan et al., 1999).

The temperature dependence of many polymers can be described using a time shift factor, a_T , and a modulus shift factor, b_T , as shown in equations 4.1 and 4.2.

$$\eta_0(T) = a_T(T)b_T\eta_0(T_0) \quad (4.1)$$

$$G_N^0(T) = b_T(T)G_N^0(T_0) \quad (4.2)$$

where T_0 is an arbitrary reference temperature. Polymers which behave in this manner are considered rheologically simple. Using the shift factors, master curves of dynamic moduli can be constructed of superimposed data generated at several temperatures. The temperature dependence of a_T for rheologically simple polymers, at temperatures well above the glass transition temperatures (T_g), often follows an Arrhenius relation. The flow activation energy (E_a), which is a measure of temperature sensitivity, is given by:

$$a_T = \exp\left[\frac{E_a}{R}\left(\frac{1}{T} - \frac{1}{T_0}\right)\right] \quad (4.3)$$

The modulus shift factor is only weakly dependant on temperature and is generally neglected.

The viscoelastic behavior of several polymer types, including LCB PE, do not follow these simple relations and are considered to be rheologically complex. These polymers do not have a single activation energy but exhibit shear dependent temperature sensitivities. At high shear rates the E_a for the loss modulus of long chain branched PE

was found to be similar to that of a linear PE. The activation energy at high shears was determined to be dominated by the reptation of linear molecules (Raju et al. 1979). However, at low shear rates the E_a is significantly higher for long chain branched PE due to the cumulative effect of the relaxations of molecules with various branch structures (Wood-Adams and Costeux, 2001).

This chapter examines the rheological behavior of the long chain branched polyolefins produced in Chapter 3. Section 4.2 explores the influence of branch density and polymer molecular weight on the rheological responses of long chain branched (LCB) homo-polyethylene. Section 4.3 examines the rheological behavior of a series of novel comb-structured polypropylenes with isotactic polypropylene backbones and poly(ethylene-co-propylene) long chain branches.

4.2 Rheological Behavior of Long Chain Branched Polyethylene

4.2.1 Experimental

A series of LCB PEs were produced in a slurry phase, semi-batch reactor using zirconocene dichloride / modified methylaluminoxane as outlined in Chapter 3 (Section 3.2). The molecular properties of the tested polymers are listed in Table 4.1.

Table 4.1. Molecular properties of long chain branched polyethylene samples

Run	M_N (g/mol)	M_w (g/mol)	M_w/M_N	LCBD ^{a)}	LCBF ^{a)}	$\eta_0^b)$ (Pa s)	n
2	60600	154000	2.54	0.33	0.12	$4.06 \cdot 10^5$	0.437
4	38900	95000	2.44	0.73	0.22	$7.86 \cdot 10^4$	0.518
5	46400	122000	2.63	0.65	0.21	$1.11 \cdot 10^5$	0.520
6	74100	197000	2.66	0.30	0.15	$7.14 \cdot 10^5$	0.442
7	66700	160000	2.40	0.35	0.17	$3.27 \cdot 10^5$	0.506
8	54100	152000	2.81	0.21	0.07	$6.46 \cdot 10^4$	0.606
9	29300	63000	2.15	1.00	0.20	$5.80 \cdot 10^3$	0.642
10	27800	57000	2.05	0.86	0.17	$3.43 \cdot 10^3$	0.679

The polymerization conditions were: catalyst = Cp_2ZrCl_2 , co-catalyst = MMAO, solvent = toluene, solvent volume = 700 ml. SB = Semi-Batch Reactor

a) Determined using ^{13}C NMR

b) Measured at 190 °C using SAOS parallel plate rheometry

The test samples were blended with 0.6 weight percent Irganox 1010 antioxidant to prevent degradation. The antioxidant was dissolved in acetone and mixed with the polymer powder. The acetone was evaporated for 24 hours in a fumehood and the polymer dried in a vacuum oven for 48 hours at 80 °C. The samples were then melt pressed (20 mm diameter, 2 mm thickness) at 180 °C and 2 MPa for 6 minutes followed by rapid quenching.

The rheological measurements were conducted on a Stresstech HR parallel plate rheometer in dynamic mode with a gap of 1.5 mm. Samples were placed in the rheometer, heated to the measurement temperature, and allowed to equilibrate for 10 minutes. The parallel plates were then moved to a gap of 1.5 mm and the excess polymer was trimmed. Samples were measured in 10 °C increments between the temperatures of 170 to 210 °C under a nitrogen blanket to prevent degradation. Strain sweeps were performed prior to frequency sweeps in order to establish the linear region. A frequency

range of 10^{-2} to 65 s^{-1} was investigated using a variable strain method. This method entails using the maximum strain that is within the linear region.

The influences of long chain branch frequency on the storage modulus $G'(\omega)$, loss modulus $G''(\omega)$, and complex viscosity η^* , as defined in equation 4.4, were investigated.

$$\eta^* = \left[\left(\frac{G'}{\omega} \right)^2 + \left(\frac{G''}{\omega} \right)^2 \right]^{\frac{1}{2}} \quad (4.4)$$

An attempt was made to superimpose the rheological data, generated at multiple temperatures, to $190 \text{ }^\circ\text{C}$ using the shift factor a_T given in Equation 4.3. This was only partially successful however, as the shift factor of several of the long chain branched PEs showed a dependence on both temperature and shear rate. Therefore the loss modulus, storage modulus, and dynamic viscosity are all given at $190 \text{ }^\circ\text{C}$. This departure from simple thermorheological behavior is dealt with in Section 4.2.2.

The long chain branched samples had very long relaxation times at low shear rates and it was not possible to obtain frequency independent viscosities from which the Newtonian viscosities (η_0) could be inferred. An attempt at fitting the viscosity data using the Cross equation, given by equation 4.5, was made.

$$\eta^*(\omega) = \frac{\eta_0}{[1 + (\lambda\omega)^n]} \quad (4.5)$$

where the value of n was assumed to be independent of temperature and the characteristic time, λ , to be proportional to η_0 . The value of λ was approximated as $365000/\eta_0$.

Unfortunately, reasonable solutions were not found for these samples using the above criteria. Figure 4.1 shows Samples 2 and 8 fitted using the Cross Equation.

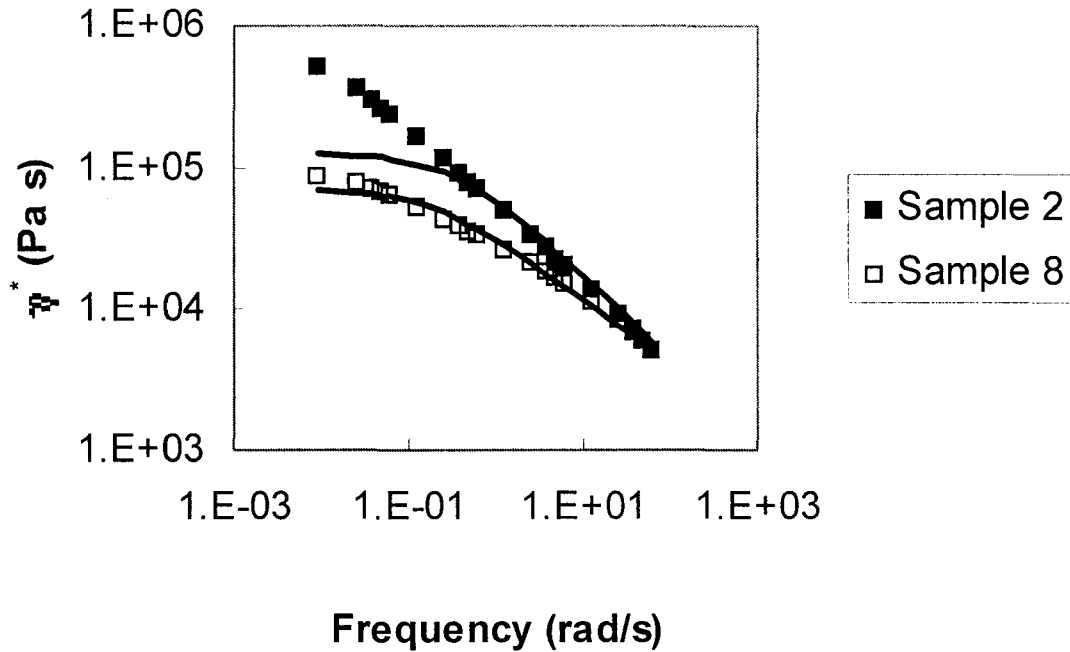


Figure 4.1 Dynamic viscosity at 190 °C fit using the Cross Equation

It can be seen that this equation gives a good approximation of the viscosity at high shear rates for both samples. At low shear rates the Cross Equation still gives an adequate estimation for Sample 8 (LCBF = 0.07) and performs poorly for Sample 2 (LCBF=0.12). The Cross Equation fails at low shear rates for PE with long chain branches. Therefore η_0 was approximated with the complex viscosity measured at $\omega = 0.01 \text{ s}^{-1}$. In order to quantify the shear thinning behavior the Power-law expression, given by Equation 4.6, was fitted to the viscosity data at high shear rates.

$$\eta = m\dot{\gamma}^{n-1} \quad (4.6)$$

where m is the consistency and n is the power law exponent which indicates the degree of non-Newtonian behavior.

4.2.2 Results and Discussion

Effect of Long Chain Branch Frequency

The long chain branch frequency of primarily linear PE has been shown to have a major role in its rheological behavior. However, distinguishing the effects of long chain branching from the influences of molecular weight and polydispersity index has proven difficult. The η_0 of polymers above the critical entanglement length (M_C) is related to the M_W by Equation 4.7, shown below.

$$\eta_0 = K_1 M_W^{3.4} \quad (4.7)$$

Consequently, doubling the M_W has the effect of increasing η_0 by an order of magnitude. Therefore, when comparing the rheological characteristics of polymers it is essential that the M_W s be similar. To this end the LCB PEs have been divided into three groups. Group 1 is composed of Runs 2, 7, and 8 with LCBFs of 0.12, 0.17, and 0.07 and M_W s of 154, 160 and 152 kmol/g, respectively. Group 2 compares Runs 4 and 5 having LCBs of 0.22 and 0.21 and M_W s of 95 and 122 kmol/g, while Group 3 compares Runs 9 and 10 with LCBFs of 0.20 and 0.17 and M_W s of 63 and 57 kg/mol.

When the M_{ws} of the PE samples are similar, the LCBF has a significant influence on the dynamic viscosity. Figure 4.2 shows the dynamic viscosity of Runs 2, 7, and 8 versus frequency at 190 °C.

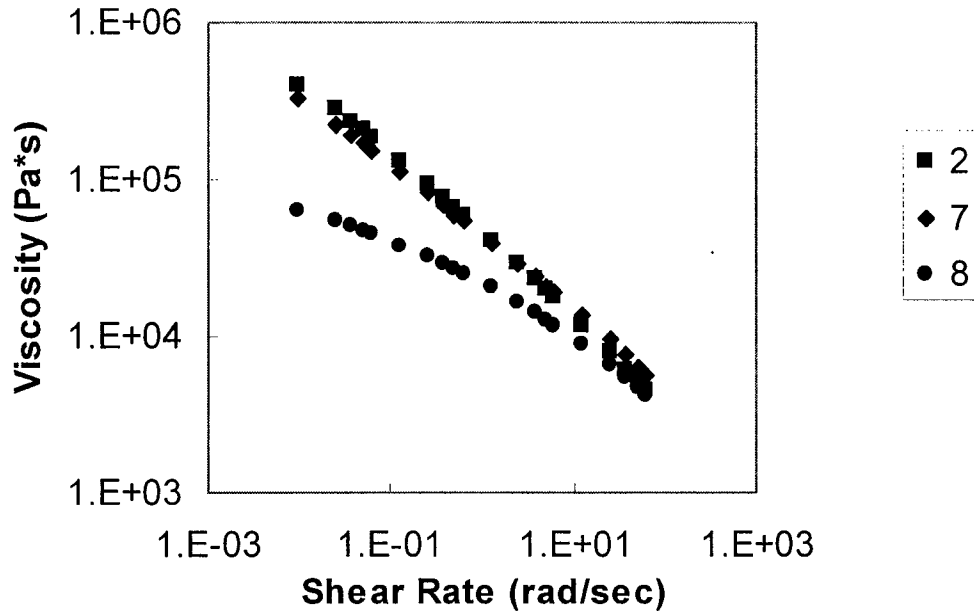


Figure 4.2 Dynamic viscosity of PE samples with M_w approximately 155 kg/mol

It is readily apparent that the LCBF had several influences on the rheological responses. Long chain branching significantly enhanced the low shear viscosity. By comparing Samples 2 and 8, with LCBFs of 0.12 and 0.07 respectively, we observe a seven fold increase in low shear viscosity. It must be further emphasized that these samples had similar M_{ws} and that this enhancement is attributed solely to the affect of long chain branching. At higher shear rates these samples all exhibited similar viscosities. This behavior was also observed in Samples 9 and 10 as shown in Figure 4.3. These samples had similar M_{ws} , 63 and 57 kmol/g, but LCBFs of 0.20 and 0.17

respectively. Branching again enhanced the low shear viscosity while having little influence on the high shear viscosity.

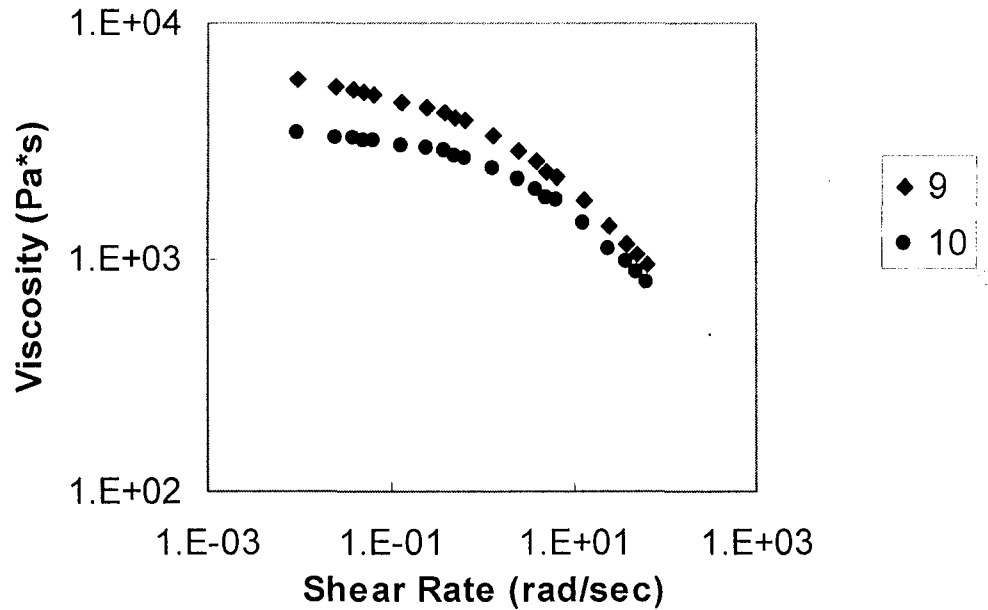


Figure 4.3 Dynamic viscosity of PE samples with M_w approximately 60 kmol/g

The flow behavior in Figures 4.2 and 4.3 can readily be explained by observing the molecular architecture of the polymer samples. At low shear rates, the viscosity is dominated by the relaxation behavior of branched polymer molecules. The long chain branches can form entanglements with nearby polymer chains. These entanglements function as temporary physical cross-links, significantly increasing the resistance to flow. An increase in branch frequency increases the amount of entanglements leading to enhanced low shear viscosities. At high shear rates, however, the viscosity is dominated by the reptation of linear chains. The long chain branches become aligned with the polymer backbones breaking the temporary physical cross-links. Consequently, samples

with similar M_{NS} but different levels of long chain branching are expected to exhibit similar high shear viscosities. This behavior was indeed observed in Figures 4.2 and 4.3. At low shear rates the viscosity of the polymer with higher levels of long chain branching exhibited significantly higher low shear viscosities. When the shear rate approached 100 s^{-1} the viscosities almost overlapped. The mechanism of increased η_0 due to the effect of long chain is shown schematically in Figure 4.4. In both diagrams there are three polymer chains with the middle molecule having 2 long chain branches. At low shear rates the branches entangle with nearby polymers, increasing the resistance to flow. At higher shear rates, the long chain branches align with the polymer backbone preventing entanglements.

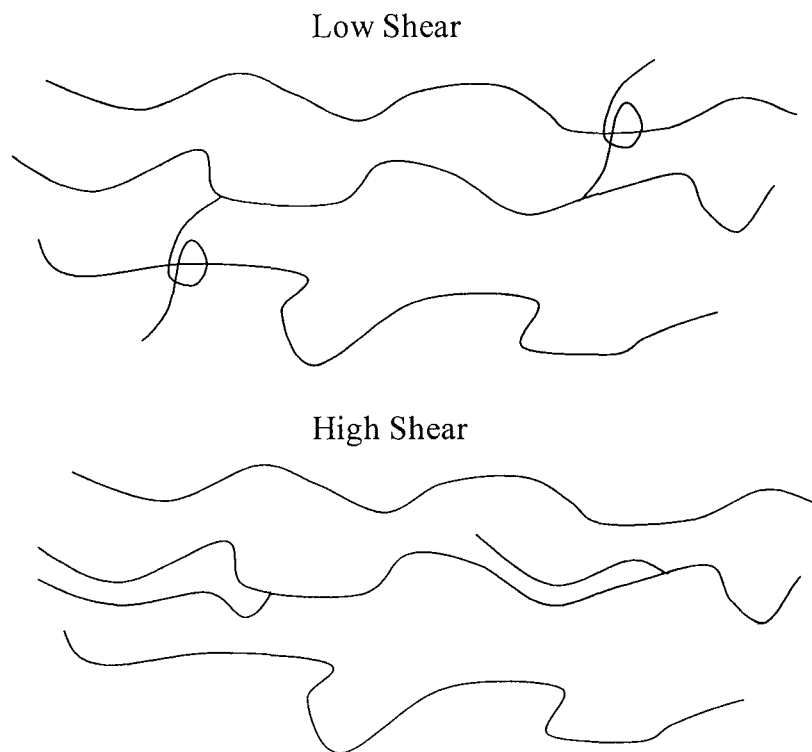


Figure 4.4 Schematic representation of long chain branching at high and low shear rates

A method of characterizing the magnitude of the shear thinning behavior is to fit the high shear viscosity with the Power-law expression given in Equation 4.6. The value of n indicates the degree of shear thinning, with a value of 1 signifying Newtonian behavior and lower values indicating increased shear thinning. The values obtained for n are given in Table 4.1. Figure 4.5 shows the influence of LCBF on the power-law exponent for Samples 2 and 8 ($M_w = 150$ kmol/g) and Samples 9 and 10 ($M_w = 60$ kmol/g).

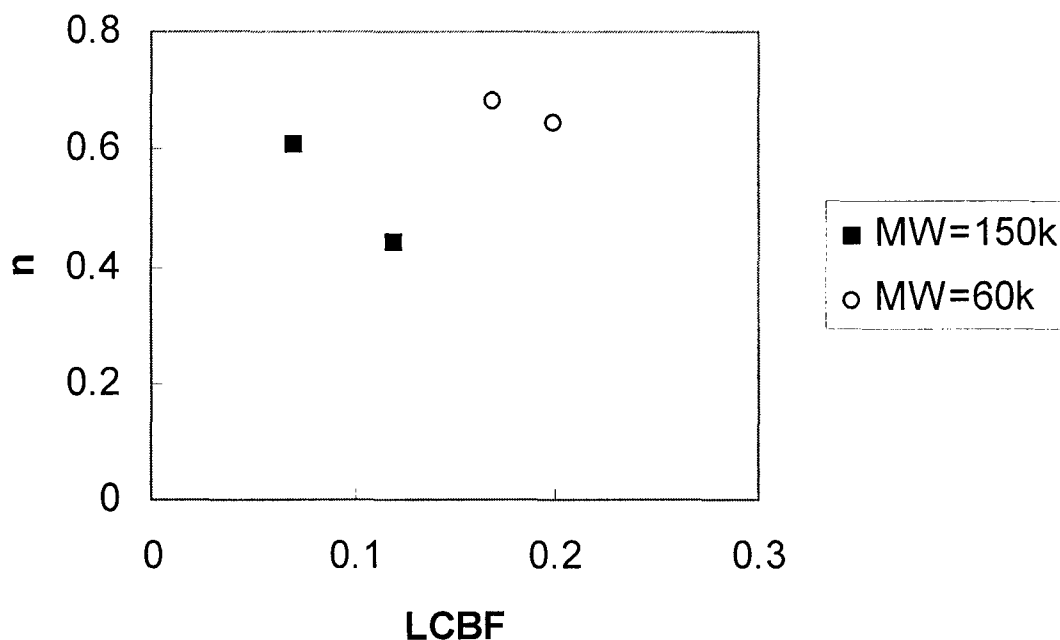


Figure 4.5 The influence of LCBF on the power-law exponent n

It can be seen that when the M_w s of the samples are similar an increase in the LCBF decreases the value of n , indicating an increase in the shear-thinning phenomenon.

This is readily explained by the increase in entanglements afforded by the increase in long chain branches. Another interesting effect is the influence of the M_w . Despite having lower LCBFs, Samples 2 and 8 both have lower values of n . Furthermore, it can be observed that the slope of a line connecting Samples 2 and 8 is significantly steeper than a line connecting Samples 9 and 10. This indicates that an increase in the LCBF at elevated M_w s produces a greater affect on shear thinning than a similar increase at lower M_w s.

The influence of branching on the shear-thinning phenomenon can also be observed with samples having different M_w s. The shear viscosity is normalized by dividing by η_0 and plotted versus the frequency. This technique eliminates the changes in η_0 caused by varying the M_w and focuses on the shear-thinning phenomenon attributed to long chain branching. The smaller the ratio of η to η_0 , the greater the amount of shear thinning. Figure 4.6 shows the normalized viscosity responses of the long chain branched PEs produced in a slurry phase semi-batch reactor.

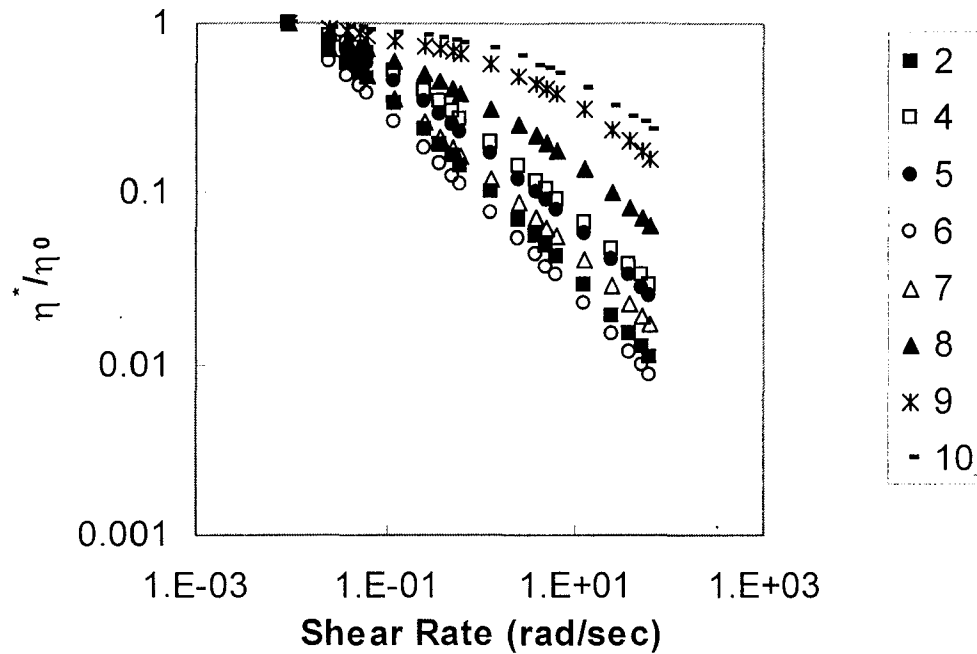


Figure 4.6 Normalized dynamic viscosity of semi-batch PE samples

It is readily apparent from Figure 4.6 that there is another mechanism, separate from the LCBF, influencing the shear viscosity. Samples with similar M_w s and different LCBFs behave in an expected manner. Sample 2, with a M_w of 154 kmol/g and a LCBF of 0.12, exhibited significantly more shear thinning than sample 8, with a M_w of 152 kmol/g and a LCBF of 0.07. Sample 2 has a greater amount of long chain branches and consequently more entanglements formed at low shear rates, increasing the shear-thinning phenomenon. However, when comparing Sample 7, with a LCBF of 0.17 and a M_w of 160 kmol/g, with Sample 10, with a LCBF of 0.17 and a M_w of 57 kmol/g, it is apparent that another mechanism occurs. Despite having similar LCBFs, these samples have significantly different flow behaviors. Sample 7 shows considerable shear thinning while Sample 10 exhibits little shear thinning. This behavior is attributed to the influence

of the LCB length. Long chain branching in homo-PE produced in a semi-batch slurry reactor is thought to be due to the incorporation of vinyl terminated macromonomers produced earlier in the reaction. The kinetics of formation of a macromonomer and a dead polymer chain are similar and they therefore have similar MWs. Consequently, polymers produced with high MWs have high MW macromonomer incorporated into their growing backbones as LCBs. These longer branches are involved in more entanglements, leading to elevated low shear viscosities. Consequently, a polymer cannot simply be characterized by knowing the LCBF. Information about the branch length must also be known. This behavior can also be observed in Sample 5 (LCBF = 0.21, $M_w = 122$ kmol/g) and Sample 9 (LCBF = 0.20, $M_w = 63$ kmol/g). Despite having similar LCBFs Sample 5 exhibits significantly greater shear thinning. The influence of branch length on the rheological responses of polyolefins will be studied in greater detail in Section 4.3.

The influence of the long chain branch frequency on the storage modulus (G') and the loss modulus (G'') was also studied. Figure 4.7 shows G' and G'' versus frequency for Samples 2 and 8.

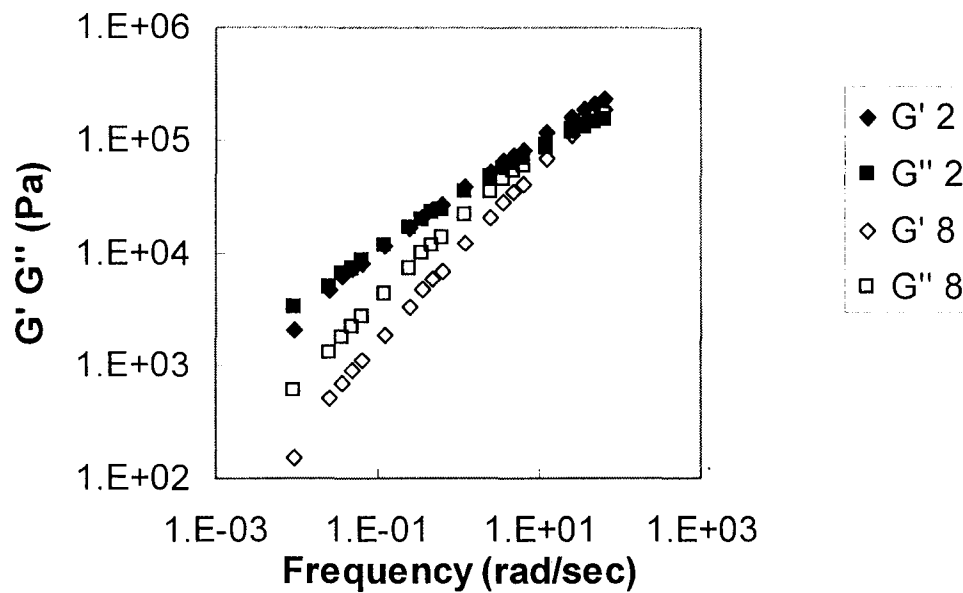


Figure 4.7 Influence of LCBF on G' and G'' for Samples 2 and 8

It is readily apparent that the LCBF significantly influenced G' and G'' . Despite having similar M_w s Samples 2 and 8 had different rheological responses. Sample 2, with a M_w of 154 kmol/g and a LCBF of 0.12, had enhanced values of G' and G'' at low shear rates compared to Sample 8, with a M_w of 152 kmol/g and a LCBF of 0.07. However, at higher shear rates the values of G' and G'' were similar for these samples. It can also be seen that Sample 2 had a broader relaxation spectrum evident by the more gradual increase of G' . These affects have been attributed to the additional modes of relaxation at low shear rates due to branching. Unfortunately, it was not possible to determine the plateau modulus (G'_0), a characteristic viscoelastic parameter which is used to determine the molecular weights between entanglements (M_e), for these samples. The loss modulus

plateau was located at a shear rate outside the experimental shear range. Samples 9 and 10 behave in a similar manner, as can be seen in Figure 4.8 which shows G' and G'' versus frequency.

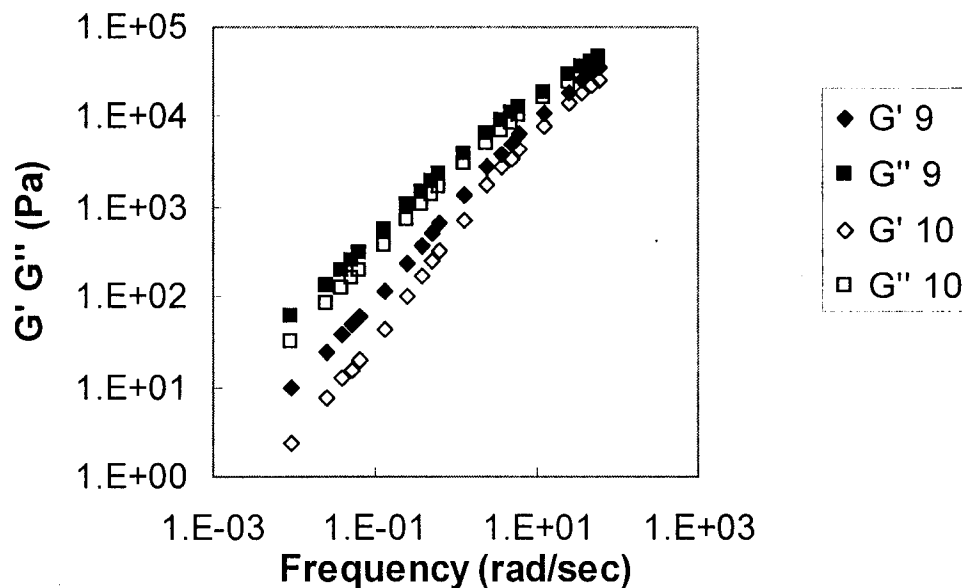


Figure 4.8 Influence of LCBF on G' and G'' for Samples 9 and 10

It can be seen that Sample 9, with a M_w of 63 kmol/g and a LCBF of 0.20, has enhanced values of G' and G'' at low shear rates compared to Sample 10, with a M_w of 57 kmol/g and a LCBF of 0.17. At higher shear rates G' and G'' are similar for both samples. Again, increased levels of long chain branching led to a broader relaxation spectrum, evident by the more gradual increase of G' . The G'_0 of these samples also could not be determined because the loss modulus plateau was located outside the experimental range. Samples 9 and 10 differ from Samples 2 and 8 in that the crossover

points G_x , which separate viscous-like and elastic-like behavior, were not apparent under the experimental frequency range.

4.2.3 Thermorheological Complexity

An attempt was made to superimpose the generated rheological data to 190 °C using the shift factor a_T given in Equation 4.3. However, the effect of temperature could not be represented by a single shift factor as a_T showed a dependency on frequency. This dependency is subtle however, and careful examination of the data is required to determine rheological complexity. Figure 4.9 shows an apparent master curve for the loss modulus of Sample 7.

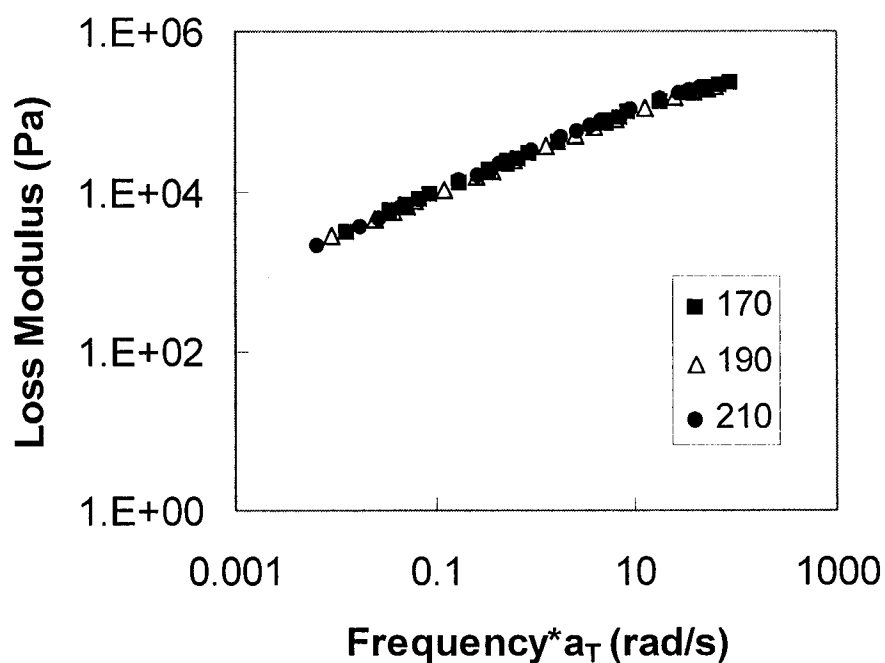


Figure 4.9 Apparent master curve of Sample 7 ($E_a = 31.4$ kJ/mol)

A single frequency shift factor was used at each temperature and the data appeared to superimpose well. However, at low and high frequencies there is a slight lack of fit in the data. This lack of fit is due to using an average activation energy to determine a_T at all frequencies. A method of detecting thermorheological complexity is to plot the magnitude of the complex modulus versus the product of η_0 and frequency. These plots are temperature independent for simple materials and temperature dependant for complex materials. Figure 4.10 shows the simple behavior of Sample 10 while Figure 4.11 shows the complex behavior of Sample 7.

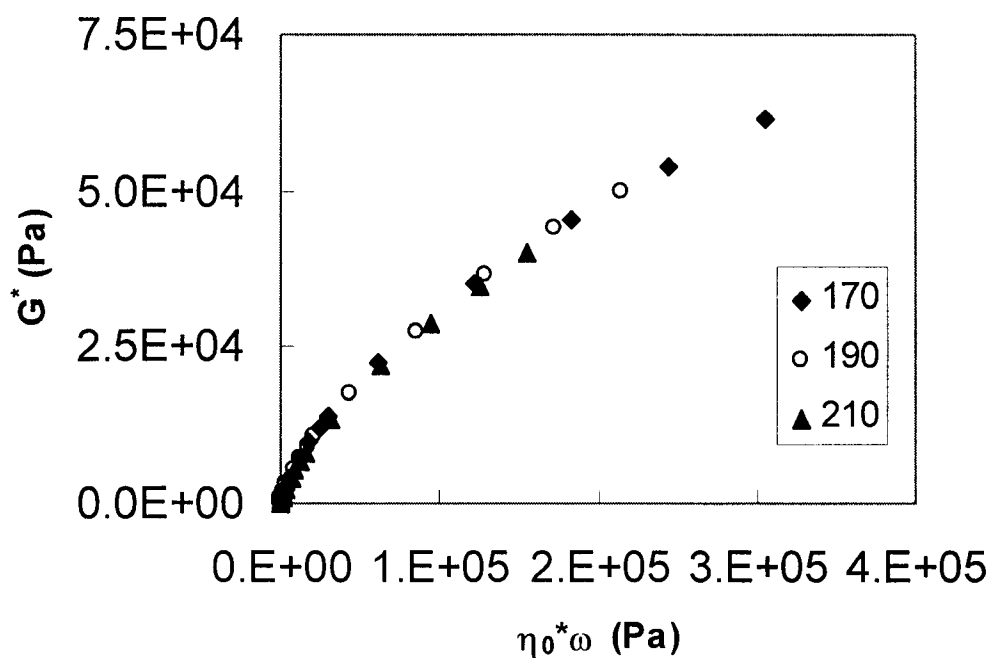


Figure 4.10 Rheologically simple behavior of Sample 10

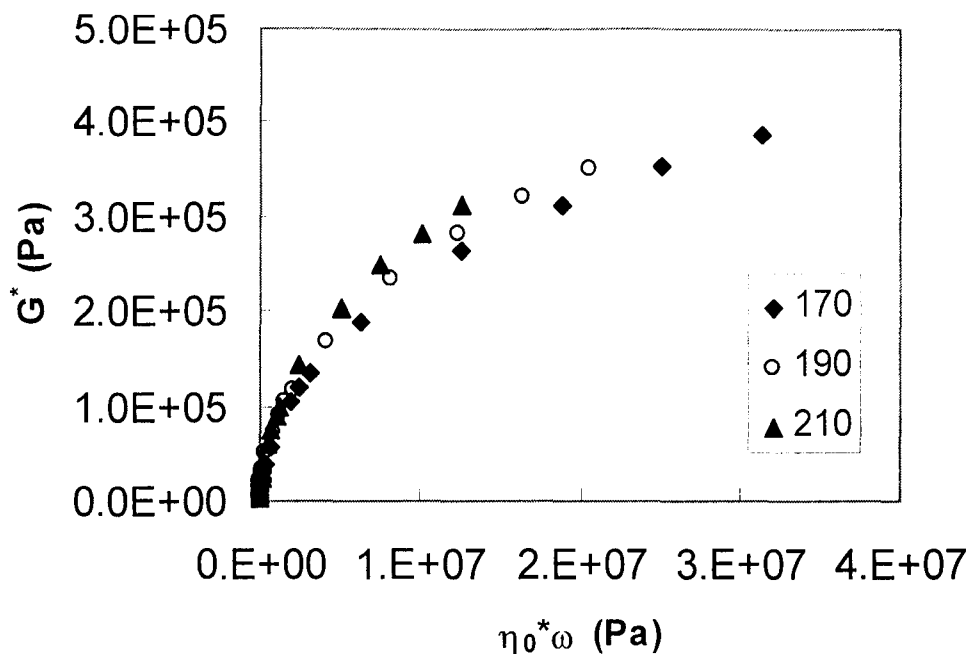


Figure 4.11 Rheologically complex behavior of Sample 7

It can be readily seen that the curves in Figure 4.10 are independent of temperature indicating rheologically simple behavior. The plot of the complex modulus versus the product of η_0 and frequency of Sample 7, shown in Figure 4.11, is obviously temperature dependent, indicating rheological complexity. Each of the samples was analyzed using this method with the majority of samples showing complex behavior.

The values of a_T at various frequencies were determined using the storage modulus. Plots of G' versus frequency at 170 °C and 210 °C were constructed for each of the samples. A value of G' at 170 °C was chosen and the value of the frequency was

noted. The frequency having the same value of G' at 210 °C was then determined. The value of a_T was calculated using Equation 4.7 shown below.

$$a_T(G', 210) = \frac{\omega_{170}}{\omega_{210}} \quad (4.7)$$

The values of a_T for the remaining values of G' were determined in a similar manner. Figure 4.12 shows the method of determining a_T used for Sample 5. The shift factors for each sample were calculated in an analogous fashion.

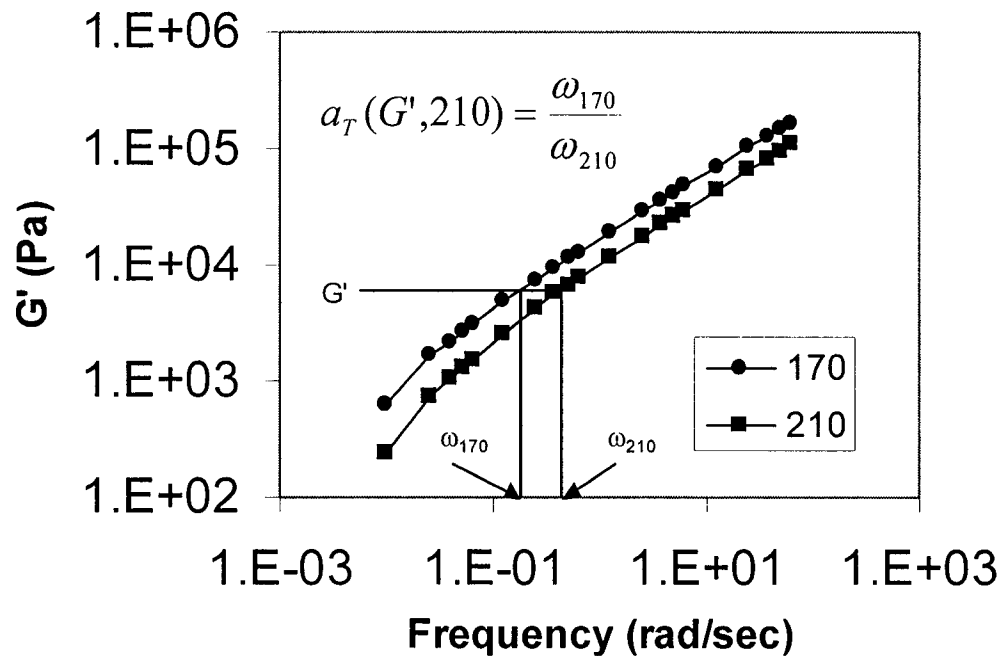


Figure 4.12 Determination of modulus-dependent shift factor for Sample 5

The activation energy at various frequencies for the samples were determined using Equation 4.3. The values of E_a for several samples are plotted versus frequency in Figure 4.13. The remaining samples are excluded to improve clarity.

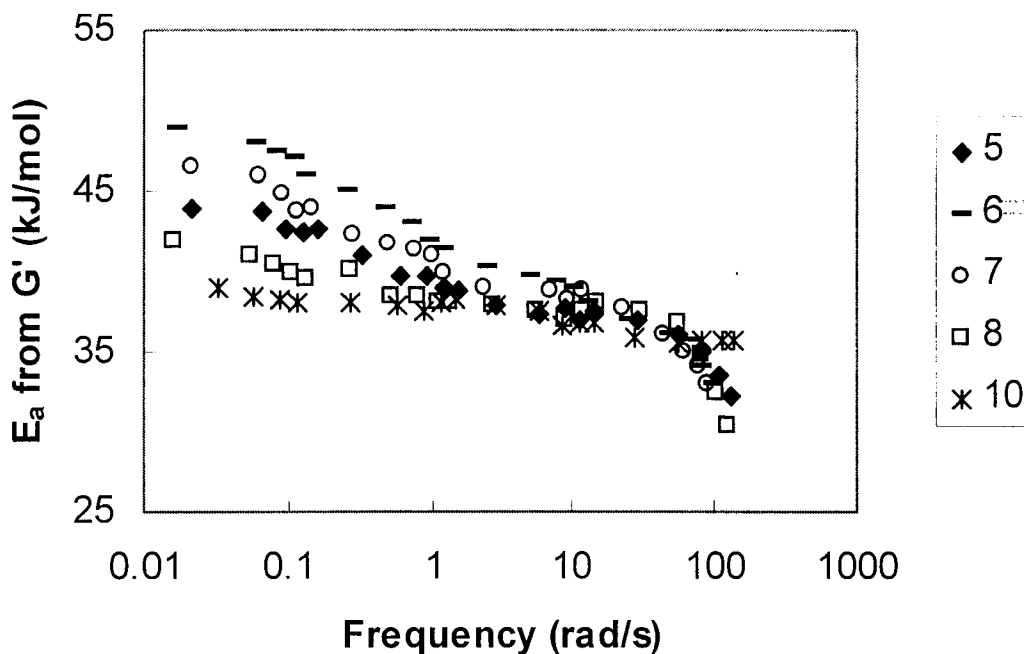


Figure 4.13 Frequency dependent activation energy

It can be seen in Figure 4.13 that Samples 5 through 8 exhibit obvious thermorheological complexity while Sample 10 exhibits simple behavior. The E_a is shear dependant with the highest values at low shear rates. The value of the activation energy at low shear rates depends on both the LCBF and on the length of LCBs, with values ranging from 39 to 49 kJ/mol. Comparing Samples 7 (LCBF = 0.17, M_w = 160 kg/mol) and 8 (LCBF = 0.07, M_w = 152 kg/mol) we see that Sample 7 has significantly higher activation energies at low show rates. This enhancement of E_a is attributed to the

increase in LCBF. Meanwhile Sample 7 (LCBF = 0.17, $M_w = 160$ kg/mol) has a similar LCBF to Sample 10 (LCBF = 0.17, $M_w = 57$ kg/mol) yet exhibits significantly different activation energies. The E_a of linear polymers, with molecular weights above the critical entanglement length, has been shown to be independent of molecular weight (Wood-Adams, et al., 2001). Therefore the increase in E_a from Sample 10 to Sample 7 is attributed to the difference in LCB length. At higher shear rates the E_a s of the samples decrease to a similar value of about 32 kJ/mol. This complex behavior arises due to multiple relaxation regimes with different temperature sensitivities. The high frequency activation energies are due primarily to the flow of linear chains. Consequently, despite having different LCBFs and M_w s, the samples all have similar high frequency E_a s. The low frequency activation energies are due to the cumulative effect of the relaxations of molecules with various branch structures. Long chain branches have different relaxation mechanisms with different temperature sensitivities than linear chains. Samples with high LCBFs or with high LCB lengths have elevated values of E_a .

4.2.3 Conclusions

The rheological properties of long chain branched polyethylenes produced in a semi-batch reactor were shown to be significantly different from their linear analogues. LCBed PEs have significantly higher η_{0s} and exhibit greater shear thinning than linear PEs with similar molecular weights. These enhancements have been attributed to the formation of additional entanglements between polymer molecules, leading to increased

resistance to flow. At higher shear rates, these entanglements break allowing normal viscosities. Consequently, elevated LCBFs lead to higher η_0 s and greater shear thinning.

Polyethylenes produced in a semi-batch reactor, with similar LCBFs but with higher M_{ws} , have longer LCBs. The longer branches allow additional entanglements, increasing the η_0 more than that predicted by the increased M_w . Also, higher M_w branches produce significantly greater shear thinning.

Long chain branching also influenced the loss modulus and storage modulus. Elevated LCBFs led to enhanced values of G' and G'' at low shear rates yet had little influence at higher shear rates. LCBed PEs also exhibited broader relaxation spectrums than linear PEs.

The long chain branched PE exhibited thermorheologically complex behavior. The temperature sensitivity of η , G' and G'' could not be summarized with a single shift factor. The activation energy, which was shear dependant, was determined using the G' . Higher LCBFs and LCB lengths led to elevated values of E_a at low shear rates. At high shear rates, the values of E_a were similar to that of linear polymers.

The work of Section 4.2 has been organized together with Section 5.2 and is being prepared for publication (Kolodka et al., 2002).

4.3 Rheological Behavior of Long Chain Branched Polypropylene

4.3.1 Experimental

A series of novel polypropylenes (PP) were produced with controlled levels of poly(ethylene-co-propylene) (EPR) long chain branches as detailed in Chapter 3 (Section 3.4). The long chain branch frequency, long chain branch length, and copolymer molecular weight were controlled yielding model long chain branched polymers. The detailed polymer characterizations are listed in Table 4.2

Table 4.2 Results of the copolymerization of propylene with poly(ethylene-co-propylene) macromonomers using semi-batch reactor

Run	Macro. M_N (g/mol) ¹	M_N ¹ (kg/mol)	PDI	Wt. % EPR ²	LCBF ²	η_0^* ($\times 10^{-3}$) (Pa s)	n
1	2560	59.0	2.7	7.6	1.8	1.03	0.63
2	3900	59.1	2.7	10.7	1.6	1.05	0.62
3	6,010	54.8	2.6	8.6	0.8	1.63	0.62
4	7,820	41.0	3.2	15.7	0.8	2.32	0.58
5	11,200	41.0	2.9	16.1	0.6	3.03	0.56
6	17,100	99.0	2.8	8.7	0.4	24.5	0.42
7	2560	97.7	2.5	--	--	10.4	0.60
8	2560	53.0	2.7	2.4	0.5	0.76	0.61
9	2560	55.2	2.4	4.5	1.0	0.68	0.63
10	2560	48.3	2.7	5.4	1.0	0.86	0.62
11	17,100	75.0	2.4	1.4	0.1	1.35	0.58
12	17,100	80.0	2.3	3.3	0.2	4.72	0.52
13	2560	248.9	2.5	8.3	8.8	n.m.	n.m.
14	2560	31.7	2.4	5.3	0.7	n.m.	n.m.
15	2560	29.4	2.4	4.5	0.8	n.m.	n.m.

The polymerization conditions were: catalyst = MBI, co-catalyst = MMAO, solvent = toluene, solvent volume = 200 ml, semi-batch reactor

1) Determined using GPC

2) Determined by massing unreacted macromonomer

The test samples were blended with 0.6 weight percent Irganox 1010 antioxidant to prevent degradation. The antioxidant was dissolved in acetone and mixed with the polymer powder. The acetone was evaporated for 24 hours in a fumehood and the polymer dried in a vacuum oven for 48 hours at 80 °C. The samples were then melt pressed (20 mm diameter, 2 mm thickness) at 180 °C and 2 MPa for 6 minutes followed by rapid quenching.

All rheological measurements were conducted on a Stresstech HR parallel plate rheometer in dynamic mode with a gap of 1.5 mm. Samples were measured in 10 °C increments between the temperatures of 170 to 220 °C under a nitrogen blanket to prevent degradation. Strain sweeps were performed prior to frequency sweeps in order to establish the linear region. A frequency range of 10^{-2} to 65 s^{-1} was investigated using a variable strain method. This method entails using the maximum strain that is within the linear region.

The influences of long chain branch length and frequency on the storage modulus $G'(\omega)$, loss modulus $G''(\omega)$, and complex viscosity η^* , as defined in Equation 4.4, were investigated. The rheological data, generated at multiple temperatures, was superimposed to 190 °C using the shift factor a_T given in equation 4.3. The activation energies were calculated using low shear viscosities as shown in equation 4.1.

The long chain branched samples had very long relaxation times at low shear rates and it was not possible to obtain frequency independent viscosities from which the Newtonian viscosities (η_0) could be inferred. An attempt at fitting the viscosity data using the Cross equation, given by Equation 4.5, was made with the value of n assumed to be independent of temperature and the characteristic time, λ , to be proportional to η_0 . Unfortunately, solutions were not found for these samples. Therefore, we have approximated η_0 with the complex viscosity measured at $\omega = 0.01 \text{ s}^{-1}$. In order to quantify the shear thinning behavior, the power-law expression, given by Equation 4.6, was fitted to the viscosity data at high shear rates.

4.3.2 Results and Discussion

Effect of Macromonomer Molecular Weight

The influences of the long chain branch length (MW) on the η^* , G' , G'' , and apparent E_a were studied. The MW, MWD, and long chain branch frequencies of Samples 3, 4, 5, 6, 9, as shown in Table 4.2, were determined to be similar, with the exception of sample 6. Therefore, we feel justified in comparing the rheological responses of these samples. Figure 4.14 shows the complex viscosities of samples with various branch lengths, ranging from well below M_C to well above.

From this figure it is readily apparent that the branch length has a significant influence on the complex viscosity over the entire frequency range studied. Sample 9,

with long chain branch lengths below M_C , behaves similarly to linear PP. The EPR branches were not long enough to form sufficient entanglements to affect the viscosity. When the branch M_N was increased to 6000 g/mol, a significant enhancement in η_0 was seen. Further increases in the branch M_N led to greater increases in η_0 . At low shear rates, the viscosity is dominated by the relaxation behavior of branched polymer molecules. An increase in branch M_N permits the formation of additional entanglements, leading to increased low shear viscosities.

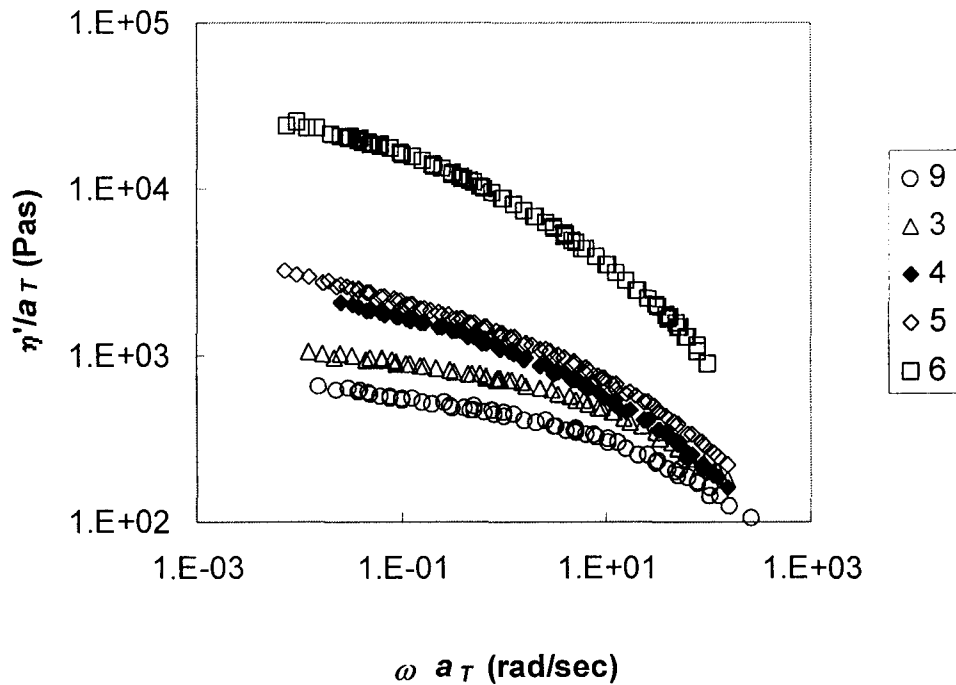


Figure 4.14 Influence of branch MW on the dynamic viscosity

It must be noted that there was a significant decrease in M_N from Sample 3 to Sample 4. Despite this decrease, the viscosity of sample 4 was markedly higher. Furthermore, there was a decrease in LCBF from Sample 4 to Sample 5, and yet the

viscosity still showed enhanced values in Sample 5. At high shear rates, the viscosity is dominated by the flow of linear chains. Consequently, because these samples had similar M_N , it was expected that the high shear viscosities would be similar. This behavior was indeed observed in Figure 4.14. When the shear rate approached 100 s^{-1} the viscosities almost overlapped. This phenomenon also had a significant influence on the shear thinning of the polymer samples.

Figure 4.15 shows a plot of the power-law exponent n , and the low shear viscosity measured at $190 \text{ }^\circ\text{C}$, versus branch length. It can be seen that increasing the M_N of the branches significantly increased the shear thinning behavior of the copolymers. The power law exponent n shows a rapid decrease with increasing branch length, indicating a further deviance from Newtonian behavior.

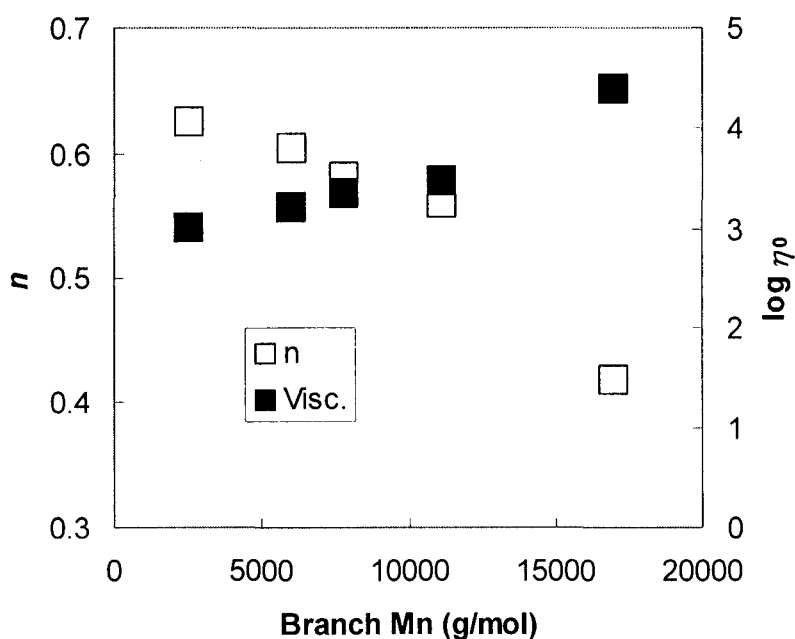


Figure 4.15 Influence of branch length on the Power-law exponent n and on the η_0

The branch length also had a significant influence on the loss modulus and storage modulus. The values of G' and G'' for Samples 3 and 5 at 170 °C are shown in Figure 4.16, with the remainders omitted to prevent crowding. Samples 3 and 5 had similar MWs and MWDs, with branch M_N of 6000 and 11100, respectively. It is readily apparent that Sample 5, with a longer branch length, had significantly higher values of G' and G'' at low shear rates, while at high shear rates they were similar.

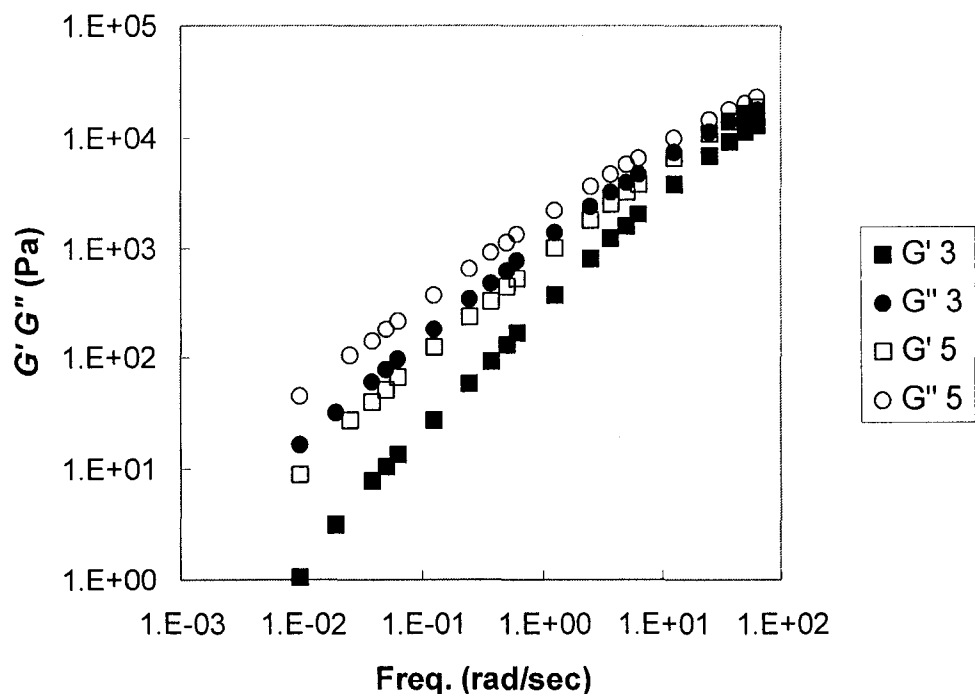


Figure 4.16 Influence of branch length on G' and G''

The branch MW had a significant influence on the flow activation energy, as can be seen in Figure 4.17. When the branch M_n was 2500 g/mol, the observed activation

energy was 37.7 kJ/mol. This is only slightly above the accepted value for linear PP (Sugimoto et al., 2001). As the branch length was increased, the E_a increased linearly to a maximum of 48.9 kJ/mol at a branch M_n of 17000. This value is significantly higher than that of linear PP, but still lower than the 55 kJ/mol reported by Kurzbeck et al. (1999) for PP modified with electron-beam irradiation.

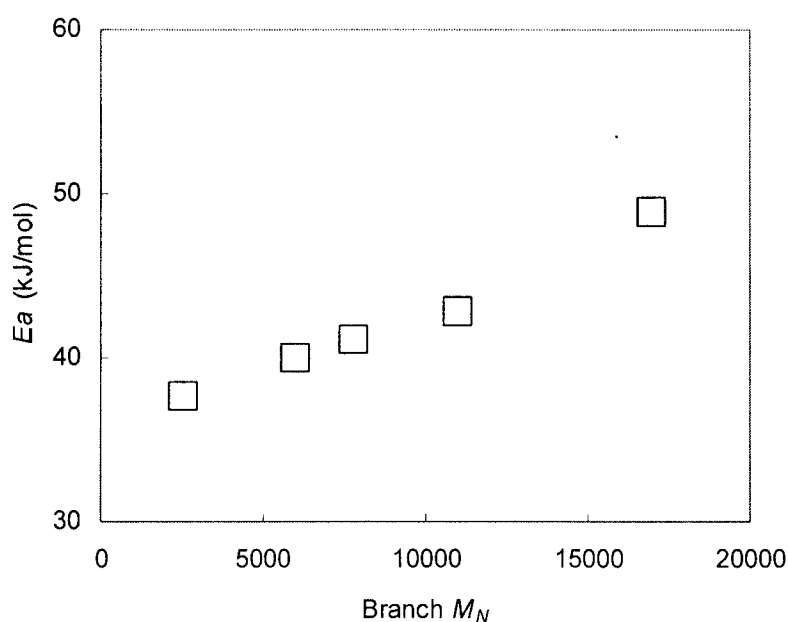


Figure 4.17 Influence of branch length on activation energy.

Effect of Long Chain Branch Frequency on the Rheology

In order to verify the influence of long chain branching beneath the critical entanglement length, the LCBF was varied from 0.5 to 1.8 with a branch M_n of 2500 g/mol. The MW and MWD of these samples were similar with M_{NS} of approximately 55000 g/mol. Figure 4.18 shows a plot of dynamic viscosity versus frequency for

Samples 8, 9, and 1. From this figure it is readily apparent that the LCBF did not have a significant influence on the η^* when the branch length was 2500 g/mol. It is theorized that the EPR branches were not long enough to form entanglements and consequently behaved as short chain branches.

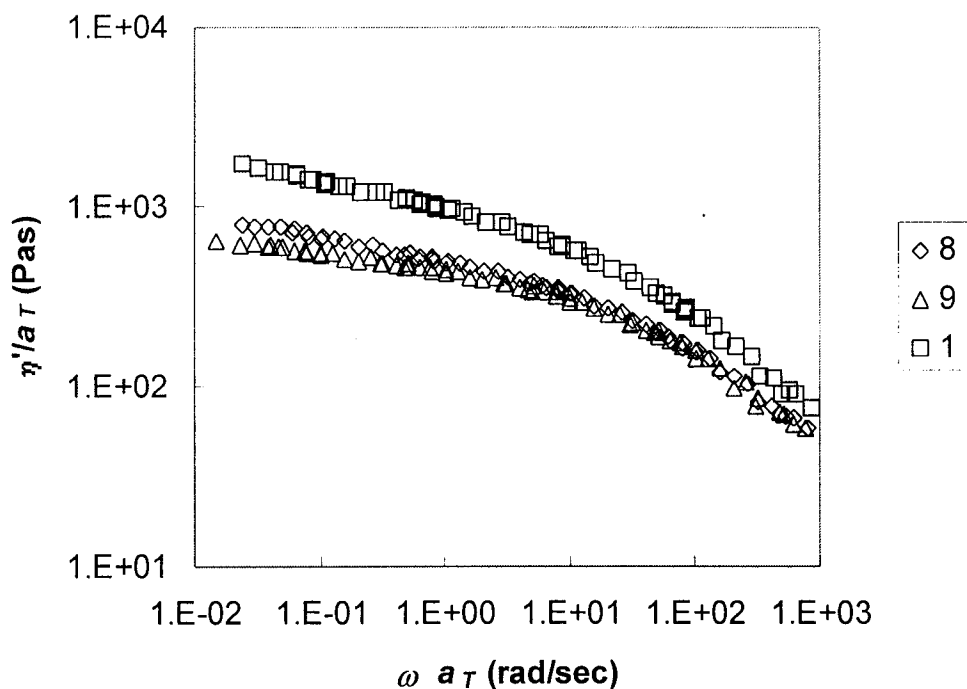


Figure 4.18 Influence of LCBF on dynamic viscosity having branches of M_N 2500 = g/mol

Figure 4.19, meanwhile, shows G' and G'' versus frequency. Again, the LCBF had little influence on the loss modulus and storage modulus when the branch M_N was 2500 g/mol. It was also shown, in Figure 4.20, that when the branch M_N was 2500 the LCBF had no significant influence on E_a .

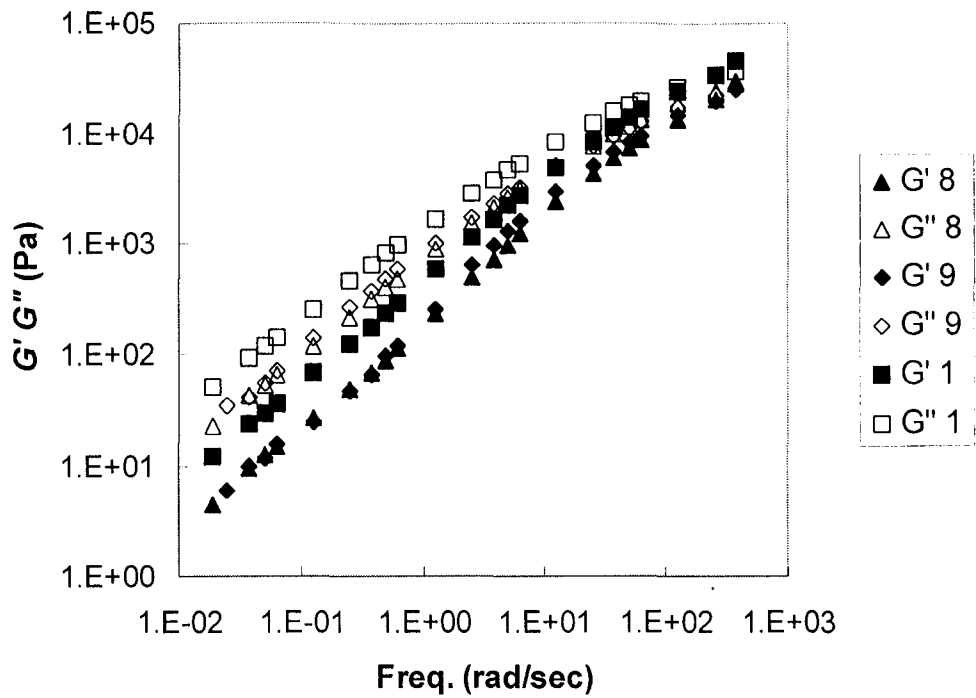


Figure 4.19 Influence of LCBF on G' and G'' with branches of $M_N = 2500$ g/mol

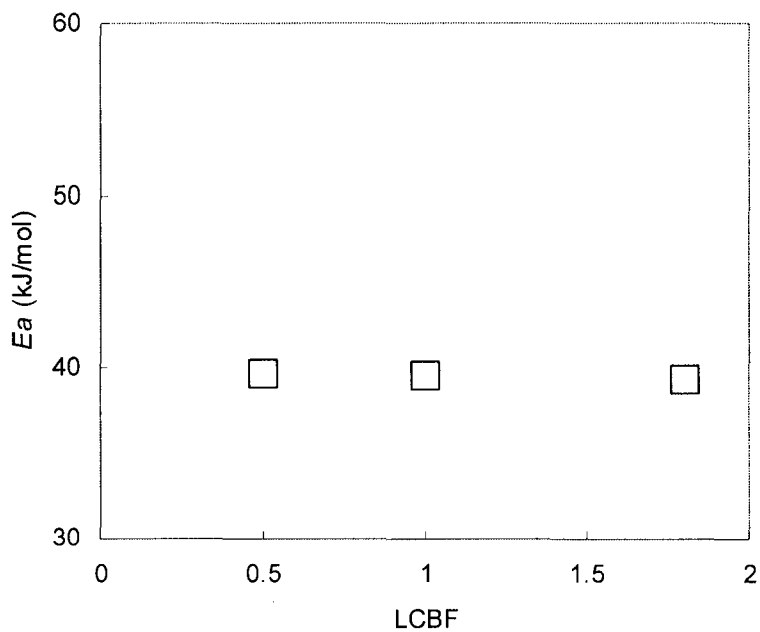


Figure 4.20 Influence of LCBF on E_a with branches of $M_N = 2500$ g/mol

The influence of the frequency of long chain branches with MWs above M_C was also studied. Figure 4.21 shows a plot of η^* versus frequency for Samples 11, 12, and 6, which have a branch M_N of 17000 g/mol. These samples have copolymer M_N ranging from 60000 to 99000 and consequently the MW may have had an influence on the observed rheological responses. It can readily be seen that the LCBF had a significant effect on the η^* over the entire frequency range. As was expected, the η_0^* was a sensitive indicator of branch frequency, with significant enhancements observed with increased LCBFs. The viscosity at low shear rates is dominated by the relaxation of branched molecules. An increase in the branching frequency increases the number of entanglements and leads to an enhancement in η_0^* . The LCBF also affected the shear-thinning phenomenon. Sample 6, with a LCBF of 0.4, exhibited considerably more shear thinning than Sample 12 with a LCBF of 0.2. Sample 12 in turn was more shear sensitive than Sample 11, with a LCBF of 0.1.

Figure 4.22 shows the influence of LCBF on G' and G'' . It is apparent that the LCBF had a strong influence on the dynamic moduli. Sample 6 had considerably higher values for both G' and G'' than Sample 11. Sample 6 also exhibited a broader relaxation spectrum as is evident by the more gradual increase in G' . This behavior is attributed to the additional modes of relaxation provided by long chain branching.

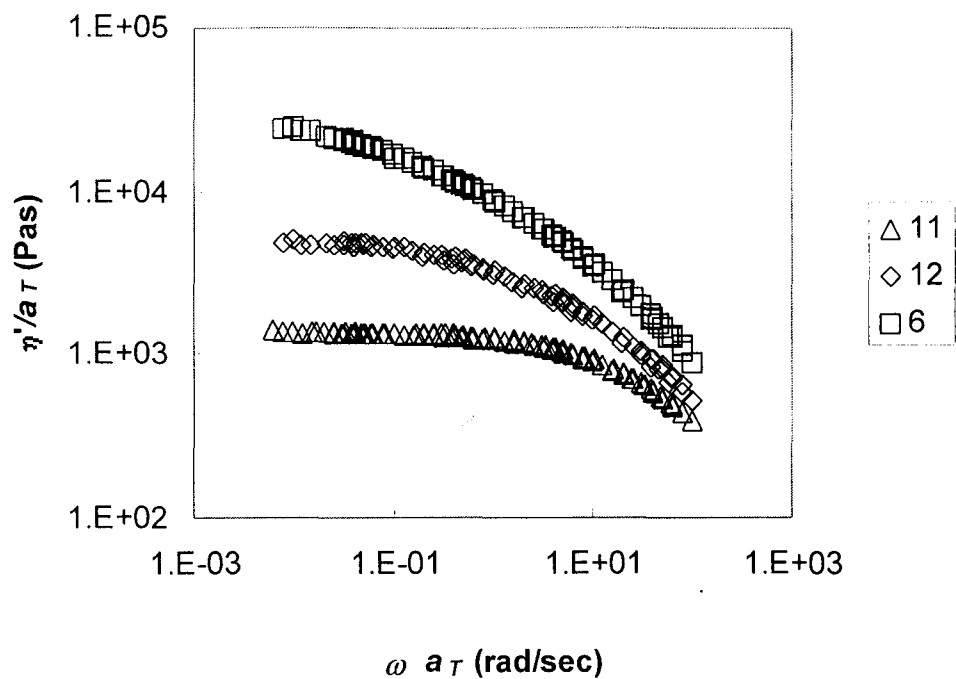


Figure 4.21 Influence of LCBF on dynamic viscosity with branches of $M_N = 17000$ g/mol

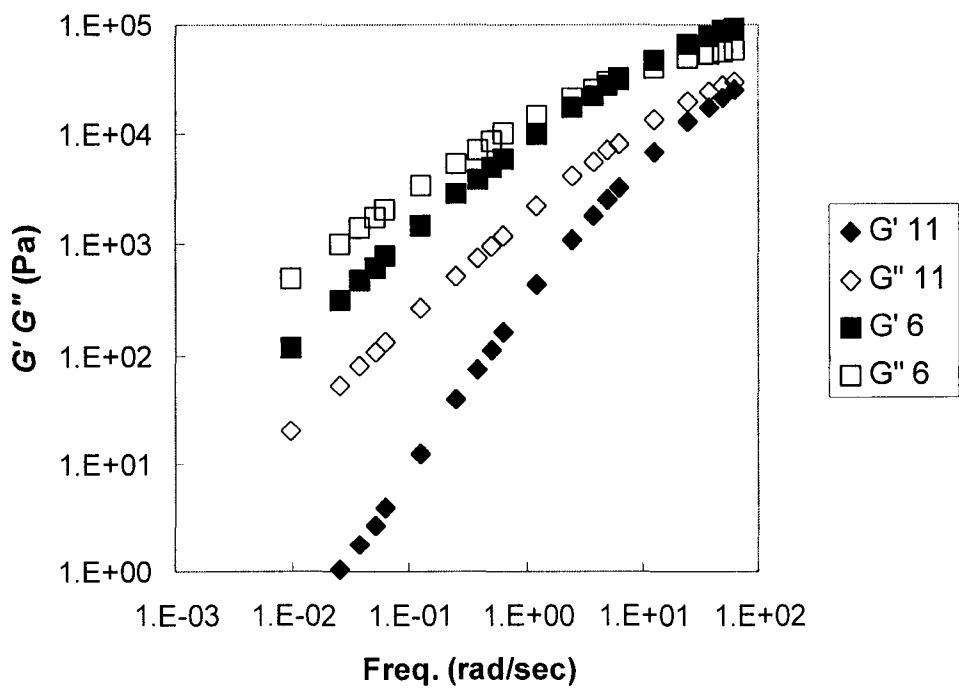


Figure 4.22 Influence of LCBF on G' and G'' with branches of $M_N = 17000$ g/mol

It is readily apparent in Figure 4.23 that the LCBF of samples with branch M_N of 17000 had a significant influence on E_a . It was observed that E_a varied linearly with LCBF.

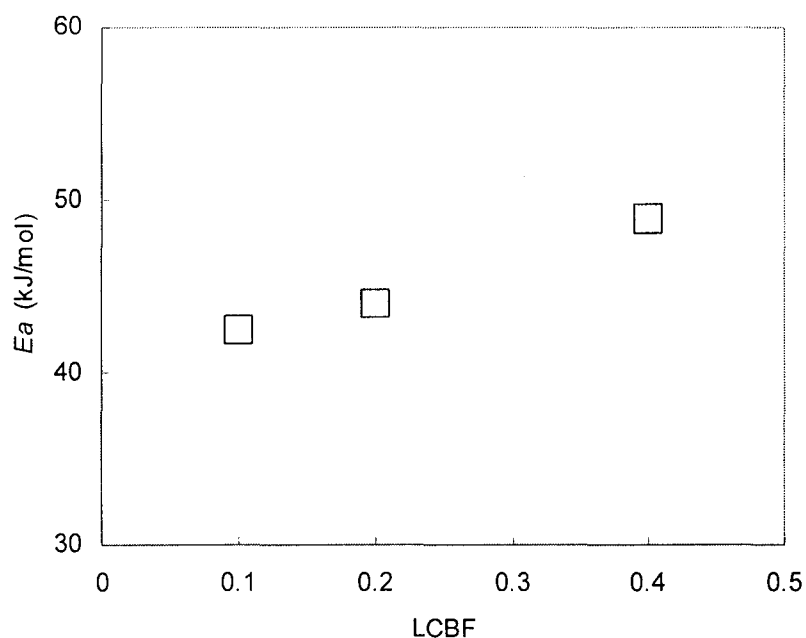


Figure 4.23 Influence of LCBF on E_a with branches of $M_N = 17000$ g/mol

It is interesting to compare the behavior observed in Figures 4.19 to 4.21 with Figures 4.22 through 4.24. When the MW of the branches was 2500 g/mol, which is below M_c , the long chain branch frequency did not appear to have a large influence on the measured rheological responses. However, when the branch length was increased to 17000 g/mol the LCBF had a strong influence on η^* , G' , and G'' and E_a .

4.3.3 Thermorheological Complexity

The long chain branched PP samples produced in this study were examined for the thermorheological complexity observed in LCB PE. The method outlined by Wood-Adams (Wood-Adams and Costeux, 2001) was used to determine rheological complexity. Plots of G^* versus $\eta_0 \times \omega$ are temperature independent for simple materials and display temperature dependence for complex materials. Using this criterion, only Sample 6 exhibited rheological complexity, as shown in Figure 4.24.

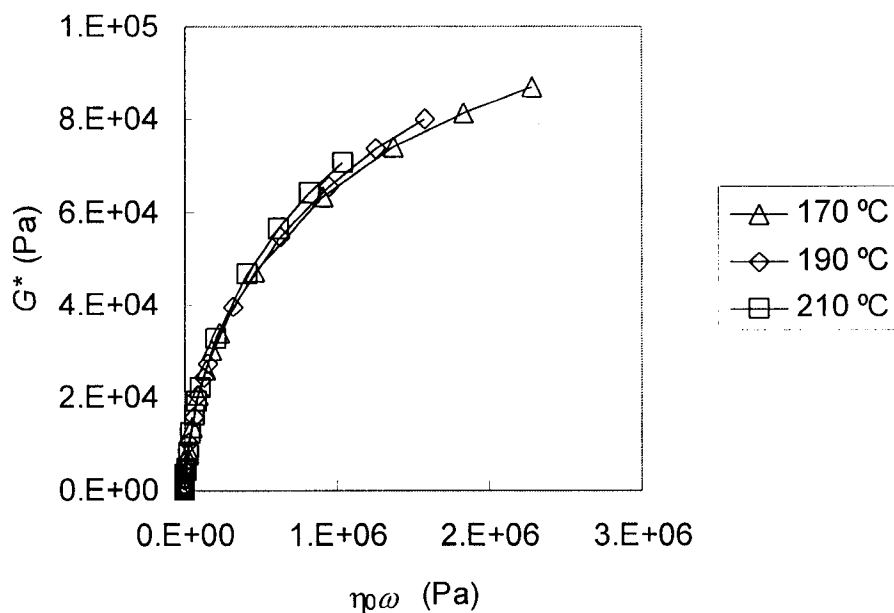


Figure 4.24 Rheological Complexity of Sample 6

The shift factor a_T was determined for the entire experimental frequency range for sample 6 using G' in the manner shown in Figure 4.12. Figure 4.25 shows the activation energy versus shear rate for Samples 1 and 6. It can be seen that Sample 1 exhibited

simple rheological behavior while the activation energy of Sample 6 showed a dependence on the shear rate. Sample 6 had an activation energy of approximately 50 kJ/mol at $\omega = 0.01 \text{ s}^{-1}$, which is similar to the value calculated using η_0 . At higher shear rates, the activation energy decreased to 29.2 kJ/mol. This behavior is attributed to the additional modes of relaxation at low shear rates caused by branched molecules. The rheological behavior at high shear rates is dominated by the reptation of linear chains. Therefore the activation energy of Sample 6 at high shear rates is similar to that of linear PP.

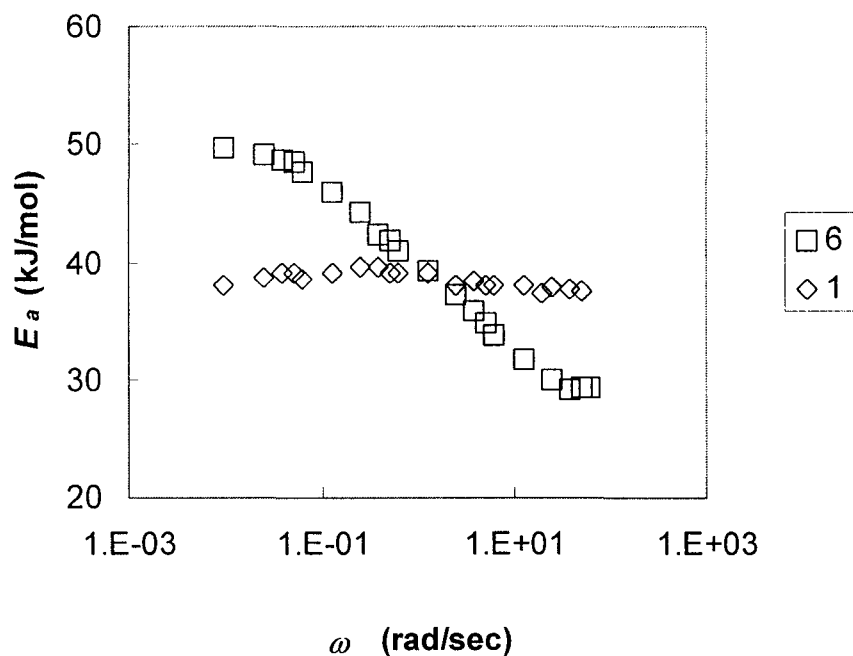


Figure 4.25 Time dependent activation energies of Sample 6

4.3.3 Conclusions

A series of model polypropylenes with poly(ethylene-co-propylene) (EPR) long chain branches were synthesized in a semi-batch reactor. The molecular weight of both the copolymer and the long chain branch were controlled as was the long chain branch frequency. The rheological behavior of the resultant long chain branched polypropylenes were measured. It was shown that when the branch M_N was less than 7000 g/mol, it behaved as a short chain branch and had little influence on the rheological responses. When the branch M_N was greater than 7000 g/mol it was long enough to form entanglements and behaved as a long chain branch. When above M_C , the branch length had a significant influence on the rheological responses. Both G' and G'' showed elevated values at low shear rates. The η_0^* was a sensitive indicator of branch length. Increasing branch M_N led to enhanced values of η_0^* . The shear-thinning phenomenon also increased with increasing branch length, as did the flow activation energy. The long chain branch frequency also had a strong influence on the rheological behavior of the polymer samples provided the branch M_N was greater than 7000 g/mol. Increases in LCBF led to increased η_0^* s, increased shear thinning, enhanced flow activation energies, and to elevated values of G' and G'' . The long chain branched samples were found to exhibit thermorheologically simple behavior, excepting Sample 6.

The work of Section 4.3 has been organized together with Section 3.4 and submitted to the journal *Macromolecules* for publication (Kolodka et al., 2002).

Chapter 5

Dynamic Mechanical Properties of Long Chain Branched Polyolefins

5.1 Introduction

Dynamic mechanical analysis (DMA) is a powerful technique for characterizing relaxations in amorphous and semi-crystalline polymers. It is sensitive to the structural heterogeneity because of the strong influence of such variables as crystallinity, lamellar thickness, and interfacial structure on the relaxation behaviour (Khanna et al., 1985). DMA also provides a quantitative method of determining the stiffness of a polymer as well as the damping characteristics at various temperatures. In extension or bending the dynamic Young's modulus (E^*) is given as stress amplitude / strain amplitude. However, when internal molecular motion occurs in the same frequency range as the imposed stress, the material responds in a visco-elastic manner and the strain response lags behind the stress. The Young's modulus is typically resolved into perfectly elastic (storage modulus) and perfectly viscous (loss modulus) components, as shown in Equation 5.1 (Wetton, 1984).

$$E^* = E' + iE'' \quad (5.1)$$

where E^* is the complex Young's modulus, E' is the storage modulus which measures the stiffness of the sample, E'' is the loss modulus, and $i = \sqrt{-1}$. The angle that reflects the time lag between the applied stress and strain is δ , and is defined by a ratio called the loss tangent, as shown in Equation 5.2.

$$\tan \delta = \frac{E''}{E'} \quad (5.2)$$

Tan δ is a damping term and is a measure of the ratio of energy dissipated as heat to the maximum energy stored in the material during one cycle of oscillation (Nielsen and Landel, 1994). Relaxation regimes in DMA appear as peaks in G'' and $\tan \delta$ and as a step transitions in G' . Typically, the relaxation points are studied using G'' or $\tan \delta$.

Polyethylene

Three relaxations are observed in polyethylene, identified as α , β , and γ in order of decreasing temperature. The α -relaxation is observed between 30 °C and the melting point, the β -relaxation between -55 and 25 °C, and the γ -relaxation between -145 and -95 °C.

The α -relaxation observed in polyolefins is generally associated with motion within the crystalline phase and intensifies with increasing crystallinity (Nitta et al., 1999). The α -relaxation is influenced by the crystallite thickness and crystal imperfections but is thought to be independent of branch type and molecular weight (Keating et al, 1999). It has been observed that the α -relaxation in polyethylenes is composed of two overlapping peaks, α_1 and α_2 (Suhm et al., 1998, Rossi et al., 1996). The α_1 relaxation is attributed to intralamellar slip and / or motion in the intercrystalline region. The α_2 relaxation is due to intracrystalline chain motion involving transitional motion of chain segments along the c-axis within the crystal lattice (Rossi et al., 1996).

The β -relaxation yields considerable information about the chain architecture of PE, although there is still some controversy regarding the origin and molecular nature of the β -relaxation. It is thought to be due to motion in the amorphous phase near branch points (Ohta and Yasuda, 1994). It has been shown that the width of the β -relaxation peak correlates well with the chemical composition distribution (CCD) of short chain branching. Polymers produced with single-site type catalysts, which provide narrow CCDs, have narrower β -relaxations located at higher temperatures than polymers produced with traditional Ziegler-Natta PEs (Stark et al., 2002). The temperature of the β -relaxation is also dependent on the branch density, with higher branch densities having lower β -relaxation temperatures (Keating and Lee, 1999). Linear polyethylene with no branching generally does not display a β -relaxation, however, researchers have observed β -relaxations in ultra high molecular weight PE (Starck et al., 2002). The β -relaxations were attributed to the glass transition of loose loop and intercrystalline tie molecules. The impact strength of the polyolefin can also be correlated to the area of the β -relaxation peak (Stark et al., 2002, Jafari and Gutpa, 2000), with greater areas providing enhanced impact strengths.

The γ -relaxation peak, although not as widely studied as the β -relaxation phenomenon, also provides information about the structure of the polymer. The γ -relaxation is generally believed to be due to crankshaft rotation of short methylene main chain segments at the surface of polymer crystals, although the exact mechanism has yet to be determined. The γ -relaxation is generally accepted as the glass transition

temperature (T_g) of PE. The γ -relaxation peak shifts to lower temperatures and sharpens with decreasing short chain branch content.

Polyolefin Blends

There has been a great deal of research focused on improving the impact strength of polypropylene by blending with olefin elastomers, such as ethylene propylene rubber (EPR). This blend has been shown to be incompatible and forms a two-phase system. When the rubber content is below approximately 30 volume percent, an isotactic polypropylene matrix with dispersed rubbery domains results (Yamaguchi et al., 1996). Impact modified polypropylene exhibits significantly higher fracture resistance, impact strength, elongation at break, and fracture toughness than unmodified polypropylene. Drawbacks include reduced modulus, tensile strength, and transparency (Pukanszky et al., 1989). Important factors influencing these properties are interfacial adhesion, the nature of the matrix and rubber, the rubber concentration, and the size, shape and dispersion of the domains (Norzalia et al., 1994). Previous studies have demonstrated that optimal toughening occurs when the rubbery domains are approximately 0.35 – 0.40 μm in diameter and are well dispersed (D'Orazio et al., 1999). It is generally accepted that the major mechanisms of toughening are shear yielding and crazing. Considerable work has also been conducted on low ethylene-content propylene copolymers. Feng et al. observed phase separation in block propylene-ethylene copolymers while random copolymers remained homogeneous (Feng et al., 1998). In contrast, Nitta et al. reported

no phase separation for polypropylene-block-poly(ethylene-co-propylene) polymers (Nitta et al., 1999).

Section 5.2 outlines the dynamic mechanical analysis of high density polyethylene synthesised using Cp_2ZrCl_2 in a semi-batch, slurry phase reactor. The polyethylene samples had long chain branch frequencies ranging from 0.03 to 0.22 branches per chain and M_w s ranging from 63 to 280 kg/mol. The details regarding the synthesis are found in Section 3.2 while the rheological properties are described in Section 4.2. Section 5.3 describes the dynamic mechanical properties of a series of novel polymers with isotactic polypropylene backbones and controlled levels of poly(ethylene-co-propylene) branches. The molecular weight of the EPR was varied from well beneath the critical entanglement length of approximately 6000 g/mol to well above, with number-average molecular weights M_N of 2500, 3900, 6000, and 11000 g/mol (Kolodka et al., 2002). The details regarding the synthesis can be found in Section 3.4 while the rheological properties are presented in Section 4.3. The amount of EPR for this study was held constant at 10% weight. The rubber content for a low molecular weight EPR sample ($M_N=2500$) was also varied, with the EPR weight percent ranging from 3.4 to 11.5. The morphological development of the various copolymers was examined using dynamic mechanical analysis. These results were then compared to commercial isotactic polypropylene and high impact polypropylene products.

5.2 Dynamic Mechanical Behaviour of Long Chain Branched Polyethylene

5.2.1 Experimental

A series of LCB PEs were produced in a slurry phase, semi-batch reactor using zirconocene dichloride / modified methylaluminoxane as outlined in Section 3.2. The molecular properties and relaxation temperatures of the tested polymers are listed in Table 5.1.

Table 5.1. Molecular properties of long chain branched polyethylene samples

Run	M _N (g/mol)	M _W (g/mol)	M _W /M _N	LCBD ^{a)}	LCBF ^{a)}	α-relax. (°C)	β-relax. (°C)	γ-relax. (°C)
1	115000	280000	2.44	0.25	0.16	53.24	--	-117.15
2	60600	154000	2.54	0.33	0.12	52.19	--	-115.72
3	46200	108000	2.34	0.10	0.03	52.35	--	-115.69
4	38900	95000	2.44	0.73	0.22	52.51	--	-116.50
5	46400	122000	2.63	0.65	0.21	51.93	--	-115.43
8	54100	152000	2.81	0.21	0.07	51.46	--	-115.41
10	27800	57000	2.05	0.86	0.17	49.13	--	-115.56

The polymerization conditions were: catalyst = Cp₂ZrCl₂, co-catalyst = MMAO, solvent = toluene, solvent volume = 700 ml. SB = Semi-Batch Reactor

1) Determined using ¹³C NMR

The test samples were blended with 0.6 weight percent Irganox 1010 antioxidant to prevent degradation. The antioxidant was dissolved in acetone and mixed with the polymer powder. The acetone was evaporated for 24 hours in a fumehood and the polymer dried in a vacuum oven for 48 hours at 80 °C. The samples were then melt

pressed (10 mm width, 2 mm thickness, and 30 mm length) at 180 °C and 2 MPa for 6 minutes followed by rapid quenching.

The mechanical properties of the copolymers were measured using a TA Instruments DMA 2980 dynamic mechanical analyzer. The storage modulus E' , the loss modulus E'' , and the loss tangent $\tan(\delta)$ ($=E'/E''$) were measured between -140 °C and 130 °C. A heating rate of 2 °C/min and a displacement of 2 μm were employed. The thermal transitions were taken as the temperature of the maximum of E'' . The measurements for all the samples were made at identical conditions and were repeated twice for a valid and reliable comparison of results.

5.2.2 Results and Discussion

The influences of long chain branch frequency and polymer M_w on the storage modulus E' , loss modulus E'' , and α , β , and γ -relaxations were investigated. Figure 5.1 shows the dynamic mechanical behaviour of Sample 2 ($M_w=154$ kg/mol, LCBF=0.12) which is representative of high density polyethylene.

It can readily be seen by observing the loss modulus that there are only two thermal relaxations present. The α -relaxation was located at 52.2 °C while the γ -relaxation was found at -115.7 °C. None of the long chain branched HDPE samples displayed a β -relaxation process. The β -relaxation peak is thought to be due to motion in the amorphous phase near branch points (Ohta and Yasuda, 1994) or to the glass

transition of loose loop and intercrystalline tie molecules in ultra high molecular weight PE (Starck et al., 2002). The branch content of these essentially linear samples was too low to produce a large enough amorphous phase to exhibit a β -relaxation process.

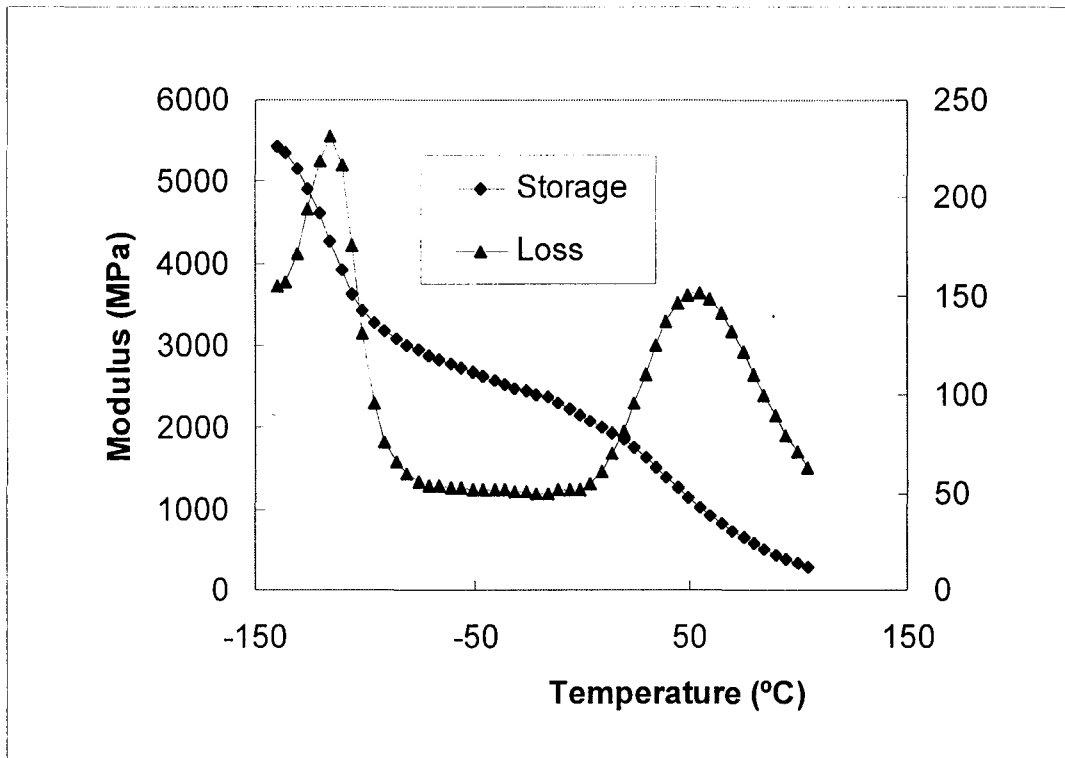


Figure 5.1 Dynamic mechanical behaviour of high density polyethylene

In order to determine the influence of long chain branching on the dynamic mechanical properties of PE an effort was made to produce samples with varying LCBFs and with similar molecular weights. The storage modulus and loss modulus of Samples 3 ($M_w=108$ kg/mol, LCBF=0.03), 4 ($M_w=95$ kg/mol, LCBF=0.22), and 5 ($M_w=122$ kg/mol, LCBF=0.21) are shown in Figure 5.2 and 5.3, respectively, while Figures 5.4 and 5.5 show Samples 2 ($M_w=154$ kg/mol, LCBF=0.12) and 8 ($M_w=152$ kg/mol,

LCBF=0.07). These samples have similar molecular weights and polydispersity indexes and therefore any variation in behaviour is attributed to long chain branching.

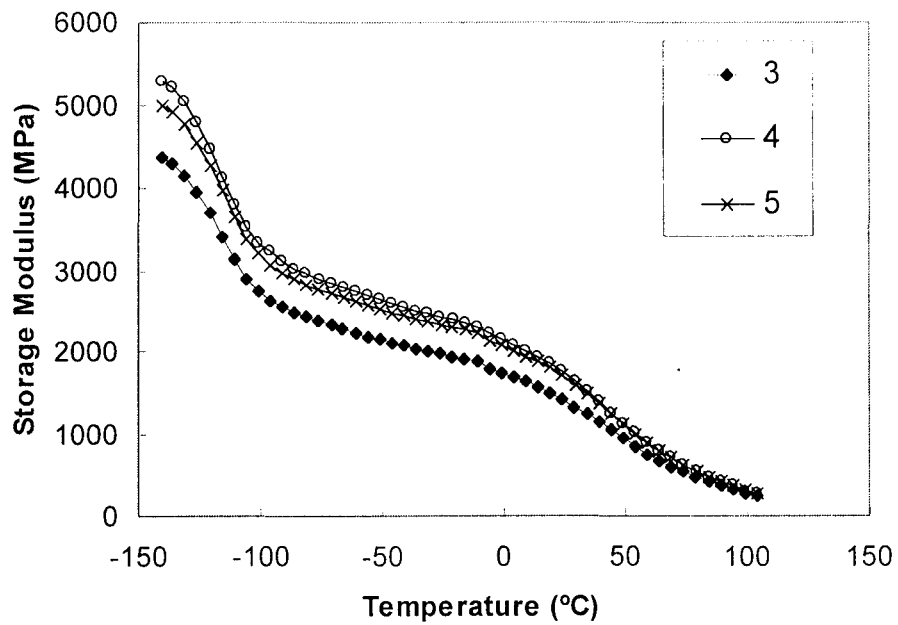


Figure 5.2 Storage Modulus of Samples 3, 4 and 5

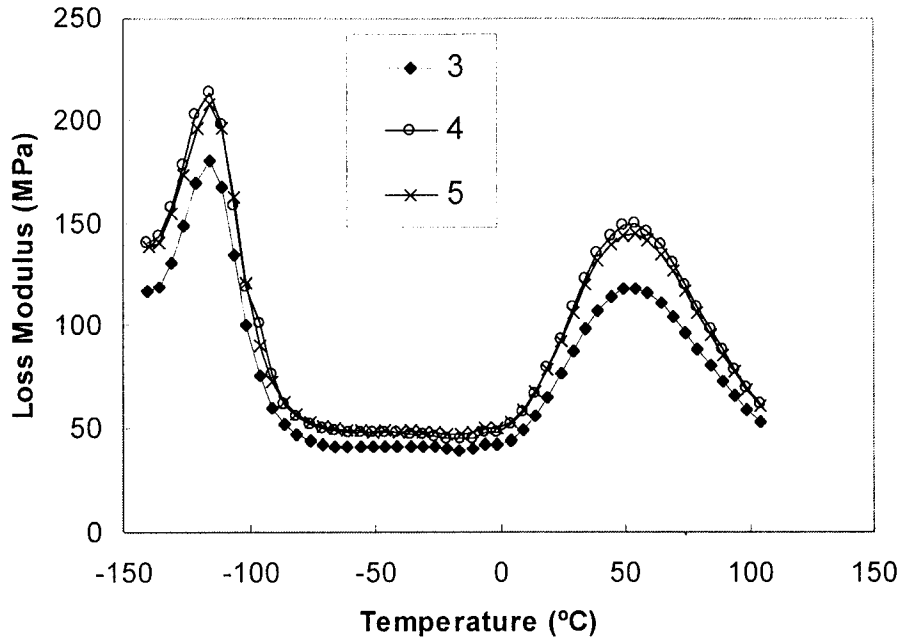


Figure 5.3 Loss modulus of Samples 3, 4 and 5

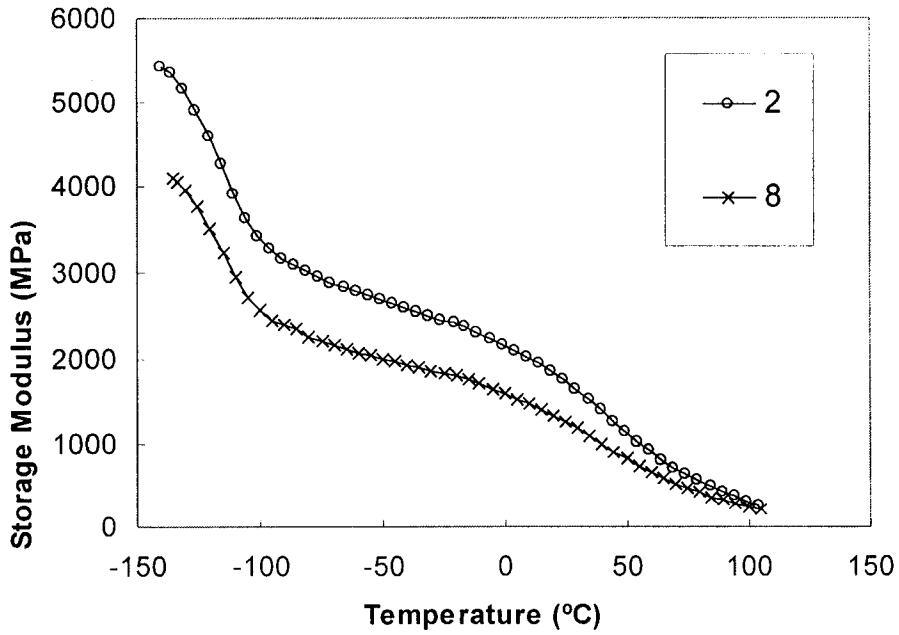


Figure 5.4 Storage modulus of Samples 2 and 8

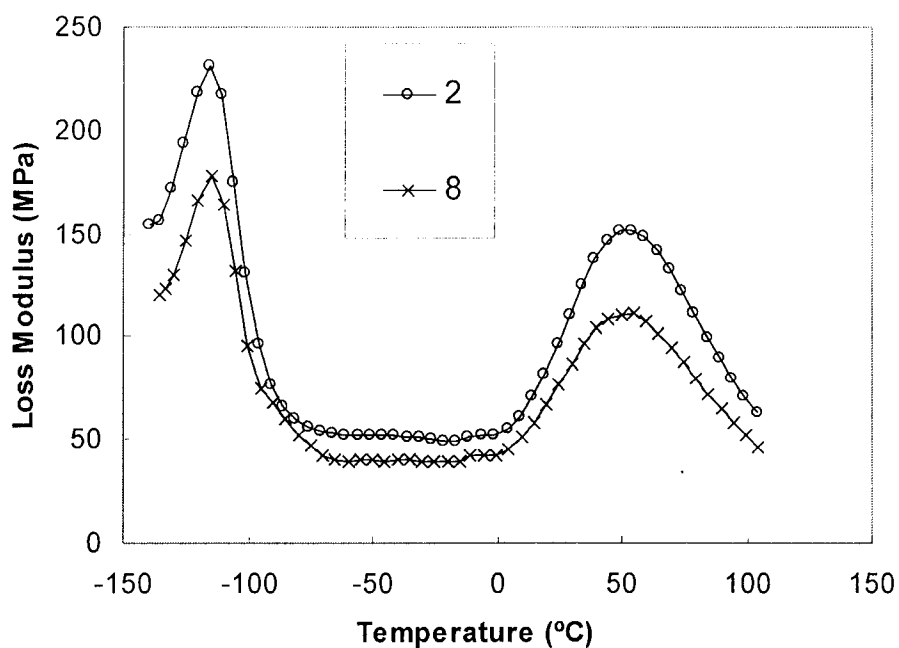


Figure 5.5 Loss modulus of Samples 2 and 8

It can readily be seen in Figures 5.2 and 5.4 that the long chain branch frequency has a significant influence on the storage modulus of polyethylene. The storage modulus of Sample 3 (LCBF=0.03), shown in Figure 5.2, is significantly lower than that of Sample 4 (LCBF=0.22) at all temperatures below the α -relaxation point. Sample 4, moreover, responds in an almost identical fashion as Sample 5 (LCBF=0.21). In a similar manner, Sample 8 (LCBF=0.07) has a significantly lower storage modulus than Sample 2 (LCBF=0.12), as seen in Figure 5.4. In all cases an increase in the long chain branch frequency led to an increase in the storage modulus at all temperatures below the α -relaxation point.

The LCBF also showed a significant influence on the loss modulus, as seen in Figures 5.3 and 5.5. In all the measured samples, an increase in the LCBF led to enhanced values of E'' . Samples 4 and 5, with similar LCBFs, responded in an almost identical manner while Sample 3 had a significantly lower E'' . Sample 2, shown in Figure 5.5 exhibited enhanced values of E'' at all measured temperatures compared to Sample 8. Studies have shown a correlation with values of the loss modulus and the impact strength (Jafari and Gutpa, 2000), with elevated values of E'' leading to improvements in impact toughness.

There has been a great deal of research conducted on polyethylene and polypropylene treated with peroxides and or radiation. The affects of such treatments are bond scission and the formation of inter and intra molecular cross-links. It has been demonstrated that the storage modulus of high molecular weight polyethylene increases with increasing radiation dosages (Birkinshaw et al., 1986). Furthermore, there was little influence on the $\tan(\delta)$ response, indicating an increase in the loss modulus. Other authors have seen an increase in E' by the addition of low levels of peroxide to PE (Kunert, 1982). With increased peroxide concentration, the E' of PE showed a sharp decline, possibly due to chain scission. The enhancement in the storage modulus has been explained by stiffening due to cross-linking in the amorphous phase, and to a suppression of c-axis slip in the lamellae by internal or surface cross-linking in the crystal phase. Long chain branching has a similar architecture to cross-linked chains, as shown in Figure 5.6, and is therefore expected to behave in a similar manner. Consequently, the

enhancements in E' and E'' observed in this work, have been attributed to the same mechanisms described in cross-linked PE.

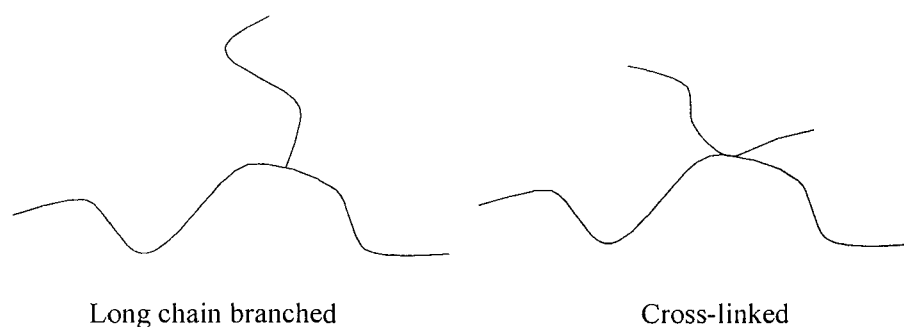


Figure 5.6 Chain architecture of branched polyethylene

The influence of molecular weight on the storage modulus and loss modulus was also examined. Two polyethylenes with widely different molecular weights but with similar long chain branch frequencies were examined. Figures 5.7 and 5.8 show the storage modulus and loss modulus of Samples 1 ($M_w=280$ kg/mol, LCBF=0.16) and 10 ($M_w=57$ kg/mol, LCBF=0.17). It can be seen that the molecular weight of the samples had little influence on the dynamic mechanical properties at temperatures above the γ -relaxation point (glass transition temperature). Despite having a M_w almost five times higher, Sample 1 behaves similarly to Sample 10 except at temperatures below -100 °C. This indicates that the molecular weight of the samples did not have a strong influence on the crystallinity.

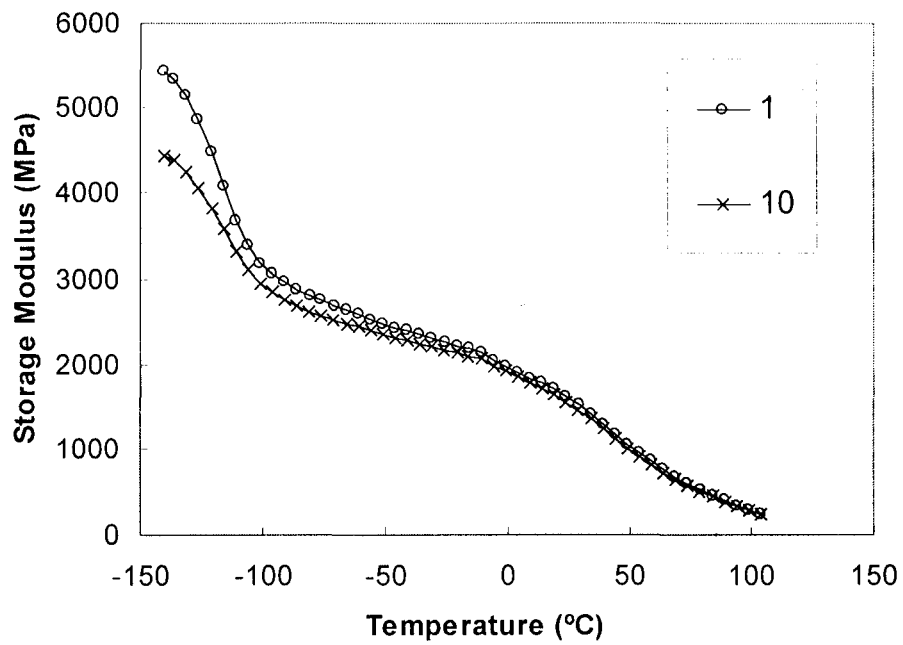


Figure 5.7 Storage modulus of Samples 1 and 10

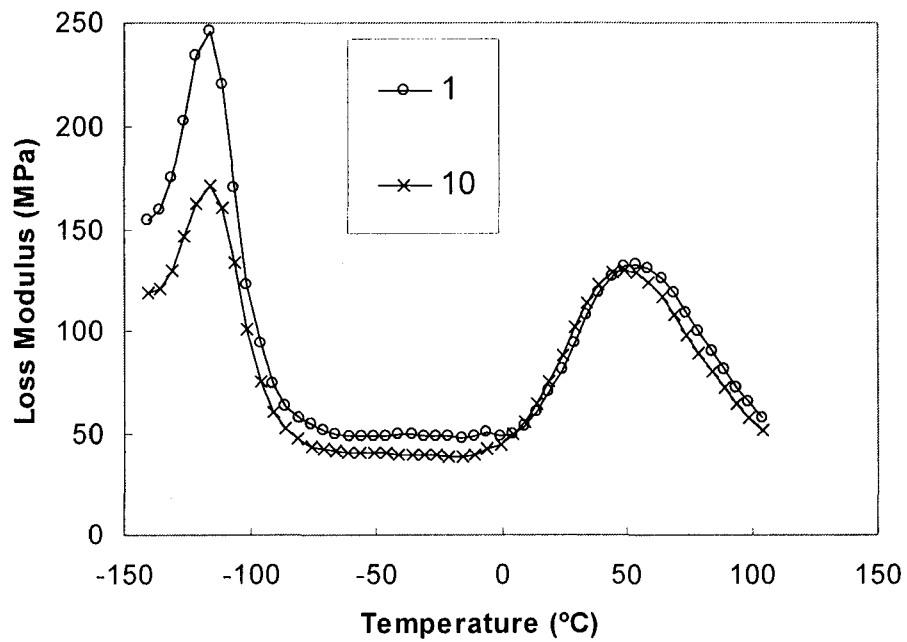


Figure 5.8 Loss modulus of Samples 1 and 10

Long chain branching appeared to have little influence on the thermal relaxations of PE. None of the samples studied exhibited a β -relaxation peak, due to their lack of short chain branches. The LCBF and M_w showed little influence on the γ -relaxation temperature, with values in the range of -115.41 to -117.15 °C. The γ -relaxation is generally believed to be due to crankshaft rotation of short methylene main chain segments at the surface of polymer crystals. The peak has been shown to shift to lower temperatures and sharpen with decreasing short chain branch content. However, long chain branching at low levels did not appear to alter the crystallinity of the polymer enough to influence the γ -relaxation process. The α -relaxation temperature also appeared to be unaffected by the M_w and LCBF of the polymer. This process, thought to be due to motion within the crystalline phase, intensifies with increasing crystallinity (Nitta et al., 2001). The α -relaxation is influenced by the crystallite thickness and crystal imperfections but is thought to be independent of branch type and molecular weight. It was demonstrated that low levels of long chain branching did not have sufficient influence on the crystallinity of PE to affect the α -relaxation temperature.

5.2.3 Conclusions

Long chain branching played a significant role in the dynamic mechanical behaviour of substantially linear polyethylene. Increasing the frequency of branching increased the stiffness of the polymer, as reflected by the increased storage modulus. Long chain branching also served to enhance the damping or energy dissipation of PE,

shown by increased values of the loss modulus. These long chain branched PEs showed behaviour similar to PE cross-linked by radiation or peroxide and a similar mechanism was used to explain the dynamic mechanical differences. The enhancements in E' were attributed to stiffening due to cross-linking in the amorphous phase, and to a suppression of c-axis slip in the lamellae by internal or surface cross-linking in the crystal phase. Long chain branching also had little influence on the crystalline structure of the PE. The α and γ relaxations showed little dependence on the LCBF.

The work of Section 5.2 has been organized together with Section 4.2 and is being prepared for publication (Kolodka et al., 2002).

5.3 Dynamic Mechanical Behaviour of Polypropylene with Poly(ethylene-co-propylene) Long Chain Branches

5.3.1 Experimental

A series of polypropylene (PP) graft copolymers with poly(ethylene-co-propylene) (EPR) branches were synthesized in a two step polymerization process. EPR macromonomers were first prepared in a high temperature high pressure continuous stirred tank reactor (CSTR) using the Dow Chemical constrained geometry catalyst (CGC). The EPR macromonomers were then copolymerized with propylene in a semi-batch reactor using rac-dimethylsilylenebis(2-methylbenz[e]indenyl) zirconium dichloride (MBI) / modified methylaluminoxane (MMAO) as detailed in Chapter 3.4.

The PP-g-EPR copolymers were compared with two commercially available polymers. Medium impact PP (SRD7-665), modified with EPR, was obtained from Union Carbide Corporation while isotactic PP was purchased from Aldrich Chemical. Table 5.2 shows the molecular characteristics of the polymer samples used in this study.

Table 5.2 GPC and ^{13}C NMR results of the polymer samples

Sample	EPR Properties			Copolymer Properties			
	M_n^a	M_w/M_n^a	F_P^b	M_n^a	M_w/M_n^b	Wt. % EPR ^c	T_g (°C)
1	3900	2.5	0.58	59000	2.7	10.7	-4.6
2	6000	2.5	0.42	55100	2.6	9.4	-2.1, -37.7
3	11100	2.5	0.28	41000	2.9	12.2	-1.7, -37.9
4	2500	2.6	0.57	53700	2.7	3.4	-1.6
5	2500	2.6	0.57	55200	2.4	5	-2.2
6	2500	2.6	0.57	59000	2.7	11.5	-6.9
iPP	-	-	-	580000	3.5	-	2.4
SRD7-665	n.a.	n.a.	0.47	n.a.	n.a.	15	0.6, -49.4

^a Molecular weights determined by GPC

^b Propylene weight fraction determined by ^{13}C NMR

^c Determined by incorporation of macromonomer and verified by ^{13}C NMR

The mechanical properties of the copolymers were measured using a TA Instruments DMA 2980 dynamic mechanical analyzer. The test samples were blended with 0.6 weight percent antioxidant and were melt pressed (10 mm width, 2 mm thickness, and 30 mm length) at 180 °C and 2 MPa for 6 minutes followed by a rapid quenching. The storage modulus E' , the loss modulus E'' , and the loss tangent $\tan(\delta)$ ($=E'/E''$) were measured between -80 °C and 120 °C. A heating rate of 2 °C/min and a displacement of 2 μm were employed. The glass transition temperature (T_g) was taken as the temperature of the maximum of E'' . The measurements for all the samples were made at identical conditions and were repeated twice for a valid and reliable comparison of results.

5.3.2 Results and Discussion

Effect of EPR Molecular Weight

The influence of the molecular weight of the grafted EPR on the morphological development of the copolymer was investigated. The M_N of the EPR branches was varied from 3900 to 11100 g/mol while the weight percent of EPR was held constant at approximately 10 percent. Figure 5.9 shows the DMA thermograms of the three samples while Table 5.2 lists the glass transition temperatures of the copolymers.

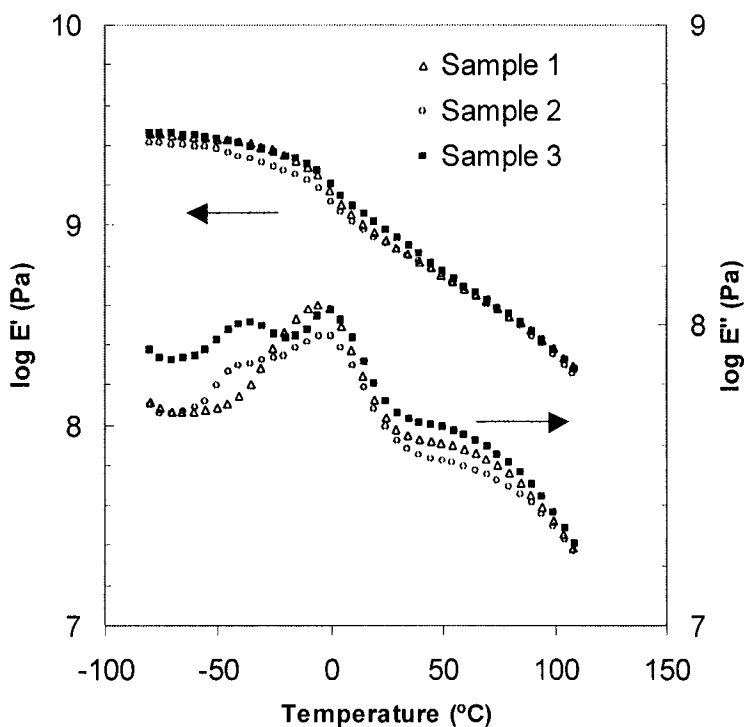


Figure 5.9 Temperature dependence of mechanical storage modulus (E') and loss modulus (E'') at 1Hz for the PP-graft-EPR copolymers with varying EPR M_N

The M_N of the EPR appears to have little influence on the storage modulus of the copolymer, but has a significant effect on the loss modulus. Sample 1 has only one dominant transition peak corresponding to the glass transition temperature (T_g) of polypropylene. At this temperature, the mobility of the chain segments increases and the storage modulus decreases dramatically. Sample 3, however, has two dominant transition peaks. The higher temperature relaxation process corresponds to the T_g of PP, while the lower relaxation process represents the T_g of the EPR branches. Meanwhile, Sample 2 has a sharp transition at the PP T_g , but shows only a shoulder at the EPR T_g . It is also of interest to note that the PP T_g of Sample 1 is slightly shifted downwards from Sample 2, which in turn is shifted downwards from Sample 3.

This behaviour can be explained by the development of EPR phase domains. Sample 1, which has short rubbery branches, behaves as a compatible homogenous system. The EPR branches are not large enough to form rubbery domains and are incorporated into the PP matrix structure. It has been shown that the T_g values of compatible or partially compatible blends shift towards each other (Choudhary et al., 1991). This is seen in the reduced T_g temperature of Sample 1. Sample 3, which has comparatively large EPR chains, assumes a two-phase morphology. The T_g of both EPR and PP can be clearly seen. The EPR branches are long enough to form rubbery domains within the PP matrix. Sample 2 exhibits only a small EPR T_g peak and appears to be a partially compatible system. The long EPR branches are large enough to form phase domains, while the small branches are homogeneously incorporated into the PP matrix. There appears to be a critical EPR branch length at a M_N of approximately 6000 g/mol.

Below 6000 g/mol, the EPR branches are incorporated into the PP matrix structure producing a compatible blend. When the critical M_N is exceeded, however, the EPR branches form rubbery phase domains. This results in a product similar to impact modified PP. Figure 5.10 shows a schematic of the developing morphology.

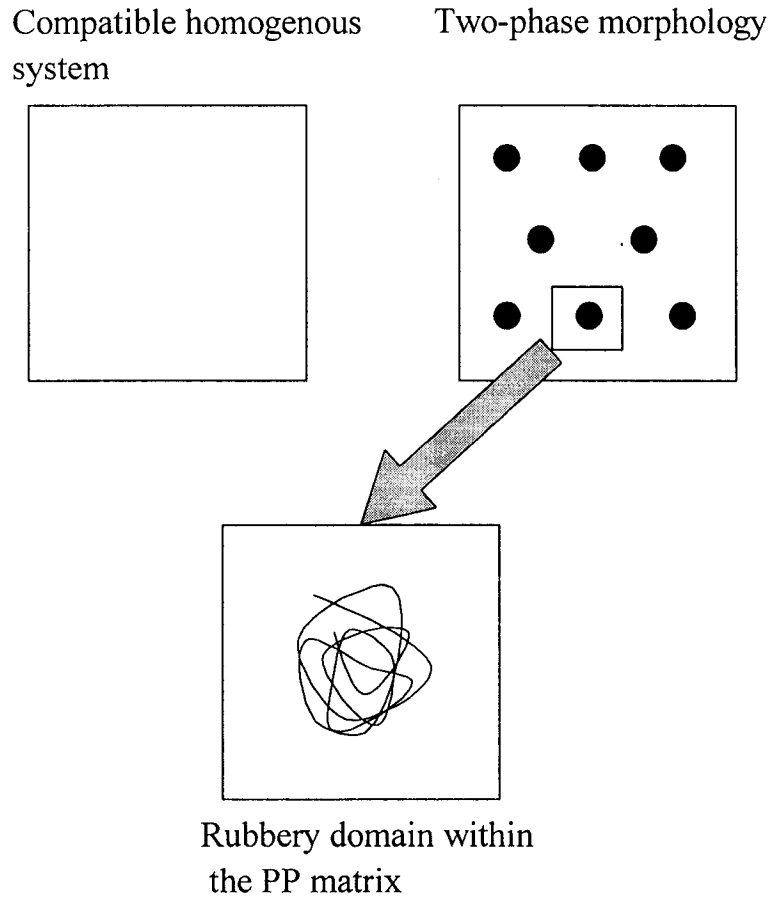


Figure 5.10 Morphological development of PP-g-EPR with increasing branch length

Figure 5.11 shows the DMA thermograms of Sample 3 and SRD7-665, a commercial medium impact polypropylene.

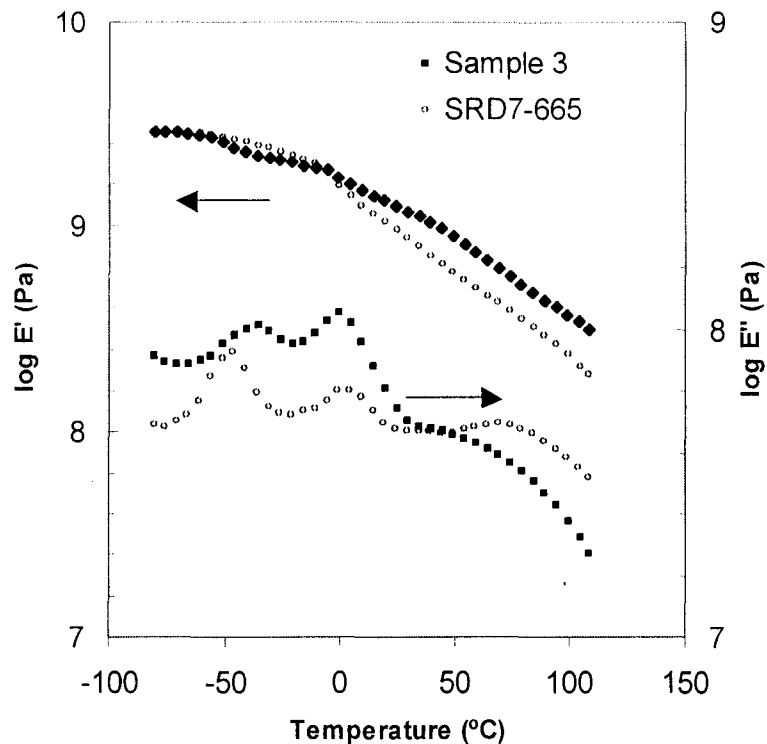


Figure 5.11 Temperature dependence of mechanical storage modulus (E') and loss modulus (E'') at 1Hz for PP-graft-EPR copolymer and commercial HIPP.

Sample 3 has a significantly higher loss modulus for temperatures below 40 °C than the commercial HIPP. It has been shown that there is a relationship between the loss modulus and the impact strength of impact modified PP (Jafari and Gupta, 2000, Karger-Kocsis and Kuleznev, 1982). Polymers with a higher loss modulus are able to absorb more mechanical energy and dissipate this energy in the form of heat. Consequently, it can be expected that Sample 3 would show improved impact properties. The increase in the loss modulus may be due to the excellent dispersion of fine rubbery domains. The domain sizes depend on the molecular weights of individual EPR branches, and are in a nano-scale for the present samples.

Effect of EPR Concentration

Several samples were produced with varying concentrations of low M_N ($M_N=2500$ g/mol) grafted EPR with the concentration varying from 3.4 to 11.5 weight percent. Figure 5.12 shows the DMA thermograms of the samples as well as a commercial isotactic PP.

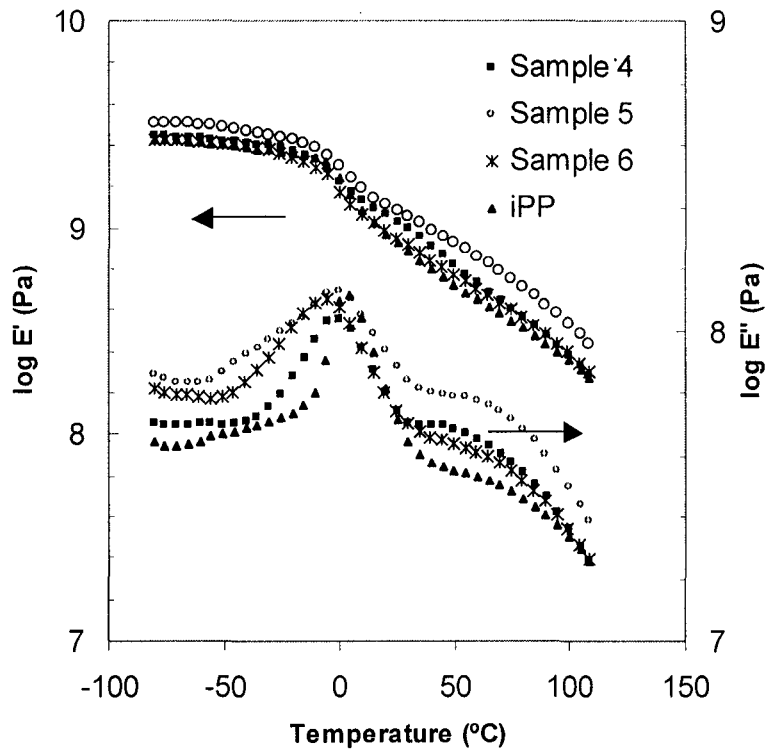


Figure 5.12 Temperature dependence of mechanical storage modulus (E') and loss modulus (E'') at 1Hz for PP-graft-EPR copolymers with varying EPR concentrations

It can be seen that each sample has only one major relaxation peak corresponding to the T_g of PP. The EPR is below the critical length of 6000 and therefore behaves as a

compatible blend. Increasing the concentration of EPR in the copolymer reduces the apparent T_g and broadens the relaxation peak. It was also observed that, at the studied EPR concentrations, increasing the amount of EPR tended to increase the loss modulus while only slightly influencing the storage modulus. The increase of E'' was only a moderate gain when compared to Samples 2 and 3 where phase domains developed.

5.3.3 Conclusions

Based on the experimental work, the following conclusions can be made:

- (1) There appeared to be a critical EPR branch length at a M_N of approximately 6000 g/mol. When the branch length was below this critical M_N , a homogenous system resulted. If this critical M_N was exceeded, a two-phase system developed, with fine rubbery domains dispersed in a PP matrix.
- (2) When a two-phase system developed, it enhanced the loss modulus of the copolymer in a manner similar to impact modified PP. In these samples, however, the domain sizes depended on the molecular weights of individual EPR branches, and were in a nano-scale. In addition, because the EPR chains were chemically grafted to the PP backbone, there was an excellent dispersion of the fine rubbery domains. This control of rubbery domain size and dispersion enabled Sample 3, with an EPR M_N of 11100 g/mol, to have a significantly higher loss modulus than a commercial impact modified PP.

- (3) The M_N of the EPR side branches had little influence on the storage modulus of the copolymer. Increasing the branch M_n from 2500 to 11100 g/mol, while holding the amount of EPR constant at 10 % weight, did not significantly change the E' .

This work has been published by Kolodka et al. (Kolodka et al., 2002).

Chapter 6

Significant Research Contributions and Recommendations for Future Work

6.1 Significant Research Contributions of the Thesis Work

This thesis work has made significant contributions to the fields of synthesizing and characterizing long chain branched polyolefins, as well as establishing the relationships between the polymer chain structures and material, rheological and dynamic mechanical properties. These contributions follow in the order outlined within the thesis.

- 1) Long chain branched polyethylene, with LCBD (carbons per 10,000 carbons) up to 1.0, was produced using the homogeneous catalyst bis(cyclopentadienyl) zirconium dichloride in a semi-batch slurry polymerization. A slurry polymerization process was believed responsible for the formation of LCB with enhanced levels of LCB attributed to the in-situ reaction of ethylene macromonomer and the encapsulation of active centres by precipitated polymer chains. The experimental conditions of reaction temperature, pressure, initial polymer concentration, and MMAO concentration, all affected LCB formation. Increasing the temperature from 60 °C to 80 °C reduced the LCBD from 0.33 to 0.10, while increasing the pressure from 2 psig to 20 psig reduced the LCBD from 0.73 to 0.30. Different MMAO / Cp₂ZrCl₂ ratios also influenced the formation of

LCB, with LCBDs ranging from 0.21 to 0.35 at ratios of 2400 to 800. This was the first reported systematic study on long chain branched polyethylene synthesized using a classic metallocene catalyst system.

- 2) Long chain branched polyethylene with controlled levels of long chain branching was synthesized using two-stage polymerization process. Narrowly dispersed poly(ethylene-co-propylene) macromonomer was first produced in a continuous stirred tank reactor. The macromonomer was subsequently copolymerized with ethylene in a semi-batch reactor using Dow Chemicals homogeneous constrained geometry catalyst (CGC-Ti). This is the first reported synthesis of polyethylene with poly(ethylene-co-propylene) branching.

This two-step reaction process was also employed to synthesize polypropylene with poly(ethylene-co-propylene) long chain branches using the catalyst system *rac*-dimethylsilylenebis(2-methylbenz[e]indenyl)zirconium dichloride / modified methylaluminoxane. It was found that the stoichiometry of the macromonomer could be used to efficiently control the long chain branch frequency (LCBF) of the copolymers without greatly influencing the molecular weights. It was also possible to control the length of the long chain branches by controlling the M_N of the macromonomer with branch lengths ranging from 2500 to 17000 g/mol. The polymers produced in this work are unique in the literature. They are the first reported polymers with controlled branch densities and branch lengths synthesized using metallocene catalysts.

- 3) The rheological properties of long chain branched homo-polyethylenes were determined to be significantly different from their linear analogues. LCBed PEs exhibited significantly higher η_{0s} and displayed greater shear thinning than linear PEs with similar molecular weights. These enhancements have been attributed to the formation of additional entanglements between polymer molecules, leading to increased resistances to flow. Polyethylenes with similar LCBFs but with higher M_{ws} showed enhancements in η_0 greater than that predicted by the increase in M_w . This affect was attributed to higher molecular weight LCBs which allowed additional entanglements. Long chain branched PE exhibited thermorheologically complex behavior. The temperature sensitivity could not be summarized with a single shift factor. The activation energy, which was shear dependant, was determined using the G' . Higher LCBFs and greater LCB lengths lead to elevated values of E_a at low shear rates. At high shear rates, the values of E_a were equivalent to that of linear polymers. The significant contribution of this work is the comparison of the influence of long chain branch frequency at different polymer molecular weights.
- 4) The rheological characteristics of a series of model polypropylenes with poly(ethylene-co-propylene) (EPR) branches were measured. The molecular weight of both the copolymer and the long chain branches were controlled, as was the long chain branch frequency. The rheological behavior of the resultant long chain branched polypropylenes were measured. It was shown that when the

branch M_N was less than 7000 g/mol, it had little influence on the rheological responses. When the branch M_N was greater than 7000 g/mol it was long enough to form entanglements and behaved as a long chain branch. When above M_C , the branch length had a significant influence on the rheological responses. Both G' and G'' showed elevated values at low shear rates. The η_0^* was a sensitive indicator of branch length. Increasing branch M_N led to enhanced values of η_0^* . The shear-thinning phenomenon also increased with increasing branch length, as did the flow activation energy. The long chain branch frequency also had a strong influence on the rheological behavior of the polymer samples provided the branch M_N was greater than 7000 g/mol. Increases in LCBF led to increased η_0^* s, increased shear thinning, enhanced flow activation energies, and to elevated values of G' and G'' . The long chain branched samples were found to exhibit thermorheologically simple behavior, excepting Sample 6. This work was the first conducted on polypropylene with various branch frequencies and branch lengths. It allowed a systematic study on the influence of branch length on the rheological characteristics independent of polymer molecular weight and branch frequency.

- 5) Long chain branching played a significant role in the dynamic mechanical behavior of substantially linear polyethylene. Increasing the frequency of branching increased the stiffness of the polymer, as reflected by the storage modulus. Long chain branching also served to enhance the damping or energy dissipation of PE, shown by increased values of the loss modulus. These long

chain branched PEs showed behavior similar to PE cross-linked by radiation or peroxide and a similar mechanism was used to explain the dynamic mechanical differences. The enhancements in E' were attributed to stiffening due to cross-linking in the amorphous phase, and to a suppression of c-axis slip in the lamellae by internal or surface cross-linking in the crystal phase. Long chain branching also had little influence on the crystalline structure of the PE. The α and γ relaxations showed little dependence on the LCBF. This work is the only known study on the influence of long chain branching on the dynamic mechanical properties of high density polyethylene.

- 6) The dynamic mechanical properties of polypropylene with poly(ethylene-co-propylene) branches of various lengths were measured. There appeared to be a critical EPR branch length at a M_N of approximately 6000 g/mol. When the branch length was below this critical M_N , a homogenous system resulted. If this critical M_N was exceeded, a two-phase system developed, with fine rubbery domains dispersed in a PP matrix. When the two-phase system developed it enhanced the loss modulus of the copolymer in a manner similar to impact modified PP. In these samples, however, the domain sizes depended on the molecular weights of individual EPR branches, and were in a nano-scale. In addition, because the EPR chains were chemically grafted to the PP backbone, there was an excellent dispersion of the fine rubbery domains. This control of rubbery domain size and dispersion enabled Sample 3, with an EPR M_N of 11100 g/mol, to have a significantly higher loss modulus than a commercial impact

modified PP. This research was the first known study on the phase separation of polypropylene with grafted poly(ethylene-co-propylene) branches.

6.2 Recommendations for Future Research

This work has helped to elucidate the influences of long chain branching on polymer properties. However, there remains significant research to be conducted which will further clarify the relationships between polymer architecture and polymer properties.

Long chain branching has been shown to have a significant influence on the melt strength of polyethylene. Little work has been done with model polymers with controlled branch density and branch length. A comprehensive study using polyethylenes with controlled branch architectures could reveal fundamental mechanisms of elongational viscosity. Furthermore, there is little work in the literature regarding the melt strength of long chain branched polypropylene. The model polymers produced in this thesis could provide significant insights into elongational viscosities with important applications in the film blowing industry.

The impact properties of polypropylene with grafted poly(ethylene-co-propylene) branches were inferred using dynamic mechanical analysis as insufficient polymer was produced to perform direct studies using such methods as Izod impact tests. A comprehensive examination using Izod impact testing could further the understanding of

the complex relationships between phase size, phase dispersion, and interfacial contact and the polymer impact properties. This Izod impact study should be accompanied by a SEM/TEM investigation on the domain morphologies.

A series of novel polymers with polyethylene backbones and with polar branches, such as acrylics, could be synthesised using the two-step polymerization process outlined in this thesis by employing several new organolanthanide complex catalysts. These novel graft copolymers should show enhanced mechanical properties over blends due to excellent distributive mixing at the molecular level and intimate contact at the interfacial boundaries.

6.3 List of Publications from this Work

Kolodka, E., W.-J. Wang, P.A. Charpentier, S. Zhu, A.E. Hamielec, “Long-chain branching in slurry polymerization of ethylene with zirconocene dichloride/modified methylaluminoxane”, *Polymer*, **41**, 3985, 2000.

Kolodka, E., W.-J. Wang, S. Zhu, A.E. Hamielec, “Molecular-Weight-Dependance on Domain Formation of Grafted Poly(ethylene-co-propylene) in a Poly(propylene) Matrix”, *Macromol. Rapid Commun.*, **23**, 470, 2002.

Kolodka, E., W.-J. Wang, S. Zhu, A.E. Hamielec, “Copolymerization of Propylene with Poly(ethylene-co-propylene) Macromonomer and Branch Chain-Length

Dependence of Rheological Properties”, accepted in *Macromolecules* for publication.

Kolodka, E., W.-J. Wang, D. Yan, S. Zhu, A.E. Hamielec, “Comparison of Rheological and Dynamic Mechanical Properties of Long Chain Branched Polyethylene Produced in CSTR and Semi-Batch Reactor Systems”, preparing for publication.

W.J. Wang, E.B. Kolodka, S. Zhu, A.E. Hamielec, “Continuous Solution Copolymerization of Ethylene and Octene-1 with a Constrained Geometry Metallocene Catalyst”, *J. Polym. Sci. Polym. Chem. Ed.* **1999**, 37, 2949.

W.J. Wang, E.B. Kolodka, S. Zhu, A.E. Hamielec, “Temperature Rising Elution Fractionation and Characterization of Ethylene/Octene-1 Copolymers Synthesised with a Constrained Geometry Catalyst”, *Macromolecular - Chemistry and Physics*, **1999**, 200, 2146.

References

- Andressen, A., H.G. Cordes, J. Herwig, W. Kaminsky, A. Merck, R. Mottweiller, J. Pein, H. Sinn, H.J. Volmer, "Halogen-Free Soluble Ziegler Catalyst for the Polymerization of Ethylene: Control of Molecular Weight by Choice of Temperature", *Angew. Chem. Int. Ed. Engl.*, **15**, 630, 1976.
- Ariffin, Z., D. Wang, Z. Wu, "Synthesis of polycarbonates using a cationic zirconocene complex", *Macromol. Rapid Commun.* **19**, 601, 1998.
- ASTM D 3124-93, "Standard Test Method for Vinylidene Unsaturation in Polyethylene by Infrared Spectrophotometry", 1994.
- ASTM D 5576-94, "Standard Practice for Determination of Structural Entities in Polyolefins by Fourier Transform Infrared Spectroscopy (FT-IR)", 1994.
- ASTM D 1238-90b, "Flow Rates of Thermoplastics by Extrusion Plastometer", 1990.
- Barsan, F., A.R. Karam, M.A. Parent, M.C. Baird, "Polymerization of Isobutylene and the Copolymerization of Isobutylene and Isoprene Initiated by the Metallocene Derivative $Cp^*TiMe_2(\mu-Me)B(C_6F_5)_3$ ", *Macromolecules*, **31**, 8439, 1998.
- Beck, S., H.H. Brintzinger, J. Suhm, R. Mulhaupt, "Propene polymerization with *rac*- $Me_2Me_2Si(2-Me-Benz[e]Ind)_2ZrX_2$ [X = Cl, Me] using different cation-generating reagents", *Macromol. Rapid Commun.*, **19**, 235, 1998.
- Bersted, B.H., J.D. Slee, C.A. Richter, "Prediction of rheological behavior of branched polyethylene from molecular structure", *J. Appl. Polym. Sci.*, **26**, 1001, 1981.

- Bersted, B.H., "On the effects of very low levels of long chain branching on rheological behavior in polyethylenes", *J. Appl. Polym. Sci.*, **30**, 3751, 1985.
- Birkinshaw, C., M. Buggy, J.J. White, "The Effect of Sterilising Radiation on the Properties of Ultra-High Molecular Weight Polyethylene", *Materials Chemistry and Physics*, **14**, 549, 1986.
- Boor, J., *Ziegler-Natta Catalysts and Polymerization*, Academic Press, New York, 1979.
- Brant, P., J.A.M. Canich, N.A. Merrill, "Ethylene/Branched Olefin Copolymers", *US Patent*, **5,444,145**, 1995a.
- Brant, P., J.A.M. Canich, "Ethylene/Longer α -olefin Copolymers", *US Patent*, **5,475,075**, 1995b.
- Brinzinger, H.-H., D. Fischer, R. Mulhaupt, B. Rieger, R.M. Waymouth, "Stereospecific Olefin Polymerization with Chiral Metallocene Catalysts", *Angew. Chem. Int. Ed. Engl.* **34**, 1143, 1995.
- Carella, J.M., W.W. Graessley, L.J. Fetters, "Effects of chain microstructure on the viscoelastic properties of linear polymer melts: polybutadienes and hydrogenated polybutadienes", *Macromolecules*, **17**, 2775, 1984.
- Carella, J.M., J.T. Gotro, W.W. Graessley, "Thermorheological Effects of Long-Chain Branching in Entangled Polymer Melts", *Macromolecules*, **19**, 659, 1986.
- Carvill, A., L. Zetta, G. Zannoni, M.C. Sacchi, "ansa-Zirconocene-Catalyzed Solution Polymerization of Propene: Influence of Polymerization Conditions on the Unsaturated Chain-End Groups", *Macromolecules*, **31**, 3783, 1998.
- Charpentier, P.A., S. Zhu, A.E. Hamielec, M.A. Brook, "Continuous Solution Polymerization of Ethylene Using Metallocene Catalyst System, Zirconocene

- Dichloride/Methylaluminoxane/trimethylaluminum”, *Ind. Eng. Chem. Res.*, **36**, 5074, 1997.
- Chien, J.C.W., B.-P. Wang, “Metallocene-Methylaluminoxane catalysts for olefin polymerization. I. Trimethylaluminum as coactivator”, *J. Polym. Sci.: Part A: Polym. Chem. Ed.*, **26**, 3089, 1988.
- Chien, J.C.W., B.-P. Wang, “Metallocene-Methylaluminoxane Catalysts for Olefin Polymerization. V. Comparison of Cp_2ZrCl_2 and CpZrCl_3 ”, *J. Polym. Sci., Part A: Polym. Chem. Ed.* **28**, 15, 1990.
- Chien, J.C.W., B. Xu, “Olefin copolymerization and olefin/diene terpolymerization with zirconocenium catalyst system”, *Makromol. Chem., Rapid Commun.*, **14**, 109, 1993.
- Choudhary, V., H.S. Varma, I.K. Varma, “Polyolefin blends: effect of EPDM rubber on crystallization, morphology and mechanical properties of polypropylene/EPDM blends. 1”, *Polymer*, **32**, 2534, 1991.
- Chung, T.C., H.L. Lu, “Synthesis of Poly(ethylene-co-*p*-methylstyrene) Copolymers by Metallocene Catalysts with Constrained Ligand Geometry”, *J. Polym. Sci. A: Polym. Chem.*, **35**, 575, 1997.
- Cossee, P., “Ziegler-Natta catalysis I. Mechanism of polymerization of α -olefins with Ziegler-Natta catalysts”, *J. Catal.* **3**, 80, 1964.
- Cruz, V.L., A. Munoz-Escalona, J. Martinez-Zalazar, “A Theoretical Study of the Comonomer Effect in the Ethylene Polymerization with Zirconocene Catalytic Systems”, *J. of Polym. Sci.: Part A: Polym. Chem.*, **36**, 1157, 1998.

- Dealy, J.M. Wissbrun, K.F., *Melt rheology and its role in Plastics Processing: Theory and Applications*, Van Nostrand Reinhold, New York, 1990.
- Deng, L., P. Margl, T. Ziegler, "A Density Functional Study of Nickel (II) Diimide Catalyzed Polymerization of Ethylene", *J. Am. Chem. Soc.*, **119**, 1094, 1997.
- De Pooter, M., P.B. Smith, K.K. Dohrer, K.F. Bennett, M.D. Meadows, C.G. Smith, H.P. Schouwenaars, R.A. Geerards, "Determination of the Composition of Common Linear Low Density Polyethylene Copolymers by ^{13}C NMR Spectroscopy", *J. Applied. Polym. Sci.*, **42**, 399, 1991.
- D'Orazio, L., C. Mancarella, E. Martuscelli, G. Sticotti, G. Cecchin, "Isotactic polypropylene/ethylene-co-propylene blends: Influence of the copolymer microstructure on rheology, morphology, and properties of injection-molded samples", *J Appl Polym Sci*, **72**, 701, 1999.
- Eskelinen, M., J.V. Seppala, "Effect of Polymerization Temperature on the Polymerization of Ethylene with Dicyclopentadienylzirconiumdichloride / Methylalumoxane Catalyst", *Eur. Polym. J.*, **32**, 331, 1996.
- Ewen, J.A., R.L. Jones, A. Razavi, J.D. Ferrara, "Syndiospecific propylene polymerizations with Group IVB metallocenes", *J. Am. Chem. Soc.*, **110**; 6255, 1988.
- Feng, Y., X. Jin, J.N. Hay, "Dynamic Mechanical Behavior Analysis for Low Ethylene Content Polypropylene Copolymers", *J Appl Polym Sci*, **68**, 395, 1998.
- Gell, C.B., W.W. Graessley, V. Efstratiadis, M. Pitsikalis, N. Hadjichristidis, "Viscoelasticity and self-diffusion in melts of entangled asymmetric star polymers", *J. Polym. Sci., Part B: Polym. Phys.* **35**, 1943, 1997.

- Giannetti, E., G.M. Nicoletti, R. Mazzocchi, "Homogeneous Ziegler-Natta Catalysis. II. Ethylene Polymerization by IVB Transition Metal Complexes/Methyl Aluminoxane Catalysts Systems", *J. Polym. Sci., Polym. Chem. Ed.* **23**, 2117, 1985.
- Gill, P.S., J.D. Lear, J.N. Leckenby, in "Measurement Techniques for Polymeric Solids", ed. R.P. Brown, B.E. Read, London: Elsevier Applied Science, 1984.
- Graessley, W.W., "Effect of long branches on the flow properties of polymers", *Acc. Chem. Res.*, **10**, 332, 1977.
- Guan, Z., P.M. Cotts, E.F. McCord, S.J. McLain, "Chain walking: A new strategy to control polymer topology" *Science*, **283**, 2059, 1999.
- Hakala, K., T. Helaja, B. Lofgren, "Metallocene/Methylaluminoxane-Catalyzed Copolymerizations of Oxygen-Functionalized Long-Chain Olefins with Ethylene", *J. of Polym. Sci.: Part A: Polym. Chem.*, **38**, 1966, 2000.
- Hamielec, A.E., J.B.P. Soares, "Polymerization Reaction Engineering Metallocene Catalysts", *Prog. Polym. Sci.*, **21**, 651, 1996.
- Han, T.K., Y.S. Ko, J.W. Park, S.I. Woo, "Determination of the Number of Active Sites for Olefin Polymerization Catalyzed over Metallocene/MAO Using the CO Inhibition Method", *Macromolecules*, **29**, 7305, 1996.
- Harkki, O., P. Lehmus, R. Leino, H.J.G. Luttikhedde, J.H. Nasman, J.V. Seppala, "Copolymerization of ethylene with 1-hexene or 1-hexadecene over siloxy-substituted metallocene catalysts", *Macromol. Chem. Phys.*, **200**, 1561, 1999.

- Harrell, E.R., N. Nakajima, "Modified Cole-Cole Plot Based on Viscoelastic Properties for Characterizing Molecular Architecture of Elastomers", *Journ. Appl. Polym. Sci.*, **29**, 995, 1984.
- Harrison, D., I.M. Coulter, S. Wang, S. Nistala, B.A. Kuntz, M. Pigeon, J. Tian, S.J. Collins, "Olefin polymerization using supported metallocene catalysts: Development of high activity catalysts for use in slurry and gas phase ethylene polymerizations", *J. Mol. Catal., A: Chem.*, **128**, 65, 1998.
- Henschke, O., A. Neubauer, M. Arnold, "Metallocene-Catalyzed Copolymerization of Propene with Polystyrene Macromonomers", *Macromolecules*, **30**, 8097, 1997.
- Herfert, N., P. Montag, G. Fink, "Ethylene, α -olefin and norbornene copolymerization with the stereorigid catalyst systems $iPr[FluCp]ZrCl_2/MAO$ and $Me_2Si[Ind]_2ZrCl_2/MAO$.
- Huang, J., G.L. Rempel, "Ziegler-Natta Catalysts or Olefin Polymerization: Mechanistic Insights from Metallocene Systems", *Prog. Polym. Sci.*, **20**, 459, 1995.
- Jafari, S.H., A.K. Gutpa, "Impact Strength and Dynamic Mechanical Properties Correlation in Elastomer-Modified Polypropylene", *J. of Applied Polym. Sci.* **78**, 962, 2000.
- James, D.E., "Encyclopedia of Polymer Science and Engineering", **V6**, H.F. Mark, N.M. Bikales, C.G. Overberger, G. Menges, J.I. Kroschwitz (eds.), New York, John Wiley & Sons, Inc., 1989.
- Johnson, L.K., C.M. Killian, M. Brookhart, "New Pd(II)-and Ni(II)-Based Catalysts for Polymerization of Ethylene and α -Olefins", *J. Am. Chem. Soc.*, **117**, 6414, 1995.

- Jordan, E.A., A.M. Donald, L.J. Fetters, J. Klein, "Transition from Linear to Star-Branched Diffusion in Entangled Polymer Melts", *ACS Polym. Prepr.*, **30**, 63, 1989.
- Kaminaka, M., K. Soga, *Makromol. Chem., Rapid Commun.*, **12**, 367, 1991.
- Kaminsky, W., K. Kulper, H.H. Brintzinger, F.R.P.W. Wild, "Polymerization of Propene and Butene with Chiral Zirconocene and Methylaluminumoxane as Cocatalyst", *Angew. Chem. Int. Ed. Engl.*, **24**, 507, 1985.
- Kaminsky, W., R. Steiger, "Polymerization of Olefins with Homogeneous Zirconocene / Aluminoxane Catalysts", *Polyhedron*, **7**, 2375, 1988.
- Kaminsky, W., M. Arndt, A. Bark, "New results of the polymerization of olefins with metallocene/aluminoxane-catalysts", *Polymer Preprints.*, **32**, 467, 1991.
- Karger-Kocsis, J., V.N. Kuleznev, "Dynamic Mechanical Properties and Morphology of Polypropylene Block Copolymers and Polypropylene/Elastomer Blends", *Polymer*, **23**, 699, 1982.
- Keating, M.Y., I.H. Lee, "Glass Transition, Crystallinity, Resin Stiffness, and Branch Distribution in Metallocene and Ziegler-Natta Ethylene 1-Olefins", *J. Macromol. Sci.-Phys.*, **B38(4)**, 379, 1999.
- Khanna, Y.P., E.A. Turi, T.J. Taylor, V.V. Vickroy, R.F. Abbot, "Dynamic mechanical relaxations in polyethylene", *Macromolecules*, **18**, 1302, 1985.
- Kim, I., J.-M. Zhou, "MAO-Free Polymerization of Propylene by *rac*-Me₂Si(1-C₅H₂-2-Me-4-^tBu)₂Zr(NMe₂)₂", *J. of Polym. Sci.: Part A: Polym. Chem.*, **37**, 1071, 1999.

- Kissin, Y.V., A.J. Brandolini, "Ethylene polymerization reactions with Ziegler-Natta catalysts. II. Ethylene polymerization reactions in the presence of deuterium", *J. Polym. Sci. Part A: Polym. Chem.*, **37**, 4274, 1999.
- Kolodka, E., W.-J. Wang, P.A. Charpentier, S. Zhu, A.E. Hamielec, "Long-chain branching in slurry polymerization of ethylene with zirconocene dichloride/modified methylaluminoxane", *Polymer*, **41**, 3985, 2000.
- Kolodka, E., W.-J. Wang, S. Zhu, A.E. Hamielec, "Molecular-Weight-Dependence on Domain Formation of Grafted Poly(ethylene-co-propylene) in a Poly(propylene) Matrix", *Macromol. Rapid Commun.*, **23**, 470, 2002.
- Kolodka, E., W.-J. Wang, S. Zhu, A.E. Hamielec, "Copolymerization of Propylene with Poly(ethylene-co-propylene) Macromonomer and Branch Chain-Length Dependence of Rheological Properties", accepted in *Macromolecules* for publication.
- Kolodka, E., W.-J. Wang, D. Yan, S. Zhu, A.E. Hamielec, "Comparison of Rheological and Dynamic Mechanical Properties of Long Chain Branched Polyethylene Produced in CSTR and Semi-Batch Reactor Systems", preparing for publication.
- Kokko, E., P. Lehmus, R. Leino, H.J.G. Luttikhedde, P. Ekholm, J.H. Nasman, J.V. Seppala, "*meso*- and *rac*-Diastereomers of 1- and 2-*tert*-Butyldimethylsiloxy-Substituted Ethylenebis(indenyl)zirconium Dichlorides for Formation of Short- and Long-Chain Branched Polyethylene", *Macromolecules*, **33**, 9200, 2000.
- Kokko, E., W.-J. Wang, J.V. Seppala, S. Zhu, "Structural Analysis of Polyethylene Prepared with *rac*-Dimethylsilylbis(indenyl)zirconium Dichloride /

- Methylaluminoxane in a High-Temperature, Continuously Stirred Tank Reactor”,
J. Polym. Sci. Part A: Polym. Chem., **40**, 3292, 2002.
- Kravchenko, R., R.M. Waymouth, “Ethylene-Propylene Copolymerization with 2-Arylindene Zirconocenes”, *Macromolecules*, **31**, 1, 1998.
- Kunert, K.A., “Influence of High Peroxide Concentration on the Mechanical Properties of Cross-Linked Low Density Polyethylene”, *J. Macromol. Sci.-Chem*, **A17(9)**, 1469, 1982.
- Kurzbeck, S., F. Oster, H. Munstedt, “Rheological properties of two polypropylenes with different molecular structure”, *J. Rheol.*, **43**, 359, 1999.
- Lai, S.Y., J.R. Wilson, G.W. Knight, J.C.Stevens, P.W.S. Chum, “Elastic Substantially Linear Olefin Polymers”, *US Patent*, **5,272,236**, 1993.
- Laun, H.M. “Orientation of macromolecules and elastic deformations in polymer melts. Influence of molecular structure on the reptation of molecules”, *Prog. Coll. Polym. Sci.*, **75**, 111, 1987.
- Leino, R., H.J.G. Luttkhedde, P. Lehmus, C.-E. Wilen, R. Sjöholm, A. Lehtonen, J.V. Seppala, J.H. Nasman, “Homogeneous α -olefin Polymerizations over Racemic Ethylene-Bridged *ansa*-Bis(2-(*tert*-butyldimethylsiloxy)-1-indenyl) and *ansa*-Bis(2-(*tert*-butyldimethylsiloxy)-4,5,6,7,-tetrahydro-1-indenyl) Metallocene Dichlorides”, *Macromolecules*, **30**, 3477, 1997.
- Lisovskii, A., M. Shuster, M. Gishvoliner, G. Lidor., M.S. Eisen, “Polymerization of Propylene by Metallocene and Ziegler-Natta Mixed Catalytic Systems. Study of Polypropylene Properties”, *J. of Polym. Sci.: Part A: Polym. Chem.*, **36**, 3063, 1998.

- Lohse, D.J., Milner, S.T., Fetters, L.J., Xenidou, M., Hadjichristidis, N., Mendelson, R.A., Garcia-Franco, C.A., Lyon, M.K., "Well-Defined, Model Long Chain Branched Polyethylene. 2. Melt Rheological Behavior", *Macromolecule*, **35**, 3066, 2002.
- Macosko, C.W., *Rheology: Principles, Measurements, and Applications*, Wiley-VCH, USA, 1994.
- Mader, D., J. Heinemann, P. Walter, R. Mulhaupt, "Influence of n-Alkyl Branches on Glass-Transition Temperatures of Branched Polyethylenes Prepared by Means of Metallocene- and Palladium-Based Catalysts", *Macromolecules*, **33**, 1254, 2000.
- Malmberg, A., E. Kokko, P. Lehmus, B. Lofgren, J.V. Seppala, "Long-Chain Branched Polyethylene Polymerized by Metallocene Catalysts Et[Ind]₂ZrCl₂ / MAO and Et[IndH₄]₂ZrCl₂ / MAO", *Macromolecules*, **31**, 8448, 1998.
- Mansel, S., E. Perez, R. Benavente, J.M. Perena, A. Bello, W. Roll, R. Kirsten, S. Beck, H.-H. Brintzinger, "Synthesis and properties of elastomeric poly(propylene)", *Macromol. Chem. Phys.*, **200**, 1292, 1999.
- Mashima, K., Y. Nakayama, A. Nakamura, "Recent Trends in the Polymerization of α -Olefins Catalyzed by Organometallic Complexes of Early Transition Metals", *Adv. Polym. Sci.*, **133**, 1, 1997.
- Matkovskii, P.E., L.N. Russiyan, V.D. Makhaev, A.K. Lee, B.G. Song, "Polymerization of Ethylene with the (C₅H₅)₂TiCl₂-(C₂H₅)₂AlCl Catalytic System under the Conditions of Classical Metallocene Catalysis", *Polymer Science, Ser. A*, **40**, 871, 1998.

- Mavridis, H., R.N. Shroff, "Temperature dependence of polyolefin melt rheology", *Polym. Eng. Sci.*, **32**, 1778, 1992.
- Meng, F., G. Yu, B. Huang, "Polymer-Supported Zirconocene Catalyst for Ethylene Polymerization", *J. of Polym. Sci.: Part A: Polym. Chem.*, **37**, 37, 1999.
- Michelotti, M., A. Altomare, F. Ciardelli, P. Ferrarini, "Ethylene / α -olefins cooligomerization versus copolymerization by zirconocene catalysts", *Polymer*, **37**, 5011, 1996.
- Milner, S.T., McLeish, T.C.B., Young, R.N., Hakiki, A., Johnson, J.M., "Dynamic Dilution, Constraint-Release, and Star-Linear Blends", *Macromolecules*, **31**, 9345, 1998
- Milner, S.T., McLeish, T.C.B., "Arm-length dependence of stress relaxation in star polymer melts" *Macromolecules*, **31**, 7479, 1998.
- Modern Plastics*, "Resins 2002", **79**, 21, 2002.
- Morrison, F.A. "Understanding of Rheology", Oxford University Press, New York, 2001.
- Munoz-Escalona, A., J. Ramos, V. Cruz, J. Marinez-Salazar, "Effect of a Second Ethylene Molecule on the Insertion of Ethylene in Zirconocene Catalyst Systems: A QM Semiempirical Study", *J. of Polym. Sci.: Part A: Polym. Chem.* **38**, 571, 2000.
- Nielsen, L.E., R.F. Landel, "Mechanical Properties of Polymers and Composites", New York: M. Dekker, 1994.
- Nitta, K.-H., T. Kawada, V.V. Prokhorov, M. Yamahiro, H. Mori, M. Terano, "Characterization and Properties of Polypropylene-block-poly(ethylene-co-

- propylene) Synthesized by Short-Period Polymerization”, *J Appl Polym Sci*, **74**, 958, 1999.
- Norzalia, S., B. Surani, M.Y. Ahmad Fuad, “Properties of Rubber-Modified Polypropylene Impact Blends”, *J Elast Plast*, **26**, 183, 1994.
- Nitta, K.-h., A. Tanaka, “Dynamic mechanical properties of metallocene catalyzed linear polyethylenes”, *Polymer*, **42**, 1219, 2001.
- Odian, G., *Principles of Polymerization*, New York, John Wiley & Sons, Inc., 1991.
- Ohta, Y., H. Yasuda, “The Influence of Short Branches on the α , β , and γ -Relaxation Processes of Ultra-High Strength Polyethylene Fibers”; *J. of Polm. Sci.: Part B: Polym. Physics*, **32**, 2241, 1994.
- Park, S., W.-J. Wang, S. Zhu, “Continuous solution copolymerization of ethylene with propylene using a constrained geometry catalyst system”, *Macromol. Chem. Phys.*, **201**, 2203, 2000.
- Pukanszky, B., F. Tudos, A. Kallo, G. Bodor, “Effect of multiple morphology on the properties of polypropylene/ethylene-propylene-diene terpolymer blends”, *Polymer*, **30**, 1411, 1989.
- Quijada, R., R. Rojas, G. Bazan, Z.J.A. Komon, R.S. Mauler, G.B. Galland, “Synthesis of Branched Polyethylene from Ethylene by Tandem Action of Iron and Zirconium Single Site Catalysts”, *Macromolecules*, **34**, 2411, 2001.
- Raju, V.R., H. Rachapudy, W.W. Graessley, “Properties of Amorphous and Crystallizable Hydrocarbon Polymers 4. Melt Rheology of Linear and Star-Branched Hydrogenated Polybutadiene”, *J. Polym. Sci., Polym. Phys. Ed.*, **17**, 1223, 1979.

- Randal, J.C. "Polymer sequence determination, carbon-13 NMR method", Academic Press, New York, 1977.
- Reinking, M.K., G. Orf, D. McFaddin, "Novel mechanism for the formation of long-chain branching in polyethylene", *J. Polym. Sci., Polym. Chem. Ed.*, **36**, 2889, 1998.
- Resconi, L., F. Piemontesi, G. Franciscano, L. Abis, T. Fiorani, "Olefin polymerization at bis(pentamethylcyclopentadienyl)zirconium and -hafnium centers: chain-transfer mechanisms", *J. Am. Chem. Soc.* **114**, 1025, 1992.
- Ribeiro, M.R., A. Deffieux, M.F. Portela, "Supported Metallocene Complexes for Ethylene and Propylene Polymerizations: Preparation and Activity", *Ind. Eng. Chem. Res.*, **36**, 1224, 1997.
- Rieger, B., C. Troll, J. Preuschen, "Ultra High Molecular Weight Polypropylene Elastomers by High Activity "Dual Side" Hafnocene Catalysts", *Macromolecules*, **35**, 5742, 2002.
- Rossi, A., J. Zhang, G. Odian, "Microstructure of ethylene - 1-butene copolymers produced by zirconocene/methylaluminumoxane catalysis", *Macromolecules*, **29**, 2331, 1996.
- Santamaria, A., "Influence of Long Chain Branching in Melt Rheology and Processing of Low Density Polyethylene", *Mater. Chem. Phys.*, **12**, 1, 1985.
- Santos, J.H.Z., M.B. Rosa, C. Krug, F.C. Stedile, M.C. Haag, J. Dupont, M.C. Forte, "Effects of Ethylene Polymerization Conditions on the Activity of SiO₂-Supported Zirconocene and on Polymer Properties", *J. of Polym. Sci.: Part A: Polym. Chem.*, **37**, 1987, 1999.

- Schneider, M.J., J. Suhm, R. Mulhaupt, M.-H. Prosenc, H.-H. Brintzinger, "Influence of Indenyl Ligand Substitution Pattern on Metallocene-Catalyzed Ethene Copolymerization with 1-Octene", *Macromolecules*, **30**, 3164, 1997a.
- Schneider, M.J., R. Mulhaupt, "Influence of indenyl ligand substitution pattern on metallocene-catalyzed propene copolymerization with 1-octene", *Macromol. Chem. Phys.*, **198**, 1121, 1997b.
- Sernetz, F.G., R. Mulhaupt, F. Amor, T. Eberle, J. Okuda, "Copolymerization of Ethene with Styrene Using Different Methylaluminoxane Activated Half-Sandwich Complexes", *J. Polym. Sci.: Part A: Polym. Chem.*, **35**, 1571, 1997a.
- Sernetz, F.G., R. Mulhaupt, "Metallocene-Catalyzed Ethene / styrene Co- and Terpolymerization with Olefinic Termonomers", *J. of Polym. Sci.: Part A: Polym. Chem.*, **35**, 2549, 1997b.
- Shaffer, W.K.A., W.H. Ray, "Polymerization of olefins through heterogeneous catalysis. XVIII. A kinetic explanation for unusual effects", *J. Applied Polym. Sci.*, **65**, 1053, 1997.
- Shiono, T., K. Soga, "Synthesis of terminally aluminum-functionalized polypropylene", *Macromolecules*, **25**, 3356, 1992.
- Shiono, T., Y. Moriki, T. Ikeda, "Copolymerization of poly(propylene) macromonomer with ethylene by (*tert*-butanamide)dimethyl(tetramethyl- η^5 -cyclopentadienyl)silanetitanium dichloride / methylaluminoxane catalyst", *Macromol. Chem. Phys.*, **198**, 3229, 1997.

- Shiono, T., S.M. Azad, T. Ikeda, "Copolymerization of Atactic Polypropene Macromonomer with Propene by an Isospecific Metallocene Catalyst", *Macromolecules*, **32**, 5723, 1999.
- Siedle, A.R., W.M. Lamanna, R.A. Newmark, J.N. Schroepfer, "Mechanism of olefin polymerization by a soluble zirconium catalyst", *J. Mol. Catal. A: Chem.*, **28**, 257, 1998.
- Sinn, H., W. Kaminsky, "Ziegler-Natta catalysis", *Advances in Organomet. Chem.*, **18**, 99, 1980.
- Small, P.A., "Long Chain Branching in Polymers", *Adv. Polym. Sci.*, **18**, 1, 1975.
- Soares, J.B.P., A.E. Hamielec, "Metallocene/Aluminoxane Catalysts for Olefin Polymerization. A Review" *Polym. React. Eng.*, **3**, 131, 1995.
- Soga, K., T. Uozumi, S. Nakamura, T. Toneri, T. Teranishi, T. Sano, T. Arai, "Structures of polyethylene and copolymers of ethylene with 1-octene and oligoethylene produced with the Cp_2ZrCl_2 and $[(C_5Me_4)SiMe_2N(t-Bu)]TiCl_2$ catalysts", *Macromol. Chem. Phys.* **197**, 4237 1996.
- Starck, P., B. Lofgren, "Thermal properties of ethylene / long chain α -olefin copolymers produced by metallocenes", *European Polymer Journal*, **38**, 97, 2002.
- Stark, P., A. Malmberg, B. Lofgren, "Thermal and Rheological Studies on the Molecular Composition and Structure of Metallocene- and Ziegler-Natta-Catalyzed Ethylene- α -Olefin Copolymers", *Journal of Applied Polymer Science*, **83**, 1140, 2002.

- Sugimoto, M., Y. Masubuchi, J. Takimoto, K. Koyama, "Melt Rheology of Polypropylene Containing Small Amounts of High Molecular Weight Chain. I. Shear Flow", *J. Polym. Sci., Part B: Polym. Physics*, **39**, 2692, 2001.
- Suhm, M.J. Schneider, R. Mulhaupt, "Temperature Dependence of Copolymerization Parameters in Ethene/1-Octene Copolymerization Using Homogeneous *rac*-Me₂Si(2-MeBenz[e]Ind)₂ZrCl₂/MAO Catalyst", *J. of Polym. Sci.: Part A: Polym. Chem.*, **35**, 735, 1997.
- Suhm, J., M.J. Schneider, R. Muelhaupt, "Influence of metallocene structures on ethene copolymerization with 1-butene and 1-octene", *J. Mol. Catal., Part A*, **128**, 215, 1998.
- Sukhova, T.A., A.N. Panin, O.N. Babkina, N.M. Bravaya, "Catalytic Systems Me₂SiCp^{*}N^tBuMX₂ / (CPh₃)(B(C₆F₅)₄) (M=Ti, X=CH₃, M=Zr, X=^tBu) in Copolymerization of Ethylene with Styrene", *J. of Polym. Sci.: Part A: Polym. Chem.*, **37**, 1083, 1999.
- Thorshaug, K., J.A. Stovngeng, E. Rytter, M. Ystenes, "Termination, Isomerization, and Propagation Reactions during Ethene Polymerization Catalyzed by Cp₂Zr-R⁺ and Cp^{*}₂Zr-R⁺. An Experimental and Theoretical Investigation", *Macromolecules*, **31**, 7149, 1998.
- Tsenoglou, C.J., Gotsis, A.D., "Rheological Characterization of Long Chain Branching in a Melt of Evolving Molecular Architecture", *Macromolecules*, **34**, 4685, 2001.
- Tsutsui, T., A. Mizuno, N. Kashiwa, "The microstructure of propylene homo- and copolymers obtained with a Cp₂ZrCl₂ and methylaluminoxane system", *Polymer*, **30**, 428, 1989.

- Uozumi, T., K. Soga, "Copolymerization of olefins with Kaminsky-Sinn-type catalysts", *Makromol. Chem.*, **193**, 823, 1992.
- Van Reenen, A.J., R. Brull, U.M. Wahner, H.G. Raubenheimer, R.D. Sanderson, H. Pasch, "The Copolymerization of Propylene with Higher, Linear α -Olefins", *J. of Polym. Sci.: Part A: Polym. Chem.*, **38**, 4110, 2000.
- Vega, J.F., Munoz-Escalona, A., Santamaria, A., Munoz, M.E., Lafuente, P., "Comparison of the Rheological Properties of Metallocene-Catalyzed and Conventional High-Density Polyethylenes", *Macromolecules*, **29**, 960, 1996.
- Wang, W.-J., D. Yan, S. Zhu, A.E. Hamielec, "Kinetics of long chain branching in continuous solution polymerization of ethylene using constrained geometry metallocene", *Macromolecules*, **31**, 8677, 1998.
- Wang, W.-J., E. Kolodka, S. Zhu, A.E. Hamielec, "Continuous Solution Copolymerization of Ethylene and Octene-1 with Constrained Geometry Metallocene Catalyst", *J. Polym. Sci., Part A: Polym. Chem.*, **37**, 2249, 1999.
- Wang, W.-J., S. Zhu, S.-J. Park, "Long Chain Branching in Ethylene/Propylene Solution Polymerization Using Constrained Geometry Catalyst", *Macromolecules*, **33**, 5770, 2000a.
- Wang, W.-J., S. Zhu, "Structural Analysis of Ethylene/Propylene Copolymers Synthesized with a Constrained Geometry Catalyst", *Macromolecules*, **33**, 1157, 2000b.
- Weng, W., E.J. Markel, A.H. Dekmezian, "Synthesis of Long-Chain Branched Propylene Polymers via Macromonomer Incorporation", *Macromol. Rapid Commun.*, **22**, 1488, 2001.

- Wester, T.S., H. Johnsen, P. Kittilsen, E. Rytter, "The effect of temperature on the polymerization of propene with dimethylsilylbis(1-indenyl)zirconium dichloride / methylaluminoxane and dimethylsilylbis(2-methyl-1-indenyl)zirconium dichloride/methylaluminoxane. Modeling of Kinetics", *Macromol. Chem. Phys.*, **199**, 1989, 1998.
- Wetton, R.E. in "Measurement Techniques for Polymeric Solids", ed. R.P. Brown, B.E. Read, London: Elsevier Applied Science, 1984.
- Whiteley, K.S., T.G. Heggs, H. Koch, R.L. Mawer, W. Immel, "Ullmann's Encyclopedia of Industrial Chemistry", **A21**, B. Elvers, S. Hawkins, G. Schultz (eds.), Weinheim, VHC Publishers Inc., 487, 1992.
- Wild, F.R.W.P., L. Zsolnai, G. Huttner, H.H. Brintzinger, "ansa-Metallocene Derivatives IV* Synthesis and Molecular Structures of Chiral ansa-Titanocene Derivatives with Bridged Tetrahydroindenyl Ligands", *J. Organometal. Chem.*, **232**, 233, 1982.
- Wild, F.R.W.P., M. Wasiucionek, G. Huttner, H.H. Brintzinger, "ansa-Metallocene Derivatives. VII* Synthesis and Crystal Structures of Chiral ansa-Zirconocene Derivatives with Ethylene-Bridged Tetrahydroindenyl Ligands", *J. Organometal. Chem.*, **288**, 63, 1985.
- Wood-Adams, P., J.M. Dealy, "Effect of Molecular Structure on the Linear Viscoelastic Behavior of Polyethylene", *Macromolecules*, **33**, 7489, 2000.
- Wood-Adams, P., S. Costeux, "Thermorheological Behavior of Polyethylene: Effects of Microstructure and Long Chain Branching", *Macromolecules*, **34**, 6291, 2001.
- Wood-Adams, P., S. Costeux, J.M. Dealy, "Linear Viscoelasticity of Substantially Linear Polyolefins: Molecular Structure Effects", *Polym. Mater.: Sci. Eng.*, **84**, 2001.

- Xu, G., S. Lin, "Titanocene-Methylaluminoxane Catalysts for Copolymerization of Styrene and Ethylene: Synthesis and Characterization of Styrene-Ethylene Copolymers", *Macromolecules*, **30**, 685, 1997.
- Yamaguchi, M., H. Miyata, K.-H. Nitta, "Compatibility of Binary Blends of Polypropylene with Ethylene- α -olefin Copolymer", *J. Appl. Polym. Sci.*, **62**, 87, 1996.
- Yan, D., W.-J. Wang, S. Zhu, "Effect of Long Chain Branching on Rheological Properties of Metallocene Polyethylene", *Polymer*, **40**, 1737, 1999.
- Yano, A., S. Hasegawa, T. Kaneko, M. Sone, M. Sato, A. Akimoto, "Ethylene/1-hexene copolymerization with $\text{Ph}_2\text{C}(\text{Cp})(\text{Flu})\text{ZrCl}_2$ derivatives: correlation between ligand structure and copolymerization behavior at high temperature", *Macromol. Chem. Phys.*, **200**, 1542, 1999.
- Yano, A., S. Yamada, A. Akimoto, "Propylene polymerization with dimethylsilylbis(3-methylcyclopentadienyl) MCl_2 [M = Ti, Zr, Hf] in combination with methylaluminoxane", *Macromol. Chem. Phys.*, **200**, 1356, 1999.